AD-A082 354 SIGNATRON INC LEXINGTON MA F/G 17/2.1
HF MOBA COMMUNICATIONS STUDY.(U)
MAR 80 A MALAG, L EHRMAN DAAK80-79-C-0773
UNCLASSIFIED A257-I CORADCOM-79-0773-1 NL

1 OF 2

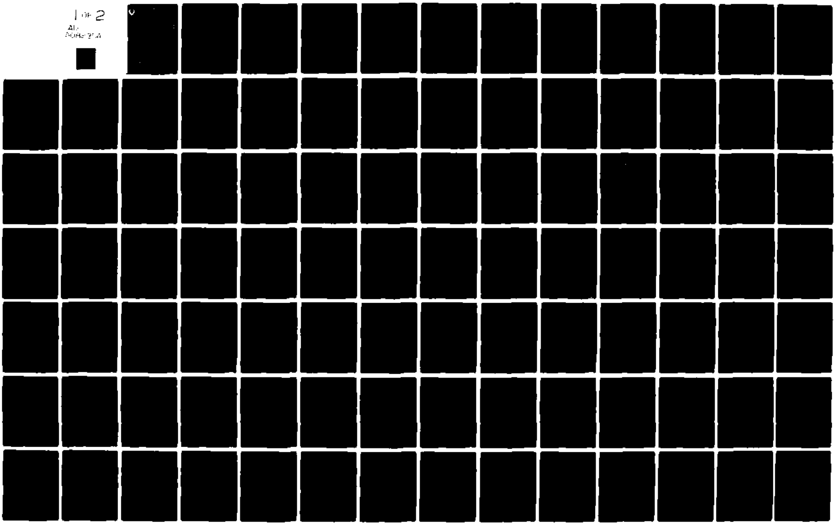

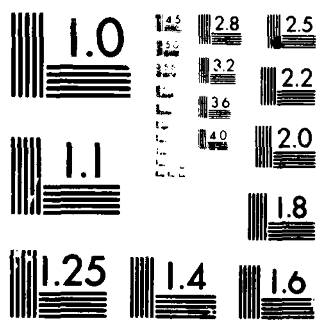

MICROCOPY RESOLUTION TEST CHART
NATIONAL BUREAU OF STANDARDS-1963-A

LEVEL II

RESEARCH AND DEVELOPMENT TECHNICAL REPORT
CORADCOM-79-0773-1

ADA082354

HF MOBA COMMUNICATIONS STUDY

DR. ALFONSO MÁLAGA
DR. LEONARD EHRMAN

SIGNATRON, INC.
12 HARTWELL AVENUE
LEXINGTON, MASSACHUSETTS 02172

7 MARCH 1980

INTERIM REPORT FOR PERIOD MARCH 1979 - JANUARY 1980

CONTRACT NO. DAAK80-79-C-0773

APPROVED FOR PUBLIC RELEASE; DISTRIBUTION UNLIMITED

PREPARED FOR:

U.S. ARMY COMMUNICATIONS SYSTEMS CENTER (CENCOMS)
FT. MONMOUTH, NEW JERSEY 07703

CORADCOM
US ARMY COMMUNICATIONS RESEARCH & DEVELOPMENT COMMAND
FORT MONMOUTH, NEW JERSEY 07703

NOTICES

Disclaimers

Disposition

UNCLASSIFIED

SECURITY CLASSIFICATION OF THIS PAGE (When Data Entered)

REPORT DOCUMENTATION PAGE

READ INSTRUCTIONS BEFORE COMPLETING FORM

1. REPORT NUMBER: CORADCOM-79-0773-1	2. GOVT ACCESSION NO.
3. RECIPIENT'S CATALOG NUMBER	
4. TITLE (and Subtitle): HF MOBA COMMUNICATIONS STUDY	5. TYPE OF REPORT & PERIOD COVERED: Interim Report. March 79 - January 80
	6. PERFORMING ORG. REPORT NUMBER: A257-I
7. AUTHOR(s): Alfonso Malaga, Leonard Ehrman	8. CONTRACT OR GRANT NUMBER(s): DAAK80-79-C-0773
9. PERFORMING ORGANIZATION NAME AND ADDRESS: SIGNATRON, Inc., 12 Hartwell Avenue, Lexington, Massachusetts 02173	10. PROGRAM ELEMENT, PROJECT, TASK AREA & WORK UNIT NUMBERS: 61102A, 1L161102AH48PN
11. CONTROLLING OFFICE NAME AND ADDRESS: John W. Walker, DRDCO-COM-D-4, U.S. Army Communications Systems Center (CENCOMS), Ft. Monmouth, N.J. 07703	12. REPORT DATE: 7 March 1980
	13. NUMBER OF PAGES: 156
14. MONITORING AGENCY NAME & ADDRESS (if different from Controlling Office): SAME	15. SECURITY CLASS. (of this report): UNCLASSIFIED
	15a. DECLASSIFICATION/DOWNGRADING SCHEDULE: N/A

12 157

16. DISTRIBUTION STATEMENT (of this Report)

Approved for Public Release; distribution unlimited

17. DISTRIBUTION STATEMENT (of the abstract entered in Block 20, if different from Report)

N/A

18. SUPPLEMENTARY NOTES

The findings in this report are not to be construed as an official Department of the Army position, unless so designated by other authorized documents.

19. KEY WORDS (Continue on reverse side if necessary and identify by block number)

HF Radio Communications
MOBA
COBA
HF Propagation in Built-up Areas

20. ABSTRACT (Continue on reverse side if necessary and identify by block number)

This report describes the results of a theoretical investigation of the various factors which affect HF radio communications in built-up (urbanized) areas. A survey of the propagation effects is given. A comparison of the range-coverage of typical Army HF radios in urban and rural areas is made.

DD FORM 1 JAN 73 1473 EDITION OF 1 NOV 65 IS OBSOLETE

UNCLASSIFIED

SECURITY CLASSIFICATION OF THIS PAGE (When Data Entered)

UNCLASSIFIED
SECURITY CLASSIFICATION OF THIS PAGE(When Data Entered)

EXECUTIVE SUMMARY

This document is the Interim Report on Contract DAAK80-79-C-0773, "HF MOBA Communications Study". The purpose of this study is to assess the advantages/disadvantages of using HF (high frequency) to communicate in built-up areas. This report is a complement to previous work done by SIGNATRON on the subject of VHF/UHF communications in built-up areas documented in the Interim and Final reports entitled, "Data Base Analysis for Military Operations in a Built-up Area (MOBA)".

The objectives of this study were: i) to establish a data base regarding HF communications in urbanized terrain and ii) to recommend propagation measurements to fill gaps in the data base and validate the findings of the study. Both of these objectives are fulfilled by this report.

The conclusions of the study are summarized as follows:

a. The range of HF communications in built-up areas is estimated to be considerably reduced compared to its range in flat obstruction-free terrain (e.g., rural). However the range reduction is not as severe at HF compared with VHF and UHF. The PRC-104 (20 watt HF manpack radio) has a rural range of 37 to 50 km. Its range in an urban area is 4.7 to 8 km. For comparison purposes, the nominal range of a VHF manpack radio such as the PRC-77 (2 watts) is 8 km. In an urban area, its range is 200 m to 1 km. Increasing the transmitted power of the PRC-77 to 20 watts would only increase its range to 2 km. A comparison of the ranges of

typical Army HF radios in rural and urban areas for voice and teletype data transmission are shown in Tables 4.1 and 4.2.

b. The reasons for range reduction in built-up areas are: (1) increased attenuation due to the presence of buildings; (2) fading due to multiple propagation paths over and around buildings; and (3) increase in the electrical noise levels in urban areas.

c. HF suffers less range reduction than VHF because the size of the buildings relative to the wavelength is smaller the lower the frequency.

d. Antenna size and/or antenna efficiency are a problem at the lower end of the HF band.

e The existing data base was found to have little quantitative data regarding the statistics and attenuation of HF signals in street-to-street communications as well as street-to building, building-to-building and intrabuilding communications.

It was therefore recommended that propagation measurements be made to fill the gaps in the existing data base.

TABLE 4.2

PREDICTED TRANSMISSION RANGE FOR
TELETYPE DATA USING HF RADIOS

Average Transmitted Power P_t (Watts)	Radio Nomenclature	Transmission Range (km) RURAL 3 MHz	RURAL 10 MHz	RURAL 30 MHz	URBAN 3 MHz	URBAN 10 MHz	URBAN 30 MHz
20	PRC-70	28.5	32	37	3.0	1.6	.33
200	GRC-106 GRC-122	51*	57	66	5.4	2.9	0.6

*Skyware interference at night.

TABLE 4.1

PREDICTED TRANSMISSION RANGE OF VARIOUS SSB-HF RADIOS

Transmitted Power, P_t	Radio	Transmission Range (km)					
		RURAL			URBAN		
(Watts PEP)	Nomenclature	3 MHz	10 MHz	30 MHz	3 MHz	10 MHz	30 MHz
15	PRC-74	34*	36	46	7.5	4.6	0.8
20	PRC-104	37*	39	50	8.0	4.7	.85
40	PRC-70	44*	46	59	9.6	5.9	1.0
100	PRC-104/FRC-93	55*	58	74	12.	7.4	1.3
400	PRC-104/GRC-106 GRC-122	78*	82	105	17.	10.5	1.8

*Skyware interference at night.

TABLE OF CONTENTS

SECTION		PAGE
1	INTRODUCTION AND SUMMARY	1-1
	1.1 Introduction	1-1
	1.2 Summary of Section 2: HF Propagation	1-3
	1.3 Summary of Section 3: AM, SSB and Digital Modulation System Performance	1-6
	1.4 Summary of Section 4: Application to Existing HF Radios	1-7
	1.5 Summary of Section 5: Conclusions and Recommendations	1-9
2	HF PROPAGATION	2-1
	2.0 Introduction	2-1
	2.1 Ground Wave Propagation	2-3
	2.2 Ground Wave Propagation over Irregular or Rough Terrain	2-15
	2.3 Ground Wave Propagation over an Inhomogeneous and Spherical Earth	2-20
	2.4 Ground Wave Propagation in Built-up Areas	2-24
	2.5 Prediction of Ground Wave Received Signal Level	2-26
	2.6 Skywave Propagation	2-31
	2.6.1 Optimum Operating Frequency	2-31
	2.6.2 Multipath Fading in Skywave Propagation	2-36
	2.6.3 Prediction of Skywave Received Signal Level	2-40
	2.7 Atmospheric and Man-Made Noise at HF	2-45
	2.8 Mode of Propagation vs. Distance	2-48
	2.9 Basic Considerations in HF Antenna Selection	2-52

SECTION		PAGE
3	AM, SSB and DIGITAL MODULATION SYSTEM PERFORMANCE	3-1
	3.0 Introduction	3-1
	3.1 AM and SSB System Performance	3-1
	3.1.1 Non-Fading AM Performance	3-2
	3.1.2 Non-Fading SSB Performance	3-4
	3.1.3 Frequency-Flat Fading AM and SSB Performance	3-9
	3.1.4 Frequency-Flat Fading AM and SSB Performance with AGC	3-20
	3.1.5 Frequency-Selective Fading AM and SSB Performance	3-24
	3.2 Digital Modulation System Performance	3-27
	3.2.1 Non-Fading NCFSK System Performance	3-32
	3.2.2 Frequency-Flat Fading NCFSK Performance	3-36
	3.2.3 Frequency-Selective Fading NCFSK Performance	3-50
4	APPLICATION TO EXISTING HF RADIOS	4-1
	4.0 Introduction	4-1
	4.1 Radio Characteristics	4-1
	4.1.1 AN/PRC-104	4-2
	4.1.2 AN/PRC-70	4-2
	4.1.3 AN/GRC-106, 106A	4-3
	4.1.4 AN/GRC-122, 142, 142B	4-3
	4.1.5 AN/FRC-93	4-4
	4.1.6 AN/PRC-74A, B, C	4-4
	4.2 Radio Performance	4-5
	4.3 Implications of the Radio Analysis	4-12
5	CONCLUSIONS AND RECOMMENDATIONS	5-1
	5.1 Conclusions	5-1
	5.2 Recommendations	5-2

LIST OF FIGURES

		PAGE
Fig. 2.0-1	Comparative Ground Wave and Ionospheric Transmission [From Crain, 1975]	2.2
Fig. 2.1-1	Plane Earth Line-of-Sight Propagation	2.5
Fig. 2.1-2	Antenna Height-Gain Factors [From Jasik, 1961]	2.9
Fig. 2.1-3	Minimum Effective Antenna Height [From Jasik, 1961]	2.10
Fig. 2.1-4	Surface Wave Attenuation Factor as a Function of the Numerical Distance	2.12
Fig. 2.1-5	World Map Showing Various Types of Terrain	2.14
Fig. 2.1-6	Ground Wave Attenuation Over Poor Ground	2.16
Fig. 2.1-7	Ground Wave Attenuation Over Good Ground	2.17
Fig. 2.1-8	Ground Wave Attenuation Over Sea Water	2.18
Fig. 2.3-1	Quantised Form of the Data Required for a Profile [from Causebrook, 1978]	2.22
Fig. 2.5-1	Normalized Nakagami-Rice Density Function	2.28
Fig. 2.6-1	Diurnal Variation of the Maximum Usable Frequency as a Function of Distance [from Sykes, et al., 1975]	2.35
Fig. 2.6-2	Diurnal Variation of the Maximum Usable Frequency for High and Low Sunspot Numbers [from Sykes, et al., 1975]	2.35
Fig. 2.6-3	Doppler Spread (Fade Rate) as a Function of Carrier Frequency for Various Local Times [from Malaga, 1978]	2.38

LIST OF FIGURES

		PAGE
Fig. 2.6-4	Doppler Spread (Fade Rate) as a Function of Carrier Frequency for Various Transmitter-Receiver Separations [from Malaga, 1978]	2.39
Fig. 2.6-5	Discrete Multipath Spread vs. Carrier Frequency at Different Times of the Day [from Malaga, 1978]	2.41
Fig. 2.6-6	Discrete Multipath Spread vs. Carrier Frequency for Various Transmitter-Receiver Separations [from Malaga, 1978]	2.42
Fig. 2.7-1	Median Values of Radio Noise Power as Recorded With a Short Vertical Lossless Antenna [from Barghausen, et al. 1969]	2.47
Fig. 2.8-1	Ground Wave and Skywave Propagation Ranges in Built-up Areas vs. Frequency for Winter Midday Conditions	2.49
Fig. 2.8-2	Ground Wave and Skywave Propagation Ranges in Built-up Areas vs. Frequency for Winter Night Conditions	2.51
Fig. 2.9-1	General Propagation Chart with Example of 800-km Circuit [from Collins Radio, 1978]	2.53
Fig. 2.9-2(a)	Vertical Radiation Pattern (in the Plane Perpendicular to the Axis of the Dipole) of a Horizontal Dipole 1/2-Wavelength Above an Earth of Finite Conductivity [from Jordan, 1950]	2.54
Fig. 2.9-2(b)	Vertical Radiation Pattern of a Vertical Dipole 1/2-Wavelength Above an Earth of Finite Conductivity [from Jordan, 1950]	2.55
Fig. 2.9-3	Comparison of the Gain of a Perfect Quarter-Wave Vertical Monopole Over Good Ground and Over Perfect Ground [from Collins Radio, 1978]	2.57
Fig. 3.1-1	Signal-To-Signal-Suppression-Noise Ratio in AM Systems With and Without Filtering vs. Diversity Order [from Jakes, 1974]	3.16

LIST OF FIGURES

		PAGE
Fig. 3.1-2	Signal-To-Signal-Suppression-Noise Ratio in AM and SSB Systems Versus Specular-To-Rayleigh Component Ratio for Single and Dual Diversity Reception	3.19
Fig. 3.1-3	Limiting Gain Relative to Mean Carrier Power [from Jakes, 1974]	3.22
Fig. 3.1-4	Effective SNR Versus Interference-To-Signal Power Ratio for AM and SSB in the Presence of Frequency Selective Fading	3.28
Fig. 3.2-1	Bit (element) error Probability Versus Signal-To-Noise Ratio [from Schwartz, Bennet and Stein, 1967]	3.35
Fig. 3.2-2	Element Error Probabilities in a Single-Channel NCFSK System Under Stable Conditions [from Akima, et al., 1969]	3.37
Fig. 3.2-3	Probability of Error for Several Systems in Rayleigh Fading [from Schwartz, Bennet, and Stein, 1967]	3.39
Fig. 3.2-4	Probability of Error for NCFSK Systems in Rician Fading [from Lindsay, 1964]	3.42
Fig. 3.2-5	Irreducible Error Probability vs. Fading Rate for NCFSK in Rayleigh Fading	3.47
Fig. 3.2-6	Signal-To-Noise Ratio Degradation vs. Fading Rate for NCFSK in Rayleigh Fading	3.49
Fig. 3.2-7	Irreducible Error Probability vs. Multipath Spread and Fade Rate for NCFSK in the Presence of Two Rician Discrete Multipath Components [from Hingorani, 1967]	3.52
Fig. 4.1	Antenna Radiation Efficiency as a Function of Electrical Length for Base-Fed Vertical Whip	4.9

SECTION 1
INTRODUCTION AND SUMMARY

1.1 Introduction

This document is the Interim Report on Contract DAAK80-79-C-0773, "HF MOBA Communications Study". This study is a continuation of the previous work done by SIGNATRON [Ehrman and Parl, 1977 and Ehrman, Malaga and Ziolkowski, 1979] on the subject of VHF/UHF radio communications in built-up areas. This report assesses the advantages/disadvantages of using HF (high frequencies) to communicate in built-up areas. The first report referenced above dealt with the study and assessment of the state-of-the-art on VHF/UHF communications in built-up areas, while the second is a report of an experimental propagation research program to gather VHF/UHF propagation data not previously available in the existing data base.

The background for this study is as follows. The present generation of mobile tactical Army radios are designed for VHF/UHF operation. The reason for this is that the VHF/UHF bands provide good performance and sufficient range when used in line-of-sight (LOS) paths and also provide relatively efficient coupling of energy from the power stage of the radio transmitter to the transmitting antenna. VHF/UHF radios, however, have virtually no over-the-horizon performance and are therefore limited to short-range communications. Longer range communications are maintained through the use of HF radio. When it is necessary for a higher headquarters to communicate with forward echelons, a communications relay is often used, with the link from the relay to the forward echelon being VHF/UHF, and the link from the relay to the headquarters being HF.

When a military operation in a built-up area (MOBA) is taking place, radio communications may need to be established over non-line-of-sight paths. The propagation path for this type of communications is a combination of diffraction over and around buildings and reflection from buildings and the ground. This communications channel exhibits Rayleigh fading due to multipath propagation and results in a communications range in urban areas which is significantly reduced relative to its nominal range in an ideal line-of-sight setting. In our previous efforts we found out that the nominal range of a typical VHF manpack radio such as the PRC-77 would be reduced from 8 km in a line-of-sight path to 1.5 km in suburban area and to ranges as short as 200 meters in a highly built-up area [Ehrman, et al., 1979]. We also found that the communications range in a built-up area was greater at the lower VHF frequencies than at the upper end of the VHF band and at UHF. This indicated that the communications range in urban areas could be improved by using HF instead of VHF/UHF. The use of HF to communicate in built-up areas might also eliminate the need for a relay for providing communications between front-line units and higher echelon units located as far as 100 miles away.

The objectives of this program were then: one, to establish what is known about HF propagation over these paths; and second, to make propagation measurements to fill in missing data and to validate the HF urban propagation model. This Interim report fulfills the first objective of the program.

The report is divided into five sections. Sections 2 and 3 contain the results of the HF data base analysis with HF propagation being discussed in Section 2 and AM, Single-Sideband (SSB) and digital system performance in Section 3. In Section 4 we assess the performance of typical Army HF radios in built-up areas. Finally, Section 5 contains the conclusions

resulting from this study and recommendations for long-term improvement of military communications in built-up areas.

In the remainder of this section, we provide a summary of Sections 2 through 5.

1.2 Summary of Section 2: HF Propagation

Section 2 presents a comprehensive summary of the various factors which affect radiowave propagation at frequencies in the HF band (3-30 MHz). The aim of this section is to provide the reader with the means for predicting the received signal and noise levels through the use of graphs and/or formulas.

HF radio signals can propagate via ground (or surface) waves and/or skywaves (ionospherically reflected waves). Hence, Section 2.1 discusses the propagation of ground waves over homogeneous smooth ground. It is shown that when the transmitter and receiver are sufficiently close, the received signal power decreases at the square of the distance, while at greater separations, it decreases as the fourth power of the distance. The minimum transmitter-receiver separation at which the received signal level begins to decrease as the fourth power of the distance depends on the frequency, polarization and type of terrain, i.e., poor ground (rocky or dry land), good ground (farm land) or sea water. In addition, the received signal level increases when the transmitting and/or receiving antennas are elevated above a minimum height. The minimum height depends also on the frequency, polarization and type of terrain. Figures and formulas are given in this section which enable the reader to evaluate the path loss (attenuation) as a function of transmitter-receiver separation, frequency, polarization and antenna height for given ground conditions. The ground conditions are specified by its conductivity and relative dielectric constant.

The path loss is further increased when the terrain is irregular. In Section 2.2 it is shown that the increase in path loss due to terrain irregularity can be accounted for by suitably modifying the conducting properties of the ground. The effects of inhomogeneous ground are discussed in Section 2.3. The ground is considered to be inhomogeneous when its conducting properties vary along the propagation path. This is the case when propagation takes place over mixed paths which include large bodies of water (lakes, sea) and various types of land (such as farm lands, deserts and cities). When propagation is over urbanized terrain, the path loss is even greater. In Section 2.4, it is shown that the effects of buildings and other urban structures such as lamp posts can be accounted for by modifying the local ground conducting properties.

The methods and theories discussed in Sections 2.1 through 2.4 are suitable for calculating (predicting) the average ground wave path loss. In practice, the received signal in urbanized terrain may exhibit fading (temporal or spatial) due to multipath propagation resulting from signals scattered and reflected from nearby structures. This has been found to be the case at VHF and UHF and also at the higher frequencies in the HF band [Ehrman, et al., 1979]. However, there is no experimental evidence regarding the statistical behavior of ground wave propagated signals at the lower end of the HF band. In Section 2.5 we discuss the possible statistical behavior of ground wave HF signals in built-up areas and present a formula for predicting the ground wave received signal level.

HF signals may also propagate via ionospheric reflection (skywaves). In Section 2.6 we discuss the various mechanisms which affect skywave propagation. It is indicated that skywave propagated signals exhibit great variability with frequency, time-of-day, transmitter-receiver separation, season, and

sunspot number. For a given set of conditions there is a maximum frequency which can be transmitted via ionospheric reflection (maximum usable frequency or MUF). For a given frequency below the MUF, there is minimum distance at which this frequency can be received (skip distance). Graphs indicating the dependence of the MUF on time-of-day and sunspot number are given in this section. We also discuss other characteristics of skywave signals such as its statistical behavior, multipath propagation and fading rate. A formula for calculating the skywave received signal level is given.

Section 2.7 discusses the various sources of noise encountered at HF: atmospheric, man-made and thermal. Graphs illustrating their relative levels as a function of frequency and environment, i.e., urban, suburban or rural, are given.

In Section 2.8 we determine which of the two types of propagation (ground wave or skywave) predominates as a function of distance and frequency and for various conditions. It is shown that during the daytime hours, the ground wave signal is stronger up to distances of 70 km at 3 MHz, up to 400 km at 10 MHz and longer at higher frequencies. Above 15 MHz there is usually no skywave return. At nighttime, however, the ground wave is stronger at distances up to 30 km at frequencies below 5 MHz. Above 5 MHz, there is no skywave signal. From these considerations, it may be concluded that HF signals in built-up areas will propagate mainly via ground wave except at night, when the skywave will interfere with the ground wave at frequencies below 5 MHz.

We conclude by discussing in Section 2.9 various factors which affect the choice of antenna polarization at HF, namely, antenna elevation pattern and antenna gain.

1.3 Summary of Section 3: AM, SSB and Digital Modulation System Performance

Nearly all Army HF radios use amplitude modulation (AM) and/or single-sideband amplitude modulation (SSB-AM) to transmit voice signals and noncoherent frequency shift keying (NCFSK) to transmit low data rate teletype information. Thus, in Section 4, the signal-to-noise ratio (SNR) out of analog AM and SSB radios, and the error rate of a digital NCFSK radio are discussed. The factors which affect the signal-to-noise ratio and error rate are the statistics of the received signal and the noise, and if the signal is fading, the fade rate and frequency selectivity.

The signal-to-noise ratio of AM and SSB systems over non-fading and fading channels is discussed in Section 3.1. In Section 3.1.1 it is shown that when the signal is not fading, the minimum required signal-to-noise ratio for voice signals of acceptable quality is 12 dB for AM radios with 6 KHz channelization and SSB radios with 3 KHz channels. For voice of good commercial quality, the required signal-to-noise ratio is 30 dB. An additional signal-to-noise ratio margin is required when the signal is fading . The margin depends on the statistics of the fading signal and the fading rate. In Section 3.1.2 it is shown that when the fading is flat and sufficiently slow (less than 1 Hz), the required additional signal-to-noise ratio margin is 1 dB if no diversity reception is used. However, if dual diversity reception is used, then the required signal-to-noise ratio is 3 dB lower. When the fading is still frequency flat but is not slow, there is a maximum effective signal-to-noise ratio which cannot be improved upon by increasing the transmitted power. The maximum effective SNR depends on the statistics of the received fading signal and is worst when the signal is Rayleigh fading. In this case, the

maximum effective SNR is around 0 dB (it depends on the modulation, i.e., AM or SSB) which is well below the minimum required SNR.

The maximum effective SNR can be improved by using diversity reception and/or automatic gain control (AGC). The improvement in the maximum SNR by using diversity reception and AGC is discussed in Sections 3.1.2 and 3.1.3 respectively.

When the channel is a multipath channel (e.g., skywave circuits or ground wave circuits in built-up areas), the fading may be frequency-selective if the bandwidth of the transmitted signal is greater than the inverse of the multipath spread (coherence bandwidth of the channel). In Section 3.1.4 it is shown that frequency selective fading also results in a maximum effective signal-to-noise ratio which depends on the signal-to-multipath-interference ratio.

The transmission of teletypewriter (digital) data using NCFSK is discussed in Section 3.2. It is shown that for a steady non-fading channel, the error rate decreases exponentially with the signal-to-noise ratio (SNR). When the channel is flat-fading, the error rate is shown to vary inversely with the signal-to-noise ratio instead of exponentially. As in the AM and SSB case, fast frequency-flat fading and/or frequency selective fading results in a maximum effective SNR or irreducible error rate.

1.4 Summary of Section 4: Application to Existing Radios

Section 4 examines the performance of various Army HF radios in both rural (ideal) and urban areas. The HF radios are the AN/PRC-104, AN/PRC-70, AN/GRC-106(106A), AN/GRC-122, AN/FRC-93 and AN/PRC-72(A,B,C). The characteristics of these radios are described in Section 4.1 and their performance is analyzed in Section 4.2. It is shown that the presence of buildings and other obstacles in urban areas significantly

reduces the range of these radios compared to their ranges in flat terrain (rural). The analysis also shows that while the range of the radios in independent of frequency in rural terrain, the range is urban terrain is almost an order of magnitude greater at 3 MHz than at 30 MHz.

The factors which limit the radio performance in any type of environment are: transmitted power, antenna gain (or efficiency), path loss and background noise. The antenna efficiency depends on its physical length relative to the wavelength. The smaller the antenna relative to the wavelength, the less efficient. For a fixed antenna length (say a 9 ft. whip), the efficiency varies from -17 dB at 3 MHz to 0 dB at 30 MHz. The path loss depends on the environment, frequency and transmitter-receiver separation (distance). In general, it increases with frequency and distance. The background noise depends on the environment (rural or urban) and in general decreases with increasing frequency.

The implications of the analysis and above mentioned effects are discussed in Section 4.3. It is pointed out that because of much lower path losses at lower frequencies, the low end of the HF band (3-10 MHz) promises to provide significantly greater coverage (range) than VHF (30-80 MHz) by a factor of 5 times. It should be pointed out though that the range comparisons mentioned above are based on low-height (5-6 ft) antenna elevations. Significant increases in range can be achieved at VHF by elevating the transmitting and/or receiving antenna above 30 ft (2 to 4 times). At HF, however, increases in range due to antenna elevation are minimal unless the antennas are raised above roof top level.

1.5 Summary of Section 5: Conclusions and Recommendations

Section 5 is the final section of this report and contains the conclusions and recommendations. As a result of the analysis we conclude that, as is the case at VHF and UHF, the range of urban HF communications will be much less than in non-urbanized terrain. However, the range reduction will be much smaller at the lower frequencies so that the 3-10 MHz band promises to provide much better coverage than VHF in urban areas. Furthermore, front line to higher echelon communications using 100 Watt HF radios will be limited to 50 km and even shorter ranges if one end of the link is in the heart of a built-up area.

The study also reveals a lack of quantitative data regarding signal attenuation in urban and suburban areas at HF. Hence, we recommend that propagation measurements be made at HF in order to fill the gap in the existing data base and to verify the findings of this study.

REFERENCES FOR SECTION 1

Ehrman, L. and S. Parl (1977), "Communications Data Base Analysis for Military Operations in a Built-up Area (MOBA/COBA)", Interim Report for Period 18 Apr 1977 - 9 Dec 1977, Report 15068.1, Contract DAAG29-77-C-0020, SIGNATRON, Inc.

Ehrman, L., A. Malaga and F. Ziolkowski (1979), "Communications Data Base Analysis for Military Operations in a Built-up Area (MOBA/COBA)", Final Report for Period 18 Apr 1977 - 9 Aug 1979, Report 15068.2, Contract DAAG29-77-C-0020, SIGNATRON, Inc.

SECTION 2
HF PROPAGATION

2.0 Introduction

At frequencies in the HF band (3-30 MHz) and below, the transmission of radio signals between a transmitter and beyond-the-horizon receivers occurs by ground (or surface) wave propagation, ionospheric reflection (skywave propagation), or a combination of both. Under normal ionospheric conditions, the signal received via ionospheric reflection becomes stronger than the ground wave beyond a certain distance depending on frequency, time of day, and the nature of the surface (i.e., sea water, smooth terrain, mountain terrain, etc.), sunspot number (SSN), polarization, etc.

Figure 2.0-1 shows the approximate distance from the transmitter at which the ground wave signal and the skywave signal are of equal amplitude as a function of frequency, for frequencies between 0.1 MHz and 30 MHz, and for the conditions prescribed, i.e., mid-day (winter time), over smooth land with typical electrical properties, and an average sunspot minimum ionosphere. Between about 1 MHz and 10 MHz a band of ranges is shown reflecting the sensitivity of the skywave to variations in the structure of the ionosphere as well as the effects of antenna polarization. Above 10 MHz the ionospheric signal, for the ranges involved, is due to ionospheric scatter. At night, ionospheric signals, for the frequencies and ranges of Figure 2.0-1, are larger; hence, Figure 2.0-1 can be interpreted as showing average expected maximum distances for which the ground wave signal is equal to a typically expected ionospheric signal. For example, at 3 MHz, during daytime, Figure 2.0-1 shows the ground wave signal to be greater than the skywave signal to distances of 90 miles. At night, this distance would typically be in the vicinity of 30 miles. This indicates that

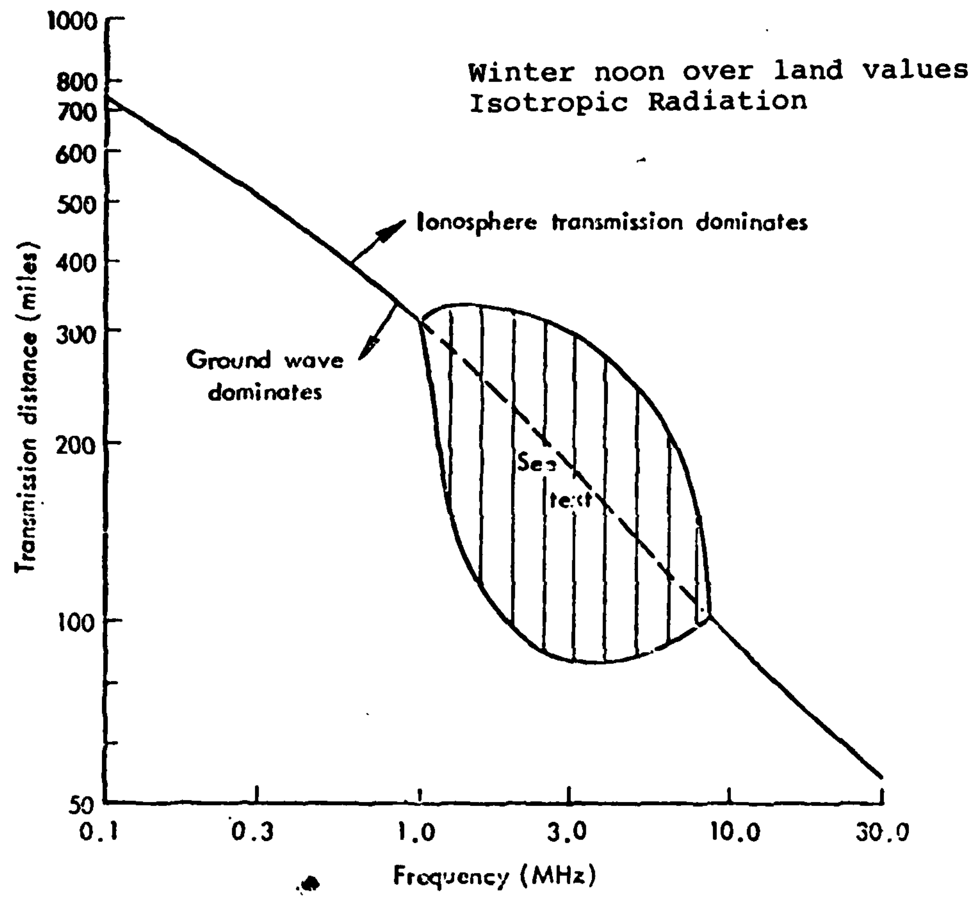

Fig. 2.0-1 Comparative Ground Wave and Ionospheric Transmission [From Crain, 1975]

short range (up to 100 miles) HF communications over a smooth (regular) ground is principally via ground wave propagation during the day-time and a combination of ground wave and skywave propagation at night. However, the curve of Fig. 2.0-1 does not include the effects of terrain irregularities such as those that might be found in urbanized areas. If these effects were included, then short range HF propagation in urbanized terrain might be a combination of ground wave and skywave propagation at all times.

Hence, in order to establish a data base for assessing the propagation mode of HF signals in built-up areas, we review in this section all the factors which affect the propagation of HF signals via the ground wave and skywave mode. In Section 2.1 we discuss basic ground wave propagation over a smooth plane earth. In Section 2.2 we discuss the effects of irregular or rough terrain. Section 2.3 deals with ground wave propagation over an inhomogeneous and spherical earth. In Section 2.4 we consider the effects of urbanized terrain (built-up areas) on ground wave propagated signals. Section 2.5 discusses the prediction of ground wave received signal level. Skywave propagation is discussed in Section 2.6. In Section 2.7 we discuss the various noise sources in the HF band. Section 2.8 summarizes the results of the previous sections by discussing the ranges where ground wave and skywave propagated signals predominate. Finally, in Section 2.9 we include some basic considerations in HF antenna selection.

2.1 Ground Wave Propagation

The theory of electromagnetic ground wave propagation over a homogeneous ground of finite conductivity was originally developed by Sommerfeld [1909] and since then the solution to this problem has been formulated in different ways by various authors. The most familiar form is that derived by

Norton [1937] and refined by King [1969].

When the transmitting and receiving antennas are placed at some height, h_t and h_r respectively, above a homogeneous ground, the results of Norton [1937] and King [1969] have shown that the ground wave field strength can be divided into three components, one of which corresponds to the direct and reflected waves of geometric optics and the other is the diffracted non-geometric-optic surface wave. The two geometric optic components are explicitly shown in Fig. 2.1-1 while the surface wave field component propagates along the surface of the ground. When the antenna heights above the ground are sufficiently great, the surface wave field at the receiving antenna is weak and the space wave (direct plus reflected wave) term predominates. Near the ground, the surface wave predominates. In general when all three components are received, the ratio of received power, P_r, to transmitter power, P_t, is given by [King, 1969]

$$\frac{P_r}{P_t} = \frac{P_o}{P_t} \left| 1 + Re^{-j\Delta} + (1-R)F(w)e^{-j\Delta} \right|^2 \qquad (2.1\text{-}1)$$

where P_o is the power that would be received in free-space if there were no obstacles present (such as the ground), R is the ground reflection coefficient, F(w) is the surface-wave attenuation factor, w is the numerical distance, and Δ is the phase shift of the reflected wave and the surface wave relative to the direct wave.

The ratio of the free-space power to transmitted power depends on the frequency (wavelength), distance between transmitter and receiver, d, and the transmitting and receiving antenna gains, g_t and g_r respectively. This ratio is given by [Bullington, 1957]:

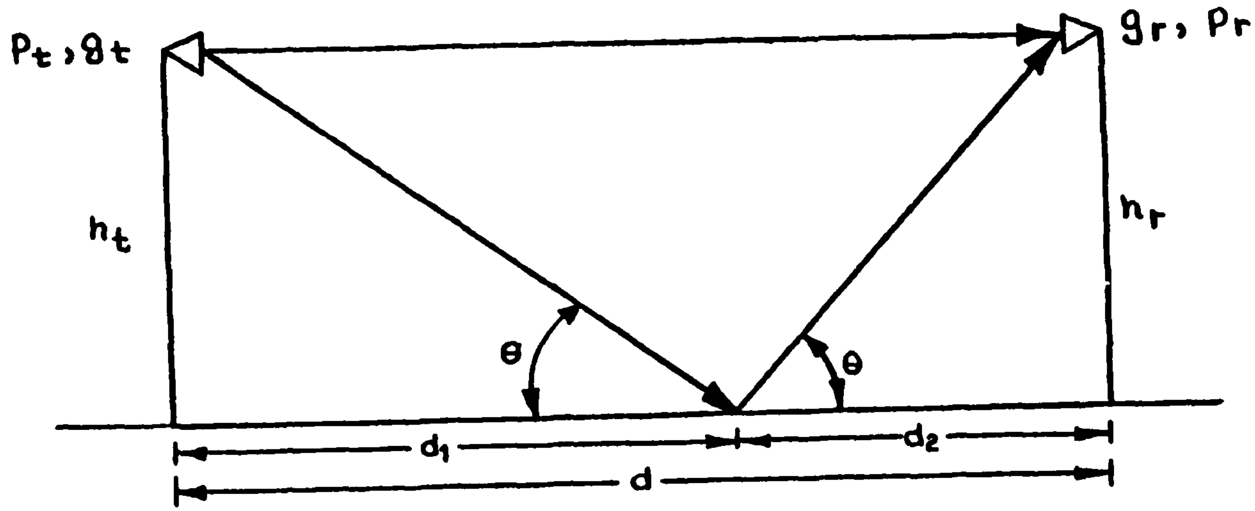

Fig. 2.1-1 Plane Earth Line-of-Sight Propagation

$$\frac{P_o}{P_t} = \left(\frac{\lambda}{4\pi d}\right)^2 g_t g_r \qquad (2.1\text{-}2)$$

Thus, in free space, the received power varies directly as the square of the wavelength and inversely as the square of the distance.

The ground reflection coefficient, R, the surface wave attenuation factor, F, the numerical distance, w, and the phase shift, Δ, depend on the polarization of the transmitted wave, the antenna heights and the ground conductivity σ and permittivity ε_r as follows:

$$R = \frac{\sin\theta - Z}{\sin\theta + Z} \qquad (2.1\text{-}3)$$

$$F(w) = 1 - j\sqrt{\pi w}\, e^{-w}\, \mathrm{erfc}\,(j\sqrt{w}) \qquad (2.1\text{-}4)$$

$$w = \frac{-j\pi d}{\lambda\cos^3\theta}\,(\sin\theta + Z)^2 \qquad (2.1\text{-}5)$$

$$Z = \begin{cases} \dfrac{\sqrt{\varepsilon_r - j60\sigma\lambda - \cos^2\theta}}{\varepsilon_r - j60\sigma\lambda}, & \text{vertical Polarization} \\ \sqrt{\varepsilon_r - j60\sigma\lambda - \cos^2\theta}, & \text{horizontal Polarization} \end{cases} \qquad (2.1\text{-}6)$$

$$\sin\theta = \frac{h_t + h_r}{d} \qquad (2.1\text{-}7)$$

$$\Delta = \frac{2\pi d}{\lambda\cos\theta}\left[1 - \sqrt{1 - \frac{4h_t h_r \cos^2\theta}{d}}\right] \qquad (2.1\text{-}8)$$

At VHF when the antennas are elevated more than one wavelength above the ground, the surface wave can be neglected and only the reflected wave will cause significant interference resulting in the well known fourth power law for the received power [e.g., Ehrman, 1977].

$$\frac{P_r}{P_t} \simeq g_t g_r \left(\frac{h_t h_r}{d^2}\right)^2 \qquad (2.1\text{-}9)$$

At HF however, typical antenna heights of 5 to 10 ft are smaller than the wavelength (in the HF band: 30 ft $<\lambda<$ 300 ft). In the case where h_t, h_r $<<\lambda$, the surface wave term cannot be neglected. The ratio of received power to transmitted power is approximately given by [Norton, 1941]

$$\frac{P_r}{P_t} = \frac{4P_o}{P_t} \left| F(w_o) \; H(q_t) H(q_r) \right|^2 \qquad (2.1\text{-}10)$$

where w_o is the numerical distance when $h_t=h_r=0$, i.e.,

$$w_o = \frac{-j\pi d Z_o^{\,2}}{\lambda} \qquad (2.1\text{-}11)$$

and Z_o is the normalized ground impedance at grazing incidence:

$$Z_o = \lim_{\theta \to o} Z \qquad (2.1\text{-}12)$$

The factor H(q) is a height-gain function which depends on the antenna heights and ground parameters and is given by [Norton, 1941]:

$$H(q) = \left[1+q^2-2q \cos b \right]^{1/2} \qquad (2.1\text{-}13)$$

where

$$q = \frac{2\pi h}{\lambda} |Z_o| \qquad (2.1\text{-}14)$$

$$b = \arg Z_o \qquad (2.1\text{-}15)$$

The height gain factor may be interpreted as the increase in received signal level when the antennas are raised above the ground (due to contributions from the space wave). Figure 2.1-2 shows the height gain factors for vertically polarized antennas over 'poor' soil and sea water.

When propagation is over 'poor' soil, the space wave (optical field) contribution to the received signal becomes significant at frequencies above 15 MHz if the antenna height is greater than 20 feet (i.e., greater than a half wavelength). Furthermore, for fixed antenna heights, the height gain increases with frequency so that at VHF most of the received signal is due to the space wave (or optical field) provided propagation is over land.

When propagation is over sea water, the space wave becomes significant at frequencies above 150 MHz so that at frequencies in the HF range (3-30 MHz) and even in the lower VHF band (30-80 MHz), the ground wave field is made up entirely of the surface wave.

The minimum antenna height at which the antenna height gain factors become significant may be obtained from Eq. (2.1-14) and is given by:

$$h_o = \frac{\lambda}{2\pi |Z_o|} \qquad (2.1\text{-}16)$$

This is the antenna height at which the space wave has equal strength as the surface wave and is shown in Fig. 2.1-3 for various ground conditions as a function of frequency.

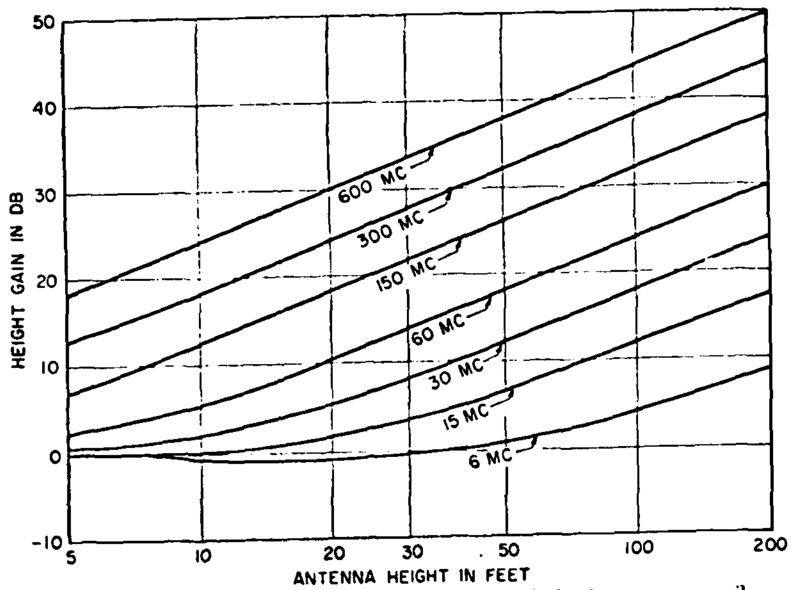

Antenna height-gain factor for vertical polarization over poor soil.

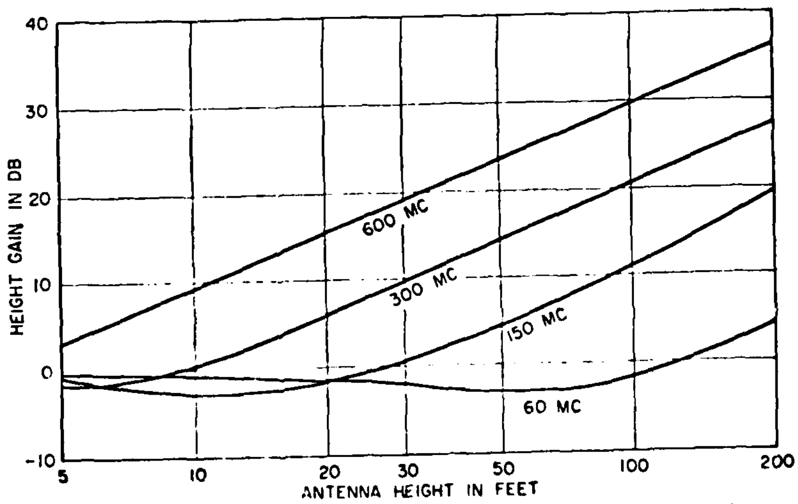

Antenna height-gain factor for vertical polarization over sea water.

Fig. 2.1-2 Antenna Height-Gain Factors [from Jasik, 1961]

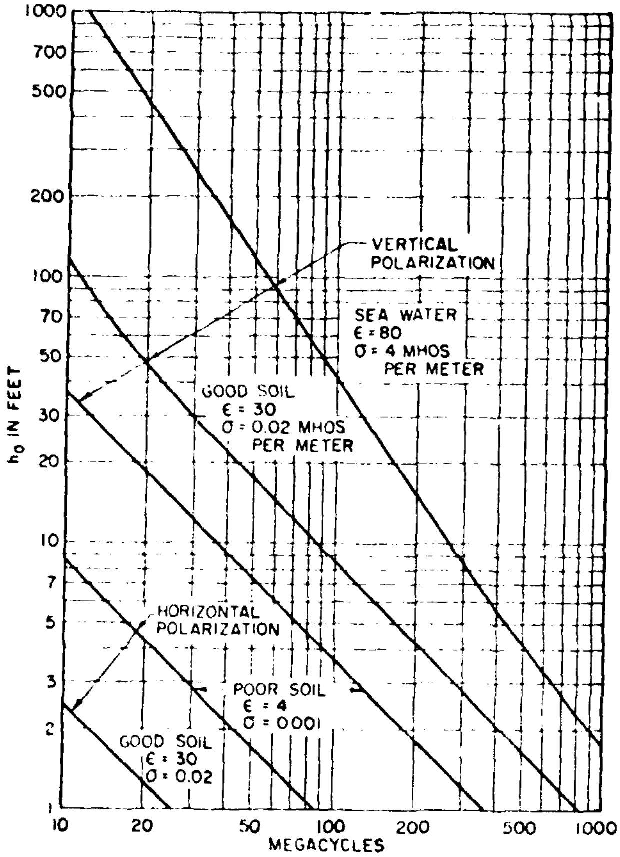

Minimum effective antenna height.

Fig. 2.1-3 Minimum Effective Antenna Height [from Jasik, 1961]

The surface wave component of the received signal is characterized by the attenuation factor F(w) and the numerical distance w which is a function of the conducting properties of the ground, the actual distance between transmitter and receiver, and the frequency. A plot of the surface wave attenuation factor F, as given by Eq. (2.1-2), is shown in Fig. 2.1-4 as a function of the magnitude and phase (argument) of the numerical distance, w. These curves show that at short numerical distances F has a value near unity. This implies that at short distances, the surface wave (and the ground wave field) decreases as the square of the distance (since $P_o \sim d^{-2}$). At the other extreme, when the magnitude of the numerical distance $|w|$ is greater than 30, the surface wave attenuation factor decreases linearly with the numerical distance (i.e., $F \sim w^{-1} \sim d^{-1}$) so that the surface wave received power decreases as the fourth power of the distance. At intermediate values of the numerical distance ($.03<w<30$) the surface wave attenuation factor is highly dependent on the argument (phase) of the numerical distance. When the argument is around 51^o, the attenuation factor has a singular point (location) where the received field is nearly zero. The argument of the numerical distance depends on the conductivity of the ground and the polarization through the argument (phase) of the normalized impedance. Table 2.1 shows values of the argument of the normalized impedance, Z, for the case of grazing incidence (or low antenna elevation so that $\theta \approx 0$) on a smooth, homogeneous flat ground (Z is given by Eq. 2.1-6).

Typical values of the ground constants ε_r and σ are given in Table 2.2 and a World Map showing various types of terrain is given in Figure 2.1-5.

At frequencies in the HF band, a smooth relatively flat earth acts as an inductive surface for vertical polarization and as a capacitive surface for horizontal polarization. The

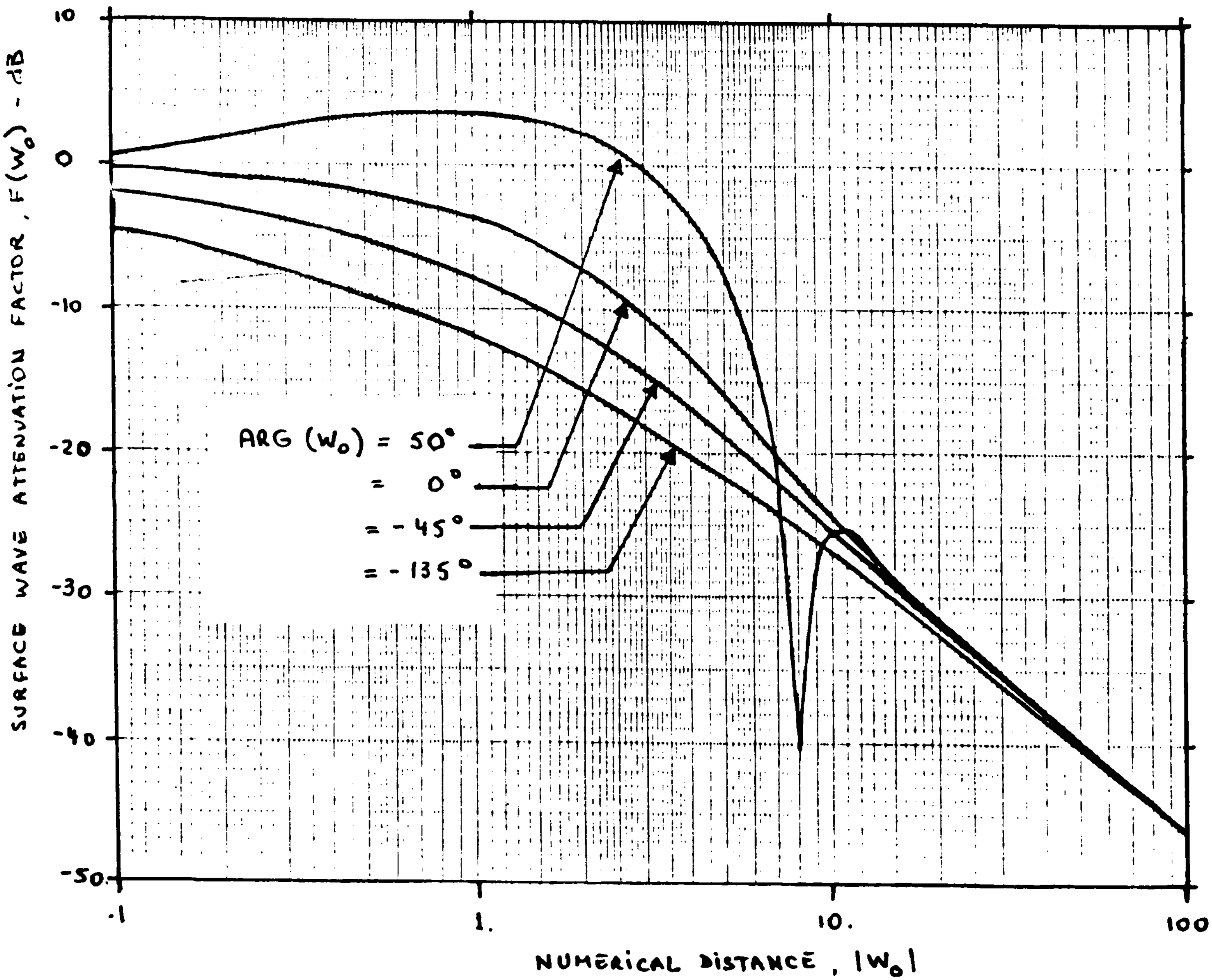

Fig. 2.1-4 Surface Wave Attenuation Factor as a Function of the Numerical Distance

Table 2.1

Relationship between Ground Conductivity, Polarization and the Argument of the Numerical Distance

Horizontal Polarization		Vertical Polarization	
Highly Capacitive	Capacitive	(Homogeneous Ground)	(Rough or Inhomogeneous Ground)
$-\frac{\pi}{2} \leq \arg Z < -\frac{\pi}{4}$	$-\frac{\pi}{4} \leq \arg Z < 0$	$0 \leq \arg Z \leq \frac{\pi}{4}$	$\frac{\pi}{4} < \arg Z \leq \frac{\pi}{2}$
$-\frac{3\pi}{2} \leq \arg W < -\pi$	$-\pi < \arg W < -\frac{\pi}{2}$	$-\frac{\pi}{2} \leq \arg W \leq 0$	$0 < \arg W \leq \frac{\pi}{2}$

Table 2.2

Typical Ground Constants

TYPE OF SURFACE	σ(mho/m)	ϵ_r
Poor Ground	0.001	4
Average Ground	0.005	15
Good Ground	0.01	15
Fresh Water	0.01	81
Sea Water	5.	81

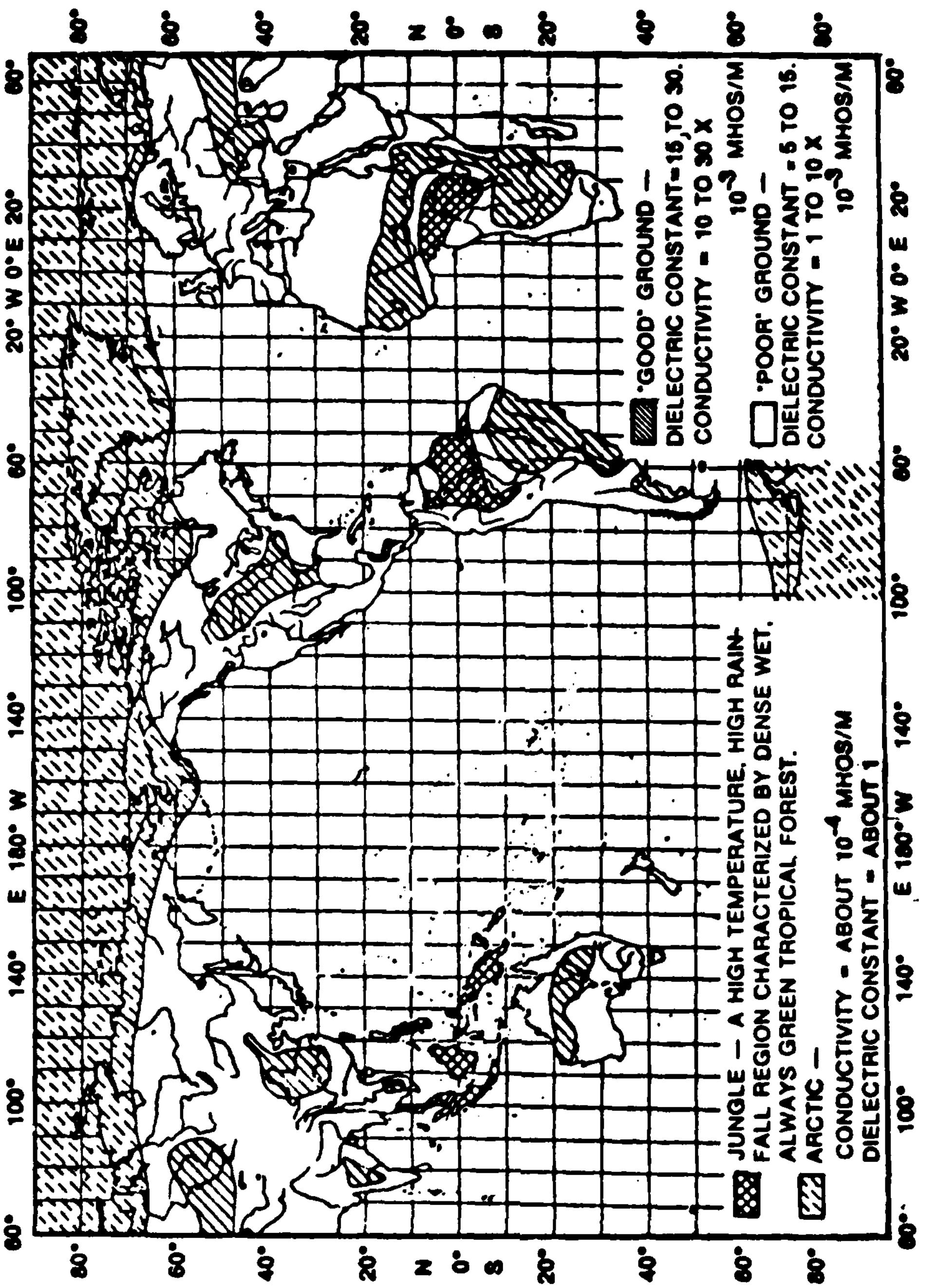

Figure 2.1-5 World Map Showing Various Types of Terrain

attenuation factor which corresponds to these cases are well behaved and have no high attenuation regions ('dead zones'). However when the surface is irregular or inhomogeneous (varying conductivity), the normalized impedance becomes highly inductive so that a high attenuation zone may exist in the ground wave field corresponding to a numerical distance with argument (phase) of around 51° (or argument of Z of around 70°).

Under equal propagation conditions (ground characteristics) and fixed frequency and distance, the numerical distance for horizontal polarization is greater than that for vertical polarization by a factor of $|\varepsilon_r - j60\sigma\lambda|^2$. Thus, even when propagation is over poor ground and the frequency is as high as 30 MHz (λ=10 m), the numerical distance for horizontal polarization is an order of magnitude (16 times) greater than the numerical distance for vertical polarization. This indicates that the attenuation for horizontal polarization is at least 20 dB greater than for vertical polarization. It is for this reason then that vertical polarization is usually preferred for ground wave transmission at frequencies in the HF band.

Summarizing, for a given polarization and frequency, curves of the ground wave propagation loss versus distance may be generated from Eqs. (2.1-2) through (2.1-10) and the universal curve (Fig. 2.1-4) of the surface wave attenuation factor versus numerical distance for the case of a flat homogeneous ground. Ground wave attenuation curves for the case of vertical polarization and propagation over poor ground, good ground, and sea water are given in Figs. 2.1-6 through 2.1-8 as a function of distance and for various frequencies.

2.2 Ground Wave Propagation over Irregular or Rough Terrain

The results of the previous section were obtained assuming a perfectly smooth boundary between the air and ground or water. However, these results can be also applied to the

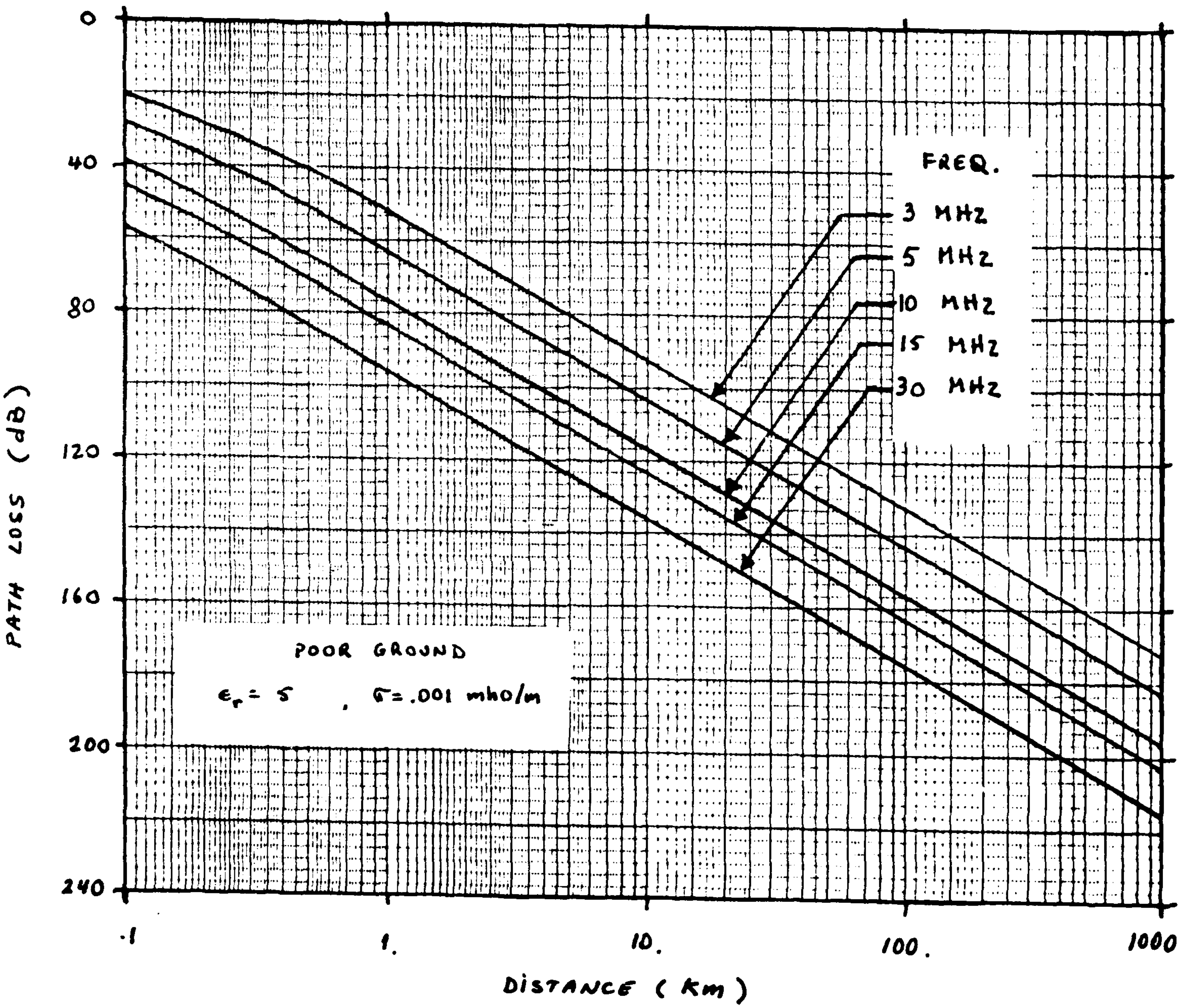

Fig. 2.1-6 Ground Wave Attenuation Over Poor Ground

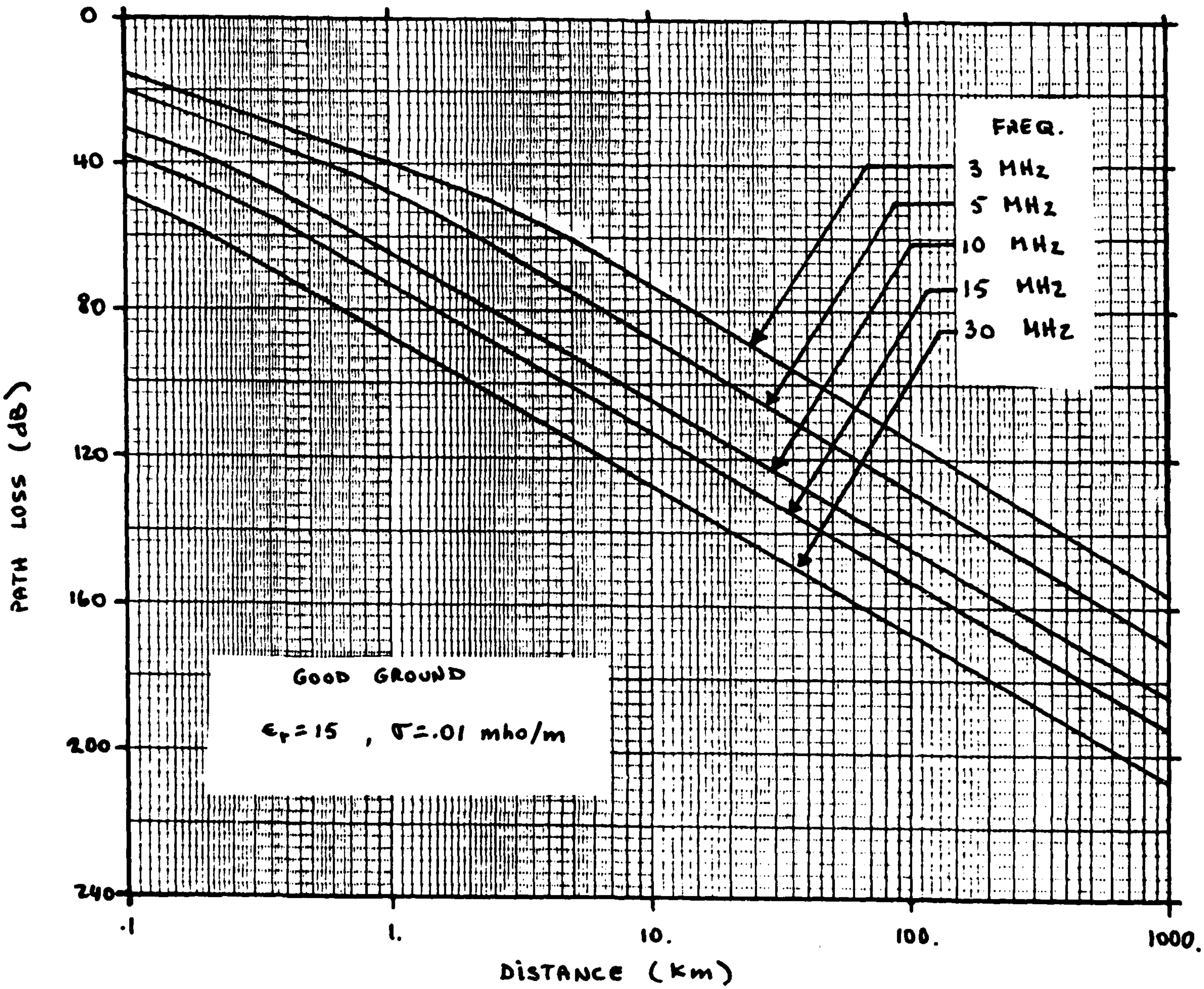

Fig. 2.1-7 Ground Wave Attenuation Over Good Ground

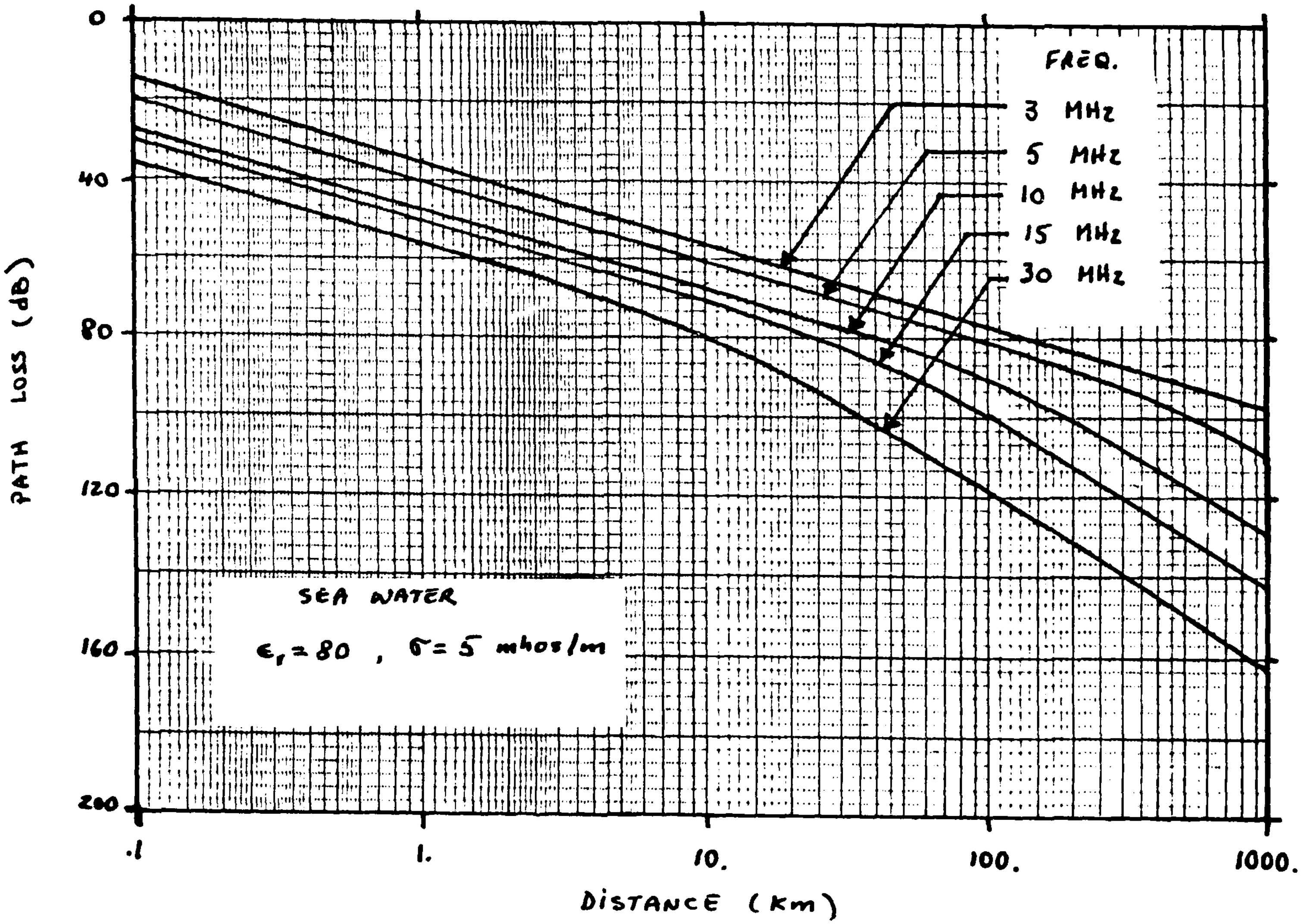

Fig. 2.1-8 Ground Wave Attenuation Over Sea Water

case of a rough or irregular terrain if the normalized impedance of the surface is suitably modified (i.e., Eq. (2.1-6)). Feinberg [1944] was the first one to show that the effect of small height irregularities (compared to the wavelength) was to decrease the apparent conductivity of the earth. However, details of his derivation were not provided and the effect of finite earth conductivity was not considered. Wait [1959] derived the effective impedance for a corrugated perfectly conducting surface. Later, Barrick [1971] derived the effective impedance of a rough surface of finite conductivity whose normalized (unmodified) surface impedance, Z, was smaller than unity, i.e., $Z \ll 1$. Hence, his results are applicable to vertically polarized surface wave propagation. Using a Fourier representation of the surface irregularities, Barrick [1971] shows that the modified effective impedance of a rough or irregular surface is given by:

$$\hat{Z} = Z + \frac{1}{4} \iint_{-\infty}^{\infty} F(p,q) W(p,q)\, dp\, dq \qquad (2.2\text{-}1)$$

where $\hat{Z}$ is the modified surface impedance, Z is the (unmodified) normalized surface impedance of the ground ignoring the irregularities (i.e., Eq. (2.1-6)), W(p,q) is the height spectral density of the surface which is defined in terms of the surface height $\xi(x,y)$ above the h=0 plane as

$$W(p,q) = \iint_{-\infty}^{\infty} < \xi(x,y)\xi(x',y') > \exp\{j(p\tau_x + q\tau_y)\} d\tau_x d\tau_y \qquad (2.2\text{-}2)$$

where $\tau_x = x-x'$, and $\tau_y = y-y'$. Thus, p and q have dimensions of inverse distance and W(p,q) is a spectral density. The function F(p,q) is a weighting function which is approximately given by (to first order in Z):

$$F(p,g) \simeq j\, p^2 k_o [(p+k_o)^2 + q^2 - k_o^2]^{-1/2} = jb \qquad (2.2\text{-}3)$$

where $k_o=2\pi/\lambda$.

When the normalized surface impedance $Z<<1$, the slightly rough or irregular surface can be conceptually replaced by a smooth flat surface at h=0 with effective impedance $\hat{Z}$ given by Eq. (2.2-1). Since W(p,q) is a spectral density, it is real and positive for all p and q. Hence, the modified surface impedance (to first order) has an additional term which is imaginary and positive when b is real and pure real and positive when b is imaginary. The former case represents a reactive contribution to $\hat{Z}$, whereas the latter is a resistive contribution.

The effect of a rough surface with spatial periods, 1/p and 1/q, all less than ℓ_o on propagating signals of varying frequencies is as follows. When the frequency of the propagating signal is such that $k_o=2\pi f/c<\pi/\ell_o<p,q$, the rough surface results in the addition of an inductive term to the effective impedance of the surface. When $k_o>\pi/\ell_o$, the effective impedance has both an additional resistive and an inductive component. Hence, at lower radio frequencies, a given rough surface will appear inductive, but at higher frequencies the resistive term will eventually increase until it is as large as the inductive term. An inductive contribution to the effective impedance may result in high attenuation areas if the argument (phase) of the effective impedance is around 70^o.

2.3 Ground Wave Propagation over an Inhomogeneous and Spherical Earth

The results of Sections 2.1 and 2.2 assumed a flat or plane earth as well as a homogeneous ground, i.e., constant conductivity and dielectric constant. When the distances involved are such that the curvature of the earth cannot be ignored and/or the ground conductivity and dielectric constant vary significantly along the propagation path (such as a mixed

sea-land path), then the surface wave attenuation factor may be computed using integral equations developed by Hufford [1952] and Ott [1971].

The integral equation obtained by Hufford [1952], which permits the calculation of the surface wave attenuation factor at a (great circle) distance, d, is given by:

$$g(d) = 1-e^{j\pi/4} \int_0^d [Z(r)+\psi]e^{-j2\pi\xi/\lambda} g(r) \sqrt{\frac{d}{\lambda r(d-r)}}\, dr \tag{2.3-1}$$

where g(d) denotes the complex surface-wave attenuation factor at a distance d, Z(r) is the normalized impedance of the ground which also varies with distance, and Ψ and ξ are defined in Fig. 2.3-1. The ratio of received power to transmitted power may be obtained by substituting g(d) for $F(w_o)$ in Eq.(2.1-10).

The integral in Eq. (2.3-1) expresses the attenuation factor at a range d in terms of its value at all ranges between zero and d. Obviously, it can only be solved numerically in a progressive manner. Causebrook [1978] and Monteath [1978] have developed a method for solving (2.3-1) numerically by dividing the profile into a set of N distances each of width D as shown in Fig. 2.3-1 and such that

$$G_N = \frac{1 - \sum_{n=1}^{N-1} Q_n I_n - Q_N A_N G_{N-1}}{1+Q_N} \tag{2.3-2}$$

where

$$Q_n = (Z_n+\psi_n)\exp\{-j2\pi\xi_n/\lambda\} \tag{2.3-3}$$

$$I_n = A_n G_{n-1} + R_n G_n \tag{2.3-4}$$

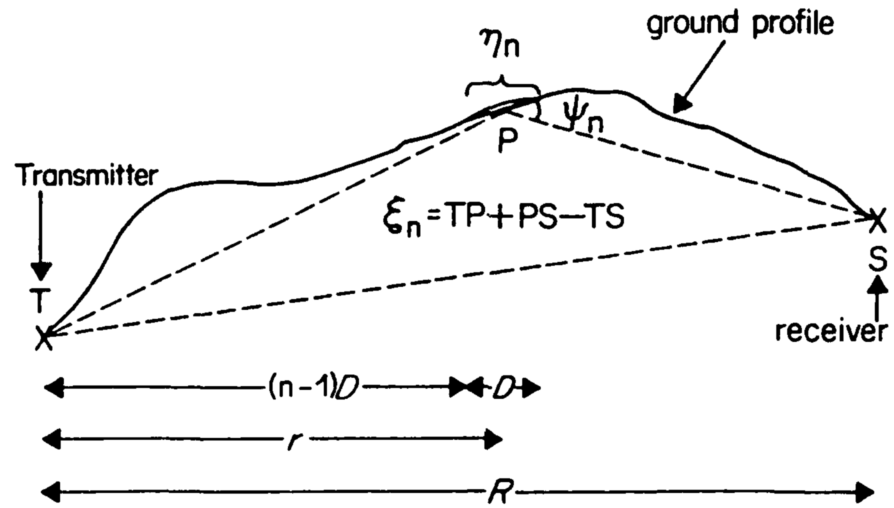

Fig. 2.3-1 Quantised Form of the Data Required for a Profile [from Causebrook, 1978]

The A_n and R_n are obtained analytically from

$$I_n = \int_{(n-1)D}^{nD} g(r) \sqrt{\frac{jND}{\lambda r(ND-r)}}\, dr \qquad (2.3\text{-}5)$$

assuming that g(r) varies linearly with r for $n \geq 2$. For n=1 g(r) is given by Eq. (2.1-4).

The interval distance, D, required for accurate computation of the surface wave attenuation depends on the desired accuracy at the extreme range of the computation. For a given accuracy smaller calculation intervals are required for spherical earth calculations than for a plane earth. The maximum permissible interval decreases as the magnitude of the attenuation factor decreases and as its phase increases. A good rule of thumb for picking the interval distance is [Monteath, 1978].

$$D < \frac{2R^2\lambda}{9d_{max}^2} \qquad (2.3\text{-}6)$$

where d_{max} is the maximum range for the computation and R is the "effective radius" of the earth (including refractive bending effects). If a plane-earth model is used then the interval distance can be picked to be 3 times greater than that given by (2.3-6).

Another integral equation which permits the calculation (numerical) of the surface wave attenuation is that derived by Ott [1971]. This integral equation is closely related to the Sommerfeld surface wave attenuation function, F(w), discussed in Section 2.1 and is given by

$$g(d) = F(d,o) - \sqrt{\frac{j}{\lambda}} \int_o^d g(r) e^{-jkw(d,r)} \{h'(r)F(d,r) - \frac{h(d)-h(r)}{d-r} + (Z-Z_r)\} \sqrt{\frac{d}{r(d-r)}}\, dr \qquad (2.3\text{-}7)$$

where g(d) is the surface wave attenuation factor (relative to free-space), F(d,r) is closely related to the Sommerfeld surface attenuation factor, and is defined as

$$F(d,r) = 1-j\sqrt{\pi p}\; e^{-u}\; \mathrm{erfc}(j\sqrt{u}) \qquad (2.3\text{-}8)$$

$$p = -j\; \frac{\pi Z^2 (d-r)}{\lambda} \qquad (2.3\text{-}9)$$

$$u = p\; \{1- \frac{h(d)-h(r)}{Z(d-r)}\} \qquad (2.3\text{-}10)$$

$$w(d,r) = \frac{[h(d)-h(r)]^2}{2(d-r)} + \frac{h^2(r)}{2r} - \frac{h^2(d)}{2d} \qquad (2.3\text{-}11)$$

The function h(r) is the terrain profile along the propagation path and h'(r) is its derivative. The factor $(Z-Z_r)$ arises in mixed-path problems. That is, Z_r is constant with distance and is defined as the normalized surface impedance near the transmitter. The factor Z varies with distance in a mixed path (inhomogeneous ground) problem. The variation of Z with r may be continuous or it may contain abrupt changes. The factor $(Z-Z_r)$ is zero for a homogeneous path, so that the integral in (2.3-7) may be interpreted as the correction factor to the Sommerfeld attenuation factor F(d,o) due to terrain variations. This equation is particularly effective for computing the additional losses introduced by mountain ridges and other large terrain variations. Methods of solving the integral equation by numerical techniques may be found in [Ott, 1971].

2.4 Ground Wave Propagation in Built-up Areas

The results presented for ground wave propagation over irregular and inhomogeneous terrain can also be applied to urban and suburban (built-up) areas. Causebrook [1977,1978] has made use of the concept of 'effective impedance' for the characterization of built-up areas and to calculate ground wave attenu-

ation at frequencies between 900 kHz and 2 MHz. The use of effective impedance will yield good average values for received field strength at distances sufficiently away from the perturbed surface (far field). But field distribution very near this surface, i.e., within a built-up area will show strong local variations, especially at frequencies where the wavelength is in the order of the building heights (i.e., HF) and will therefore in general deviate substantially from expected values.

Man-made structures, such as lamp-posts, steel-framing, wiring and plumbing may be considered as grounded parasitic monopoles, which carry induced currents in the presence of an electric field. Causebrook [1977] has derived the "effective impedance" of a built-up area by considering the effect of man-made structures as forming a 'bed of nails'. In highly built-up areas, he also makes an analogy to grooves cut in a highly conductive surface (buildings) exposing poorer conductivity at the ground (streets). If B is the fraction of an area in question which is covered by buildings, Causebrook's [1977] analysis gives the effective surface impedance as a function of mean building height, H, and building density B for the case of vertically polarized waves as:

$$Z(H) = Z(o)+j\frac{2\pi H}{\lambda}\left[1-\frac{1}{10B}\ln(1+10B)\right], \quad B<.3$$

$$Z(H) = (1-B)\left[Z(o)+j\frac{\pi H}{\lambda}\right], \quad .3\leq B<1 \qquad (2.4\text{-}1)$$

where Z(0) is the normalized surface impedance at ground level and Z(H) is the value at a level H which is the height taken for the structures. Equation (2.4-1) indicates that the effective surface impedance in a built-up area requires an extra imaginary term in the presence of buildings. Thus a built-up area can be conceptually replaced by a smooth flat surface (as long as B and H do not change very much over the range of interest) at H=0

with effective impedance Z(H) given by (2.4-1). The average (expected) ground wave propagation loss may then be computed according to the theory of Section 2.1. If the terrain is highly irregular and/or the mean building height, H, and the building density change considerably over the range of interest, then Z(H) may be used to calculate the inhomogeneous surface wave attentuation factor using the integral equations described in Section 2.3.

2.5 Prediction of Ground Wave Received Signal Level

The theories described in Sections 2.1 through 2.4 permit the computation of the ground wave attenuation versus distance not only for areas of constant (although maybe modified) surface impedance but also for a continuously varying impedance. However, these theories do not account for off-axis scattering terms which may be present especially in the case of ground wave propagation in built-up areas between elevated antennas. It is likely that off-axis scattered fields would contribute an additional random component to the total received field. Currently, there is no information in the literature regarding the statistics of HF ground wave signals in built-up areas. However, if the off-axis scattered field is made up of multiple reflected waves as is the case at VHF and UHF, then the scattered field would exhibit complex Gaussian statistics, i.e., its envelope would be Rayleigh distributed and its phase would be uniformly distributed. Furthermore, if we regard the surface wave field as a steady (non-fading) sinusoidal component, as is normally assumed, then the envelope of the received signal would have Rice-Nakagami statistics. Its envelope would have probability density given by [Beckmann, 1967]

$$p(R) = \frac{R}{\sigma^2} \exp\left[-\frac{1}{2\sigma^2}(R^2+A^2)\right] I_o\left(\frac{AR}{\sigma^2}\right), \quad R \geq 0 \qquad (2.5\text{-}1)$$

where

- R is the amplitude of the received signal.
- A is the amplitude of the steady surface wave component
- σ is the rms value of the scattered component
- $I_o(x)$ is the modified Bessel function of the first kind and zero order.

When the scattered field is weak compared to the surface wave component, i.e., $A^2/2\sigma^2 >> 1$, then

$$p(R) \simeq \delta(R-A) \qquad (2.5\text{-}2)$$

which is the commonly made assumption when dealing with ground wave propagation at low frequencies and at HF in open terrain. On the other hand, if the scattered field component is strong compared to the surface wave component, as is the case at VHF and especially UHF, i.e., $A^2/2\sigma^2 << 1$, then

$$p(r) \simeq \frac{R}{\sigma^2} \exp\ [-R^2/2\sigma^2] \qquad (2.5\text{-}3)$$

which is the Rayleigh density function. Plots of the density function of (2.5-1) are given in Fig. 2.5-1, as a function of the ratio A/σ.

The ground wave received signal level is thus completely specified by the received specular (or surface wave component) power, $P_r=A^2$, and the surface wave-to-scattered field ratio, $A^2/2\sigma^2$. The surface wave received power can be predicted according to the formula

$$P_r = P_o(f,d) - A_m(f,d) + H_t(h_t,f) + H_r(h_r,f) \qquad (2.5\text{-}4)$$

where all quantities are in dB and

- P_o is the power received if we assume free space transmission as given by Eq. (2.1-2)

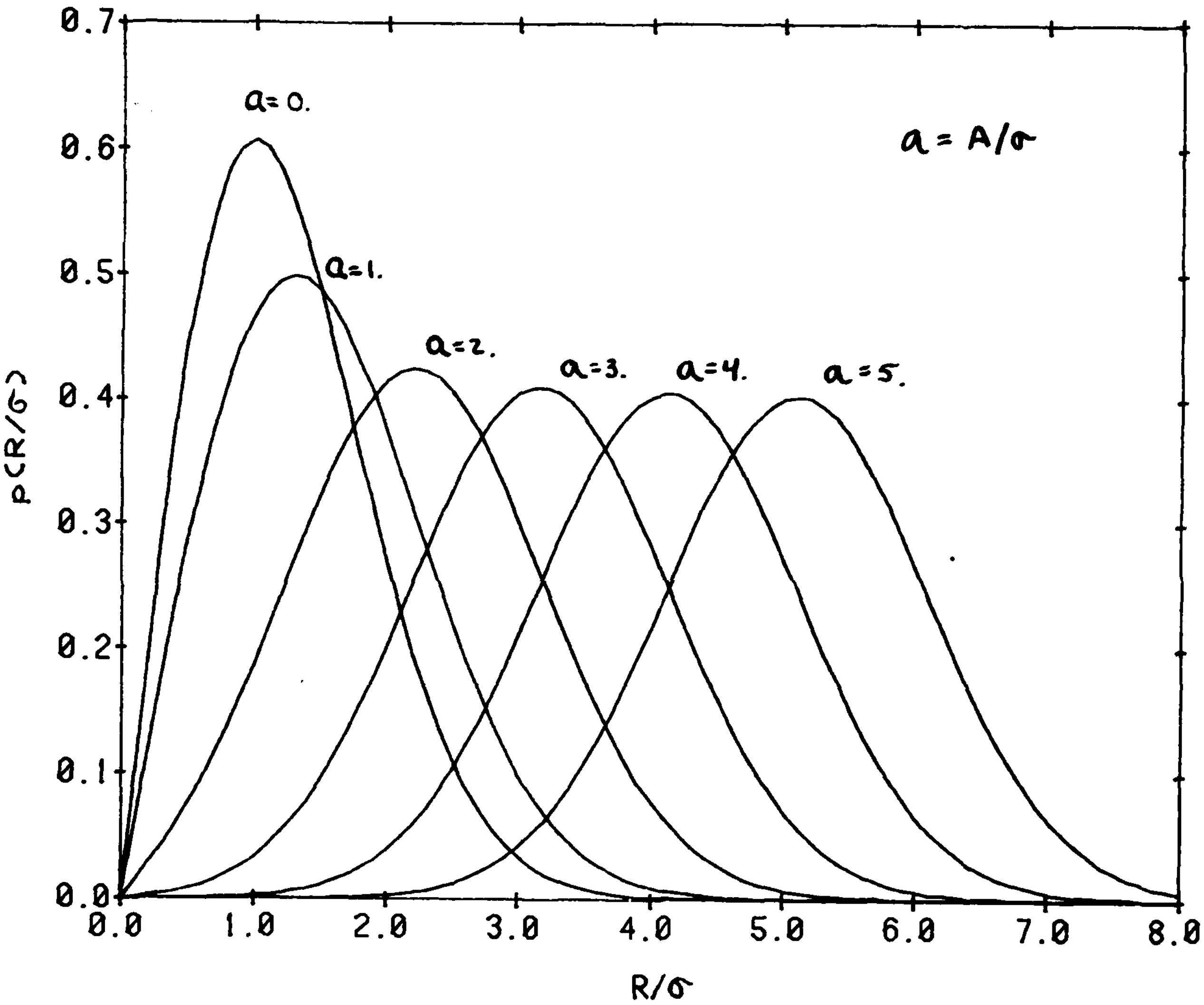

Fig. 2.5-1 Normalized Nakagami-Rice Density Function

$A_m(f,d)$ is the attenuation of the surface wave relative to free-space attenuation in a built-up area characterized by its effective surface impedance. In the case of vertically polarized waves, the effective surface impedance is given by Eq. (2.4-1). The attenuation factor $A_m(f,d)$ is defined below and varies depending on whether we are dealing with homogeneous (flat terrain) or inhomogeneous (irregular terrain or varying building density) ground.

$H_t(h_t,f)$ and $H_r(h_r,f)$ are height-gain factors expressed in dB and account for the effects of antenna elevation. They are local terrain dependent and are defined by Eq. (2.1-13).

When the terrain is homogeneous (flat and constant ground conductivity) the attenuation factor $A_m(f,d)$ is defined as:

$$A_m(f,d) = -20 \log_{10}[2F(w_o,Z)] \qquad (2.5\text{-}5)$$

where $F(w_o,Z)$ is the Sommerfeld surface wave attenuation factor defined in Eq. (2.1-4), w_o is the numerical distance at grazing incidence defined in Eqs. (2.1-2) and (2.1-6), and Z is the effective surface impedance defined in Eq. (2.4-1). For a given distance d, and impedance, Z, $F(w_o,Z)$ may be determined from Fig. 2.1-4.

If the terrain is highly irregular and/or the ground conductivity changes (continuously or abruptly) throughout the propagation range, then the attenuation factor $A_m(f,d)$ is defined as:

$$A_m(f,d) = -20 \log_{10}[2g(d)] \qquad (2.5\text{-}6a)$$

where g(d) is the surface wave attenuation defined by the integral equations (2.3-1) or (2.3-7). Note that if Eq. (2.3-7) is used, then (2.5-6) may be rewritten as:

$$A_m(f,d) = -20 \log_{10}[2F(w_o,Z)] -20 \log_{10}(1-x) \qquad (2.5\text{-}6b)$$

where x is the ratio of the integral in Eq. (2.3-7) to the first term $F(d,0)=F(w_o,Z)$. Since $F(w_o,Z)\leq 1$ when $0<x<1$ (2.5-5) and (2.5-6) are positive, the second term in (2.5-6b) represents the excess loss due to terrain irregularities and/or inhomogeneous paths. If the excess loss is due to the curvature of the earth or terrain irregularities such as mountain ridges, then the second term in (2.5-6b) is entirely analogous to the diffraction losses encountered at VHF and UHF and maybe computed in a similar manner [e.g., see Ehrman, 1977]. However, if the second term is due to changes in the conductivity of the ground along the propagation path, then it must be computed from Eq. (2.3-7) using numerical techniques described in [Ott, 1971].

The ratio of specular to scattered power, $A^2/2\sigma^2 = P_r/2\sigma^2$, has yet to be determined and may be significant in built-up areas especially at the high end of the HF band and when the antennas are elevated above the ground. If the scattered component is significant, then the received signal will exhibit fading. If the fading rate of the scattered field is f_s (for a description of the scattered field, see Ehrman, 1977), then the average number of fades of the amplitude of the received signal below a level R per unit time is given by the following [Rice, 1948]:

$$N(R) = f_s \frac{R}{\sigma} \sqrt{2\pi} \exp\left[-\frac{R^2+A^2}{2\sigma^2}\right] I_o\left(\frac{RA}{\sigma^2}\right) \qquad (2.5\text{-}7)$$

Note that as the ratio of specular (surface wave) to scattered power ratio, $A^2/2\sigma^2$, increases the average number of fades below level R per unit time decreases exponentially. If

$A^2/2\sigma^2>4$, it is negligible for any value of R so that no fading is observed.

The expected fade duration (below level R) is given by [Halpern, 1977]

$$T(R) = \frac{1}{N(R)} \int_0^R p(r)dr$$

$$= \frac{1}{f_s(\frac{R}{\sigma})\sqrt{2\pi}\; I_0(\frac{RA}{\sigma})} \sum_{n=1}^{\infty} (\frac{R}{A})^n \; I_n(\frac{RA}{\sigma^2}) \qquad (2.5\text{-}8)$$

which is negligible when R<A/2 and $A^2/2\sigma^2>>1$.

2.6 Skywave Propagation

Long distance HF propagation is mainly via the ionospneric-skywave mode. Signals propagated via this mode are unstable compared with ground wave propagated signals, for the strength of the ionospheric signals is dependent upon many factors related to the condition of the ionosphere which generally varies from hour to hour, day to day, and season to season. Reliable communications for a given circuit can generally be obtained if the operating frequency lies between a lower (LUF) and a maximum usable or operational (MUF) frequency limit. For a given path, these frequency limits are determined by the ionospheric characteristics at a given time.

2.6.1 Optimum Operating Frequency

Ionospheric propagation is influenced by the presence of four ionized layers, identified as the D, E, F_1 and F_2 layers. Their heights and ionization levels are closely related to solar radiation so that there are important diurnal variations (day versus night) and seasonal variations which are

related to the relative position of the sun. At HF the D-layer acts primarily as an absorbing medium and is not a significant reflecting layer. The F_1-layer, which is of low ionization, is closely associated with the E-layer and is seldom distinguishable from the E-layer. Thus, reference to the F_1-layer is seldom made, and the term F-layer implies the F_2-layer. Consequently, ionospheric reflection of HF signals is due almost wholly to the presence of the E-layer and the F-layer.

The critical frequency for a layer is the maximum frequency for which a vertically incident wave reflects from that layer. Signals transmitted at frequencies above the critical frequency will penetrate the layer and may reflect from higher layers. Accordingly, the critical frequency of the F-layer is always higher than the critical frequency of the E-layer. A frequency which is not reflected from a given ionospheric layer at vertical incidence may, however, be reflected from that layer when a more grazing oblique incidence is used. The maximum frequency that can be reflected for a given angle of incidence on a layer, and corresponding to a given distance between transmitter and receiver, is called the maximum usable frequency or MUF. The MUF is minimum for a vertically incident signal and increases with decreasing grazing angle (or with increasing angle of incidence on the layer). Since the grazing (i.e., elevation) angle decreases with increasing transmitter-receiver separation, the MUF increases with increasing transmitter-receiver separation. Thus, a signal at some given frequency above the critical frequency of a layer will be reflected by the layer at all grazing angles less than some maximum angle. This results in reception of the signal at receiver distances beyond some minimum distance called the skip-distance. The important point we are making here is that for a given transmitter-receiver separation there corresponds an

MUF. Communication at a given distance using a signal frequency nearly equal to the MUF for that distance (i.e., skip-distance) can also be achieved at greater distances (skip-zone) but not at lesser distances.

The LUF is determined in part by ionospheric absorption which results in attenuation of the signal below a usable level. Ionospheric absorption is caused principally by passage of the transmitted signal through the D-layer, and the resulting attenuation increases with decreasing frequency. In general, to minimize absorption, the signal carrier frequency must be adjusted as close to the MUF as conditions existing at any time will permit. Unlike the MUF, the LUF is not a critical frequency and does not depend totally upon the condition of the ionosphere. The LUF is the lowest frequency that will give satisfactory reception, i.e, sufficient SNR at the receiver, and is affected by transmitted power, antenna gains, receiver sensitivity, path loss, etc. Operating at a signal below the LUF is possible but results in degraded performance (e.g., higher error rates with digital communications, or lower reliability with analog transmission). With sufficiently high transmitting power and/or antenna gains, the increased ionospheric absorption at relatively low frequencies may be overcome resulting in low values of LUF. The usable bandwidth determined by the LUF and the MUF is an important parameter in a system which uses wideband (spread spectrum) signals for a low probability of intercept or for interference rejection.

In order to minimize ionospheric attenuation and fading due to multipath, the optimum operating frequency for HF skywave propagation is usually close to the MUF. How close the optimum operating frequency should be to the MUF is determined by the bandwidth of the transmitted signal. For narrowband (3-6 kHz) systems, the optimum operating frequency (FOT) for a

given time of day and season, is defined as the maximum frequency having ionospheric support on 90% or more of the days during the month. For broadband systems, the optimum operating frequency must be sufficiently below the MUF so that all frequencies in the band have ionospheric support on 90% or more of the days during the month. If the MUF were invariant, it would be a simple matter to set the operating frequency according to the guidelines described above. In actuality, the MUF is highly variable and must be treated statistically.

The variability of the MUF is closely related to the variability of the ionosphere. Conditions of the ionosphere vary throughout the day with the angle of the sun (solar zenith angle). In addition, they also vary with the season of the year, and vary in synchronism with the eleven-year sunspot cycle. The MUF increases with transmitting distance, is higher during the daylight hours, and increases as the sunspot number (SSN) increases. Although the MUF changes with the season, the changes are somewhat dependent upon the geographic location and local time. In general, the daytime MUF tends to be higher in the winter than in the summer, while the nighttime MUF is slightly higher in the summer than in the winter. Values of the SSN range from about 5 during lows to approximately 100 to 130 during the highs. A new low interval started in the year 1976.

Computer programs are used in system design to predict the MUF, optimum frequency and available signal-to-noise ratio for particular HF paths based upon transmitted power and antenna characteristics. One such program is the OT/ITS HFMUFES-4 [1976] program for predicting the performance of HF skywave telecommunication systems. Figure 2.6-1 shows the diurnal variation in the monthly median value of the MUF for several single-hop distances, and SSN=110. The trends shown in the figure are consistent with what might be observed anywhere

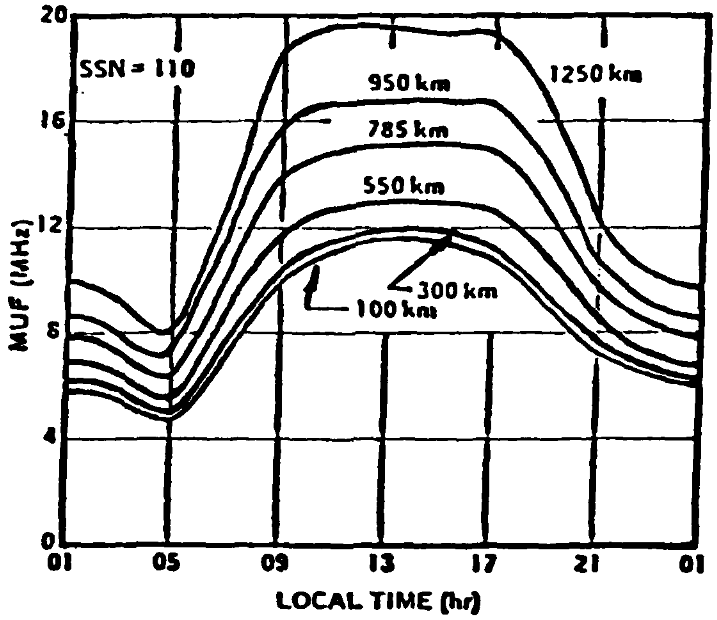

Fig. 2.6-1 Diurnal Variation of the Maximum Usable Frequency as a Function of Distance (from Sykes, et al., 1975)

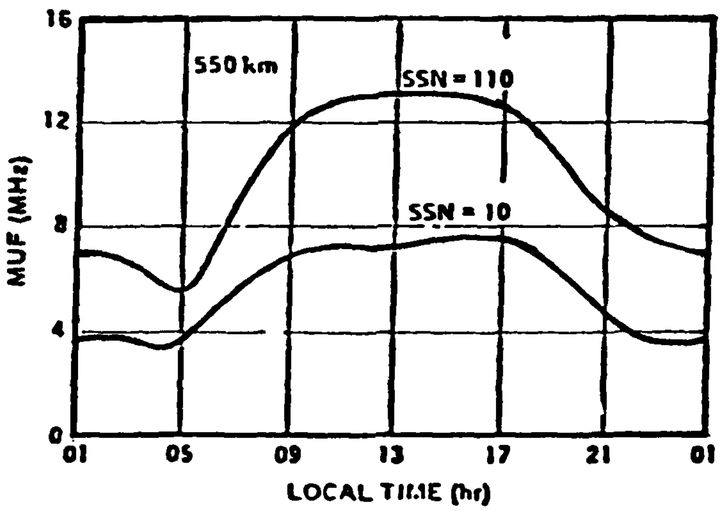

Fig. 2.6-2 Diurnal Variation of the Maximum Usable Frequency for High and Low Sunspot Numbers (from Sykes, et al., 1975)

in the world. The greatest diurnal variation in the MUF occurs at the longest distance with most of the change occurring during sunrise and sunset. Figure 2.6-2 shows the diurnal variation of the MUF at a distance of 550 Km for both high and low sunspot numbers. Note that the MUF for SSN=110 is about 1.7 times that for SSN=10 for all hours of the day.

In addition to the somewhat regular or normal variations in the ionosphere there are occasional irregular and unpredictable variations generally referred to as sudden ionospheric disturbances. These disturbances generally last from about ten minutes to an hour and result in extremely high absorption causing a loss of signal or fade out. The disturbances occur simultaneously throughout the portion of the earth illuminated by the sun; they do not occur at night. Another type of disturbance is the ionospheric storm wherein the ionosphere deviates from its normal layer stratification and becomes turbulent. These storms generally result in erratic communications and usually require the use of a lower operating frequency to prevent outage. The effects of ionospheric storms are greater near the polar regions and are somewhat predictable in short-term forecases available internationally from NOAA.

2.6.2 Multipath Fading in Skywave Propagation

When the operating frequency is below the MUF, skywave propagation results in multiple propagation paths, each with different propagation times, attenuation and Doppler shifts. The multipath is a consequence of energy radiated at different elevation angles being reflected from different layers in the ionosphere, and also from multihop propagation. Thus, in general, the received skywave field is of the form

$$E_S(f,t) = E_o e^{j2\pi ft} \sum_{n=1}^{N} c_n(t) \exp\{-j2\pi(ft_n - V_n t\} \quad (2.6\text{-}1)$$

where E_o is the field that would be received at an equivalent distance in free space at an operating frequency f, assumed to be below the MUF, t_n is the time delay of each ionospheric return, V_n is the Doppler shift of each return and $c_n(t)$ is the time varying attenuation of each return relative to the free space attenuation E_o. The number of ionospheric returns depends on the operating frequency, transmitter-receiver separation and time of day. If the transmitter and receiver are sufficiently close, the received signal described by (2.6-1) includes the ground wave signal discussed earlier.

The presence of multiple returns in the skywave field results in fading and the fading rate is determined by the relative Doppler shifts of the various returns. The Doppler shifts of the individual returns are related to diurnal changes in the ionization levels in the various layers as well as the heights of the layers. A model which relates the Doppler shifts and path delays to the various parameters of a two-layer ionosphere are discussed in [Malaga, et al., 1978]. Typical fading rates (Doppler spread), which are well within observed values, are given in Figure 2.6-3 for various times of day for a 3000 km link. Note that for a fixed frequency below the MUF, the Doppler spread is greatest at sunrise (and sunset) and decreases so that at noon it is negligible. Figure 2.6-4 shows the Doppler spread for various transmitter-receiver separations at a local time of 900 hrs. These curves show that the MUF increases with distance as discussed earlier. However, as the operating frequency approaches the MUF, the fading rate (Doppler spread), B_D, approaches zero. The reason is that at the MUF, there is only one skywave return. At frequencies close to the MUF, the fading rate is slow (~1 Hz).

When the delay differential between the last and first ionospheric returns or the ground wave (multipath spread) is

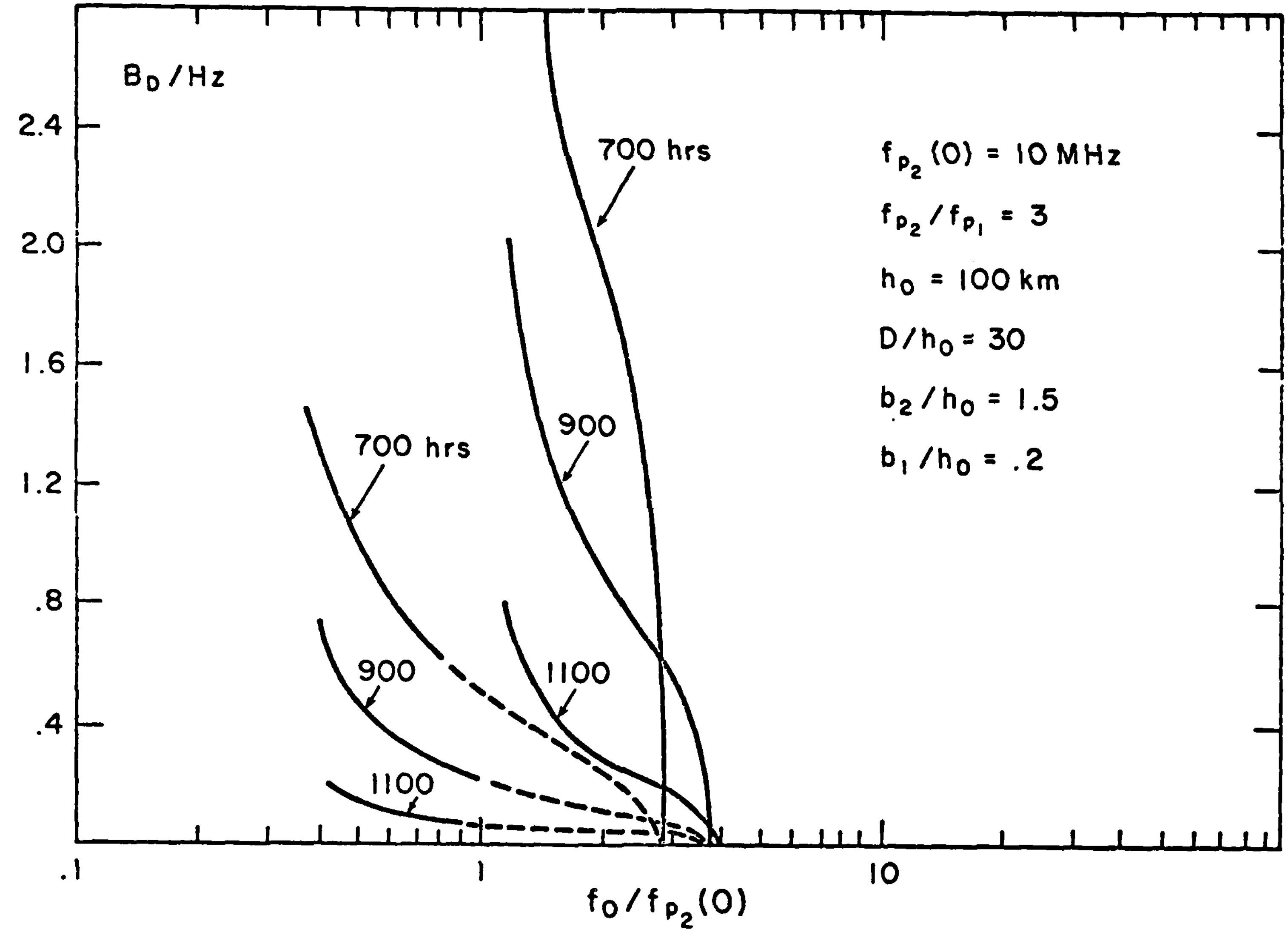

Fig. 2.6-3 Doppler Spread (Fade Rate) as a Function of Carrier Frequency for Various Local Times (from Malaga, 1978)

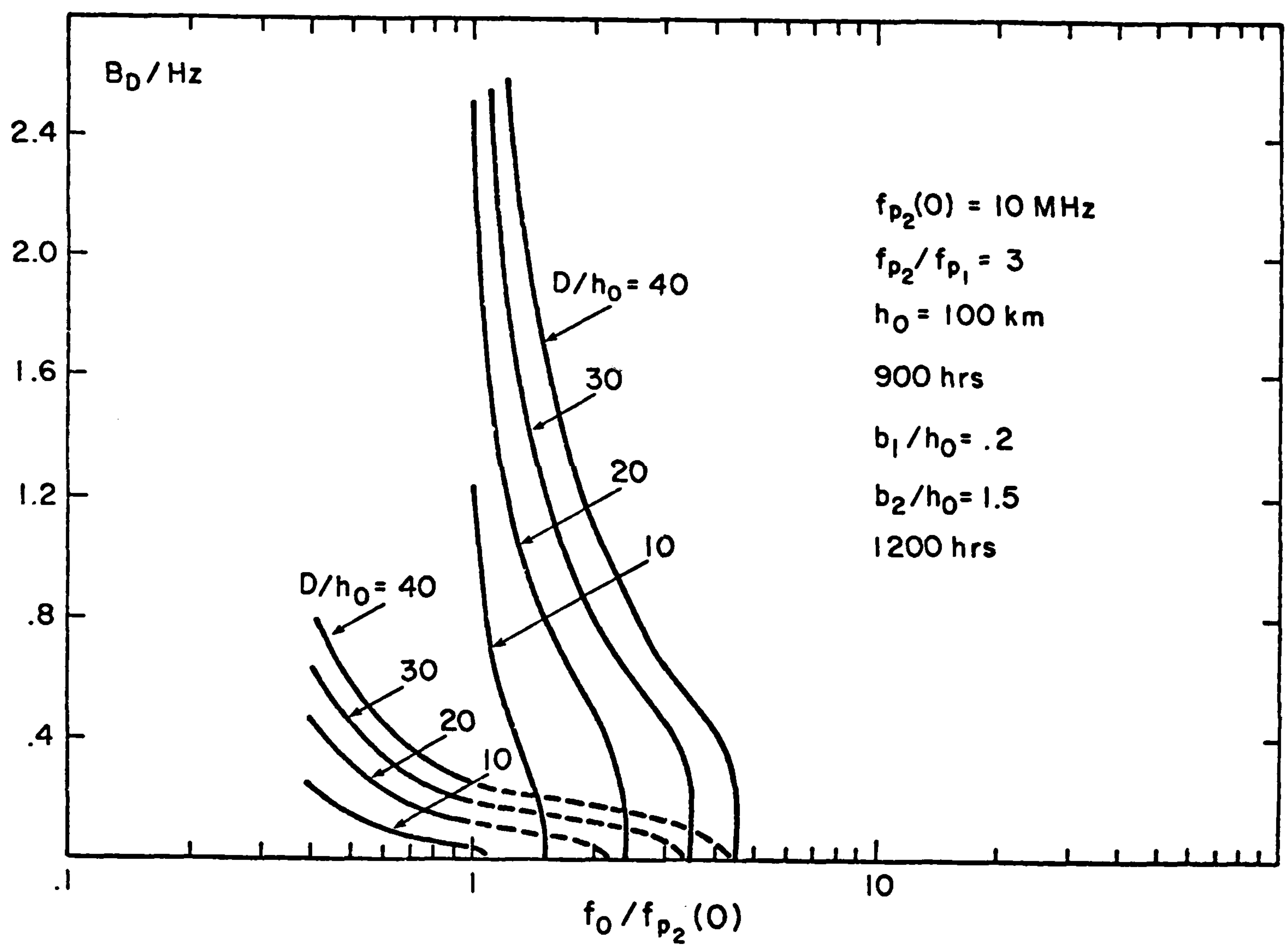

Fig. 2.6-4 Doppler Spread (Fade Rate) as a Function of Carrier Frequency for Various Transmitter-Receiver Separations (from Malaga, 1978)

greater than the inverse of the bandwidth of the transmitted signal, the multipath fading is frequency selective, that is the various frequency components in the transmitted signal fade independently. This effect results in severe distortion of analog signals and large error rates in digital signal transmission. Typical values of the multipath spread for various times of the day (3000 km link) are shown in Figure 2.6-5 and for various transmitter-receiver separations in Figure 2.6-6. These curves show that the multipath spread for HF skywave propagation is typically in the order of 1 msec or less at frequencies below the MUF. The inverse of the multipath spread is the coherence bandwidth which is a measure of the maximum frequency separation for which two transmitted frequencies will still be strongly correlated after reflection from the ionosphere. Thus, the coherence bandwidth for HF skywave transmission is typically in the order of a few kHz at frequencies below the MUF. This implies that SSB-AM signals (3 kHz bandwidth) might exhibit flat-fading rather than frequency selective fading under certain conditions. However, wideband HF signal transmission will always exhibit frequency selective fading.

2.6.3 Prediction of Skywave Received Signal Level

As discussed earlier, the skywave received signal level at a frequency below the MUF is a function of the SSN, season, geographic location, time of day and frequency. For a given frequency and any specified time, the median received skywave signal level in dBW (dB above 1 watt) is given by:

$$P_r = P_t + G_t + G_r - L(f,t) \qquad (2.6\text{-}2)$$

where

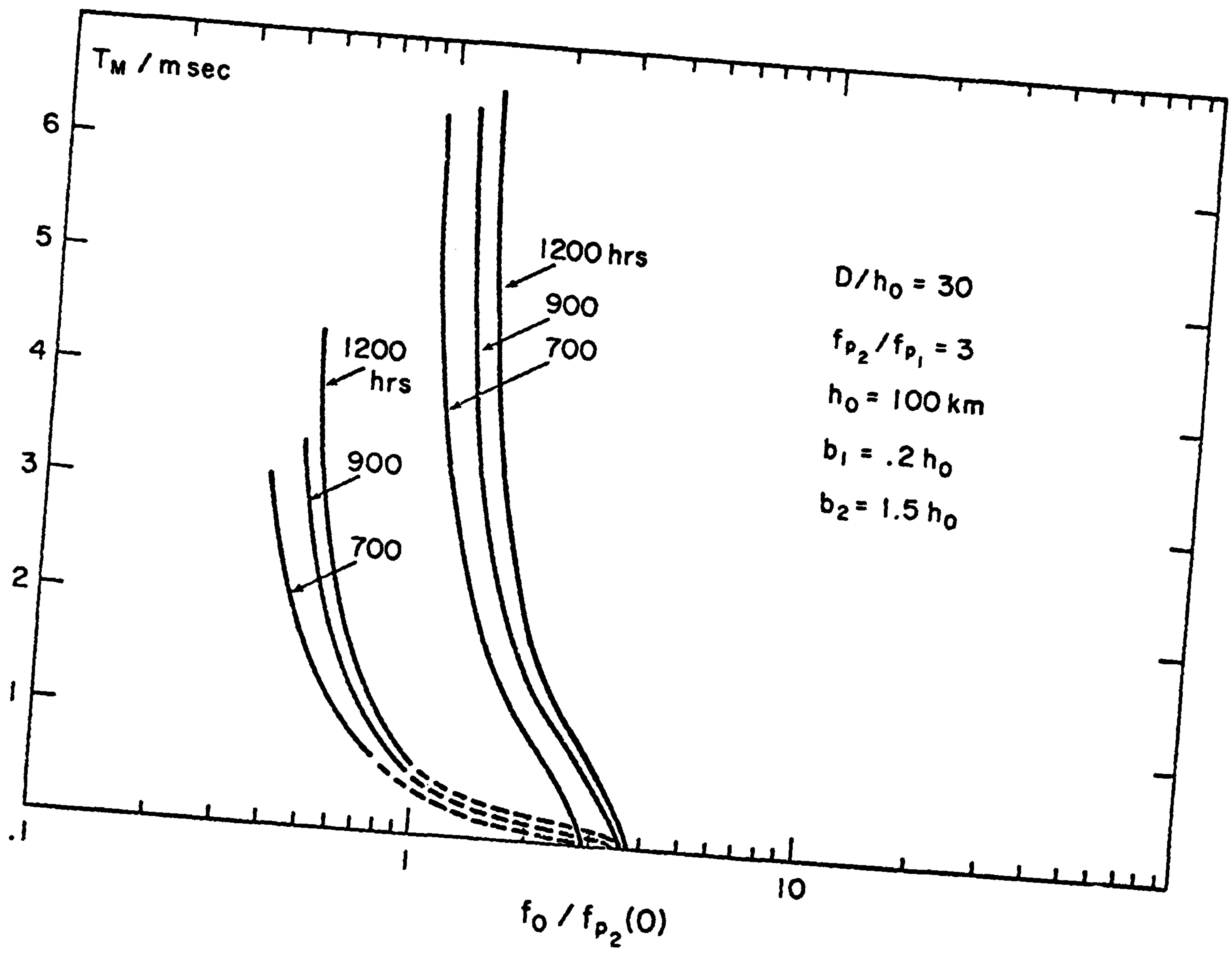

Fig. 2.6-5 Discrete multipath spread vs. carrier frequency at different times of the day (from Malaga, 1978)

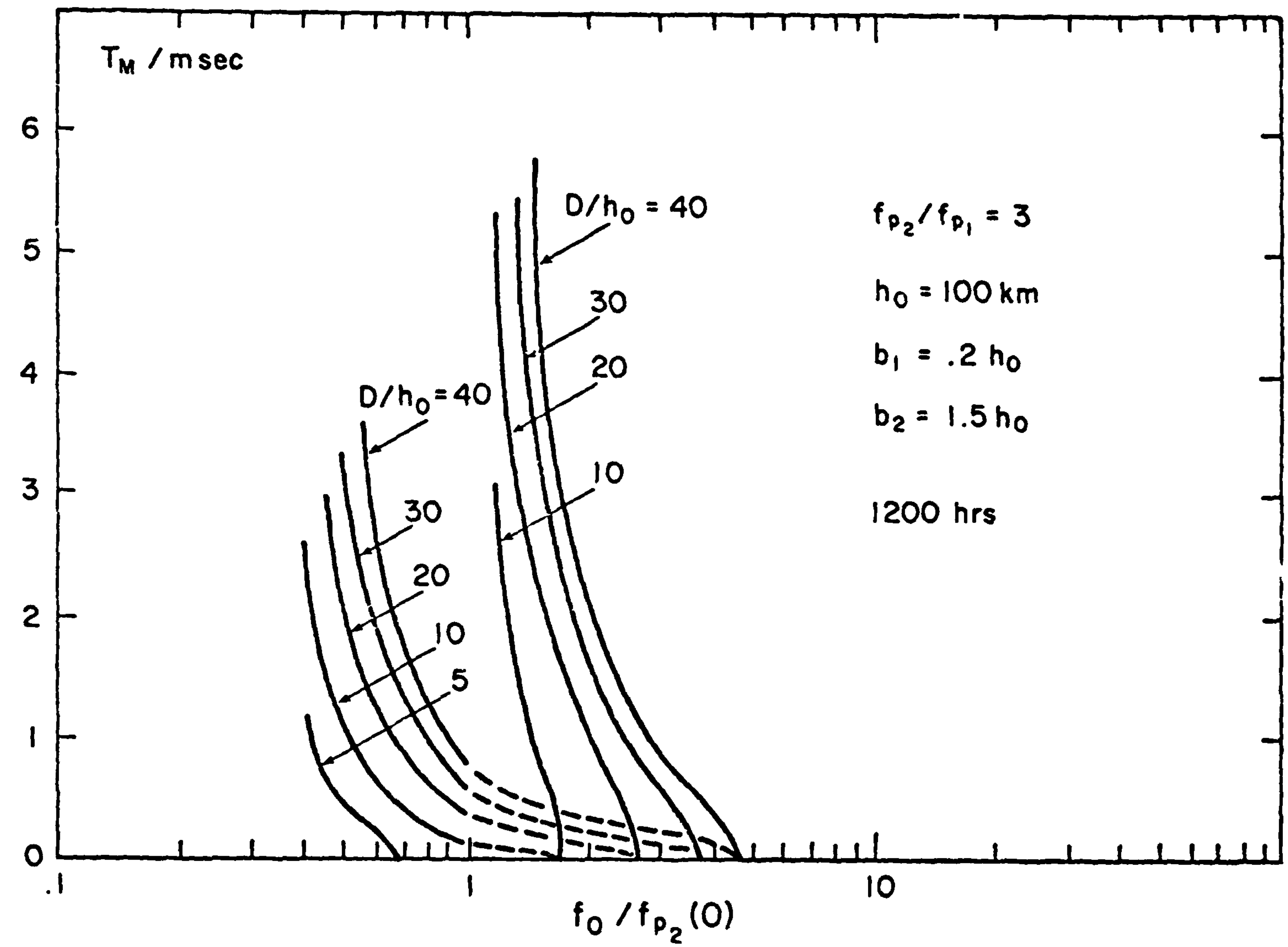

Fig. 2.6-6 Discrete multipath spread vs. carrier frequency for various transmitter-receiver separations (from Malaga, 1978)

P_t = transmitter power delivered to antenna input (dBW)

G_T = power gain of transmitting antenna (dB) in direction of propagation path relative to isotropic antenna in free space.

G_r = power gain of receiving antenna (dB) in direction of propagation path relative to isotropic antenna in free space.

L = total attenuation in the propagation path (dB) defined below.

The total path attenuation, L, is calculated for the specific propagation path at the operating frequency and is composed of four major loss mechanisms:

$$L = L_F + L_A + L_G + L_P \qquad (2.6\text{-}3)$$

where L_F is the free space transmission loss expected between ideal, loss-free, isotropic, transmitting and receiving antennas in free space which represents the major loss mechanism. For a single-hop transmission, the path length, D, between transmitter and receiver is the length of the path the signal travels from the transmitting antenna to the most probably reflecting layer and back to the receiving antenna. The free-space loss depends on the frequency (and wavelength) and path length as follows:

$$L_F = 20 \log_{10}(4\pi D/\lambda) \qquad (2.6\text{-}4)$$

Under certain conditions, the second major loss is the absorption loss (L_A) resulting from passage of the signal through the D-layer. L_A is calculated from a semi-empirical formula using the following variables: geographic latitude of

the reflection point, sunspot number (SSN), solar zenith angle at a particular time and season, angle of incidence of the signal ray path on the reflecting layer, gyrofrequency, winter anomaly factor, number of hops and operating frequency. During the night when solar zenith angle is much greater than 90^{o}, the ionospheric absorption loss becomes insignificant. A formula relating all these factors is given by Barghausen, et al., [1969]:

$$L_A = \frac{286(1+.0087\ x_n)(1+.005S)(\cos \chi)\ N \sec \phi}{\nu^2/4\pi + (f+f_H)^2} \qquad (2.6\text{-}5)$$

where

x_n	=	geographic latitude in degrees measured positive from the equator.
S	=	smoothed 13-month sunspot number
χ	=	solar zenith angle
ϕ	=	angle of incidence of radio signal measured from vertical
ν	=	collision number (=20 at 63 km altitude)
f	=	operating frequency in MHz.
f_H	=	gyro frequency at absorbing height in MHz (1 MHz)
N	=	number of hops.

The third major loss (L_G) applies only to multiple-hop propagation involving reflection of the radio wave from the earth's surface and depends on the reflection coefficients (conductivity and dielectric constant) of the ground at the point of reflection and the take-off angle of the ray above the horizon. A fourth loss factor (L_p) is the excess system loss

which is included to account for the day to day variations in the ionospheric conditions (e.g., SSN) from the monthly median and includes other losses not explicitly attributable to the three major loss mechanisms. The excess system loss includes such factors as ionospheric focusing, deviative absorption (when operating very close to the MUF), polarization losses, and the contribution of signals from different paths.

A detailed explanation of the median propagation loss factors is presented along with expressions for calculating the individual major loss terms in a report by Barghausen, et al., [1969]. This reference is the basis for the revised OT/ITS long term ionospheric prediction program [Haydon, et al., 1976].

The skywave received signal level fluctuates randomly (with a median value given by (2.6-2)). The statistics of these fluctuations have been found to be Rayleigh (Eq. (2.5-3)) distributed [Shaver, et al., 1967] if no ground wave component is present. When the ground wave is of comparable strength to the skywave field, the statistics of the ground wave plus skywave field are given by the Rice-Nakagami distribution (see Eq. (2.5-1)).

2.7 Atmospheric and Man-Made Noise at HF

The required signal strength for satisfactory HF communications depends to some extent on the receiver's sensitivity and noise factor, but is strongly dependent upon the external noise at the receiving antenna. The three types of noise with which the HF signal must contend are galactic, atmospheric and man-made; of these, the latter two predominate at HF. The average power of man-made noise varies over a wide range, more with time and location than atmospheric noise and is subdivided

according to the receiving environment as urban, suburban or rural noise. Atmospheric noise depends upon the frequency, time of day, season and geographic location of the receiver. Figure 2.7-1 shows typical plots [Barghausen, et al., 1969] of the noise levels above receiver thermal noise power (KT_oB) from various sources as a function of frequency. The curves of atmospheric noise show that the highest noise levels occur during the night hours in the summer time while the lowest noise levels occur in the morning hours during the winter months. In general, man-made noise levels exceed atmospheric noise at the upper end of the HF band (15-30 MHz). Below 15 MHz, man-made noise exceeds atmospheric noise in the winter time while atmospheric noise predominates in suburban and rural areas during the summer months.

The curves of Fig. 2.7-1 may be used to predict the average noise levels from:

$$N = F + \log_{10}B - 204 \qquad (2.7\text{-}1)$$

where

N	=	noise level in dBw
B	=	receiver bandwidth in Hz
F	=	noise power (figure 2.7-1) above KT_oB.

The noise level predicted by Eq. (2.7-1) is independent of the receiving antenna gain (or directivity). This is because atmospheric noise is considered to be omnidirectional in both azimuth and elevation. Man-made noise on the other hand tends to arrive at low elevation angles. In this case, the actual received man-made noise level would be weighted by the antenna directivity at low elevation angles.

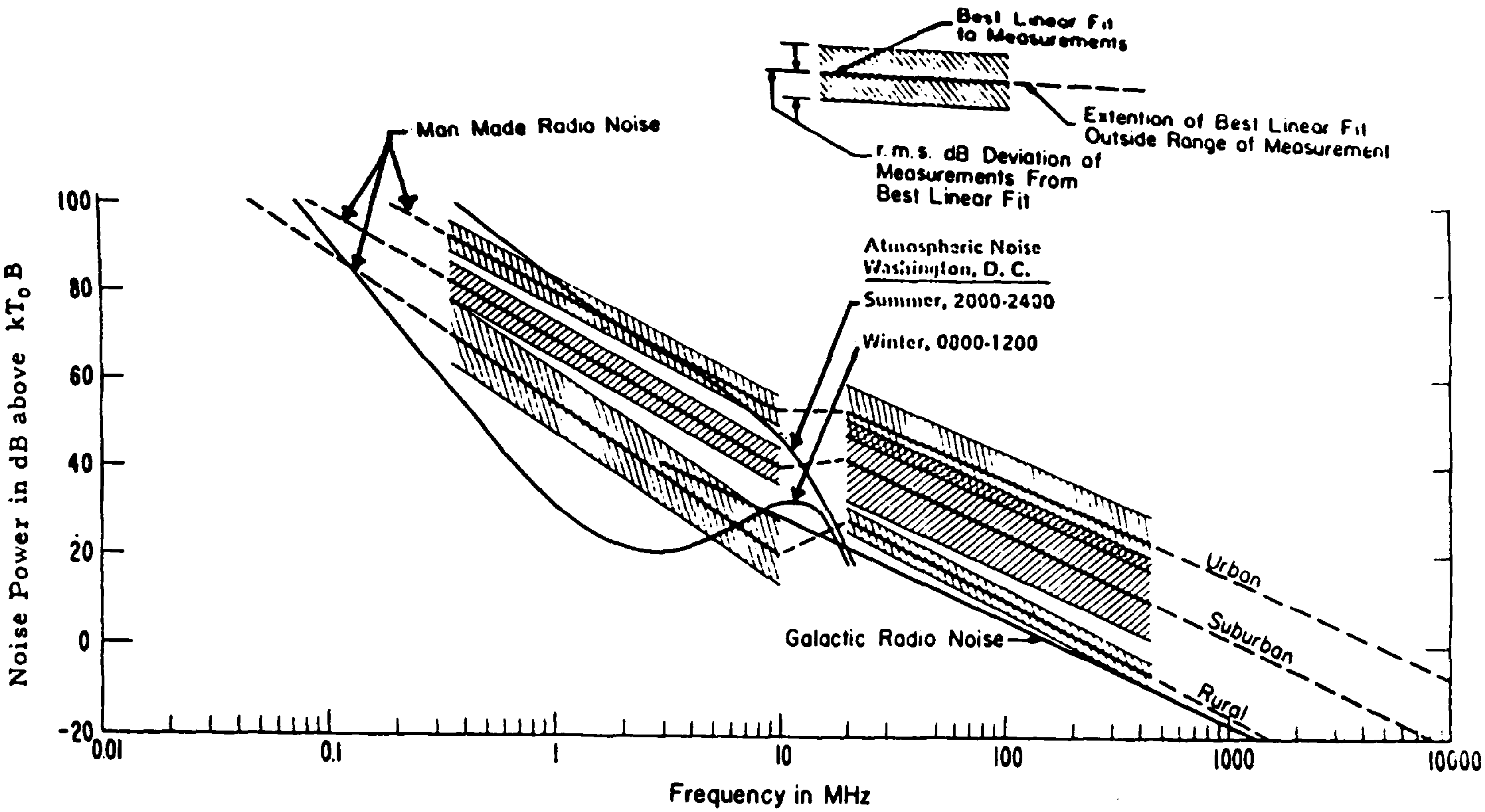

Fig. 2.7-1 . Median values of radio noise power as recorded with a short vertical lossless antenna.

(from Barghausen, et al. 1969)

2.8 Mode of Propagation vs. Distance

The previous sections have dealt with a description of the two modes of propagation encountered at HF. In this section, we discuss the conditions under which the ground wave is the predominant mode of propagation.

The curves of Figure 2.8-1 represent the distance at which skywave propagated signals and ground wave propagated signals are of equal amplitude as a function of the operating frequency and for the conditions specified: winter midday sky-wave propagation, omnidirectional (isotropic) antenna radiation and ground wave propagation over a dense urban area. The cross-hatched area reflects the variability of the ionospheric conditions between a low sunspot number (10) and high sunspot number (110). Thus, the region above the cross-hatched area indicates the distances at which the skywave signal is stronger than the ground wave signal while at the distances below the cross-hatched area, the ground wave signal is stronger than the skywave return. It should be mentioned however that the regions of Fig. 2.8-1 have been determined assuming isotropic radiation (i.e., equal excitation of the ground wave and sky-wave). When vertical polarization is used, the range of the ground wave is greater because of greater antenna gain at lower elevation angles. If horizontal polarization is used, the range of the ground wave is shorter because of lower antenna gain at the lower elevation angles. Keeping this in mind, the curves of Fig. 2.8-1 show that the maximum distance at which ground wave propagation predominates increases from a low of 70 km at 3 MHz to 1000 km at 15 MHz. At frequencies above 15 MHz, there is no skywave return while at frequencies below 3 MHz the skywave signal is strongly attenuated due to absorption in the D region of the ionosphere.

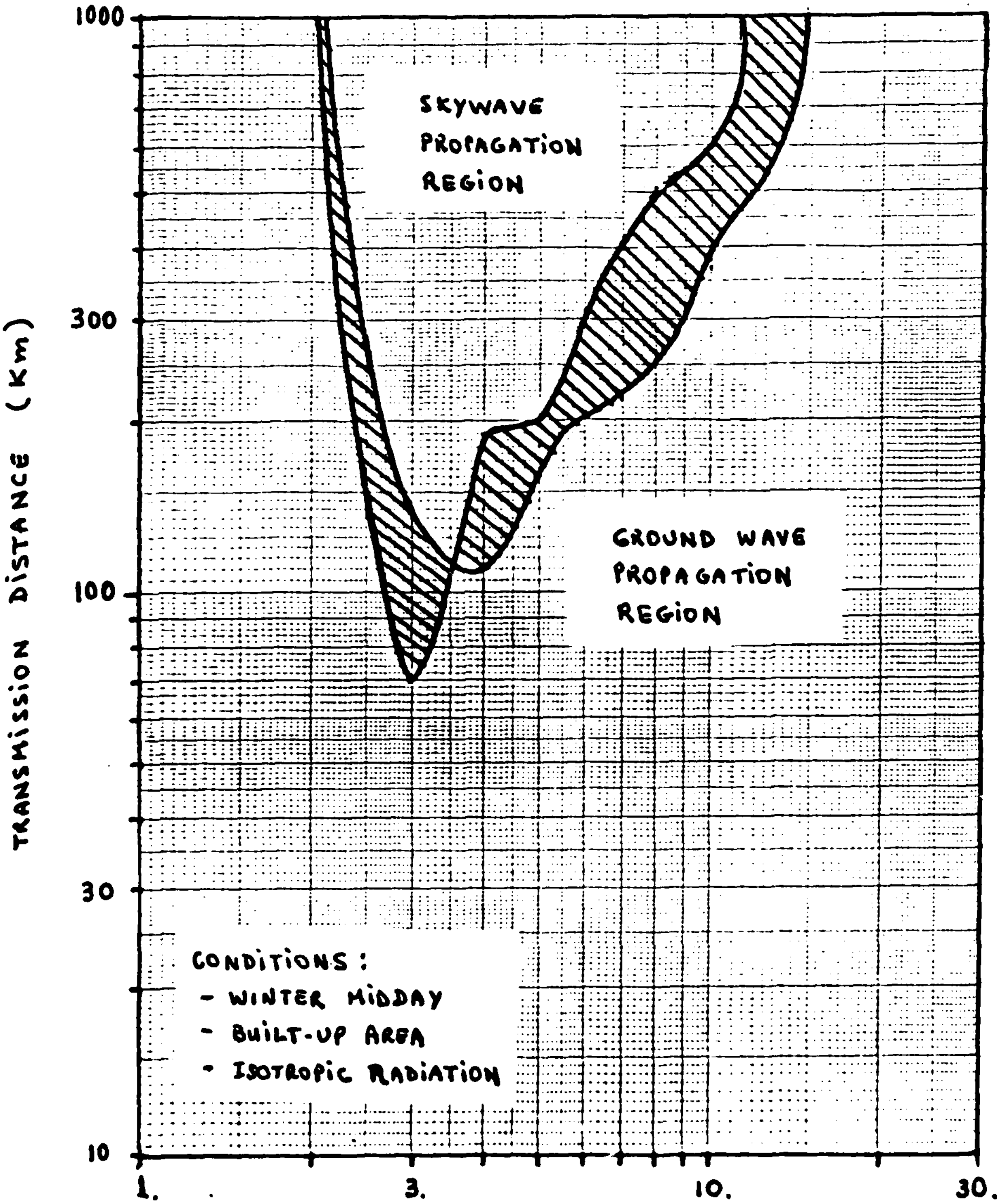

Fig. 2.8-1 Ground Wave and Skywave Propagation ranges in built-up areas vs. frequency for Winter mid-day conditions

At night, the D region disappears so that the skywave signal suffers less attenuation and the ranges for which ground wave propagation predominate (for a fixed frequency) decrease. This is reflected by the curves of Figure 2.8-2 where we have also plotted the distance at which skywave and ground wave propagated signals are of equal strength as a function of frequency and under winter night conditions assuming isotropic radiation. Figure 2.8-2 shows that the maximum distance at which the ground wave is stronger than the skywave at night decreases from 70 km at 1 MHz to 35 km at 4 MHz. At frequencies above 5 or 6 MHz there is no skywave return. Hence, above this frequency there is only a ground wave propagated signal. During the summer time the maximum range for ground wave propagation is similar as that during the winter except that skywave propagation is possible at higher frequencies (15 to 20 MHz during the day).

Figures 2.8-1 and 2.8-2 only provide a degree of perspective relative to normal experience. For example, any 3 MHz signals received up to distances of 70 km are normally propagated via the ground wave mode while those beyond 140 km are due to ionospheric propagation. However, Figures 2.8-1 and 2.8-2 do not indicate the system parameters necessary to provide a specified communications capability. This will be discussed in Sections 3 and 4.

As a final comment regarding the propagation mode for short distance HF transmissions, it should be pointed out that in calculating the propagation loss for skywave transmission we did not account for reflection from the sporadic E layer. This layer is not always present, as are the E-layer (during the day) and the F-layer (day and night), but occurs rather unpredictably but frequently enough in the middle latitudes to permit sporadic E propagation from 25 to 50% of the time at frequencies up to 15 MHz. When this layer is present, the range

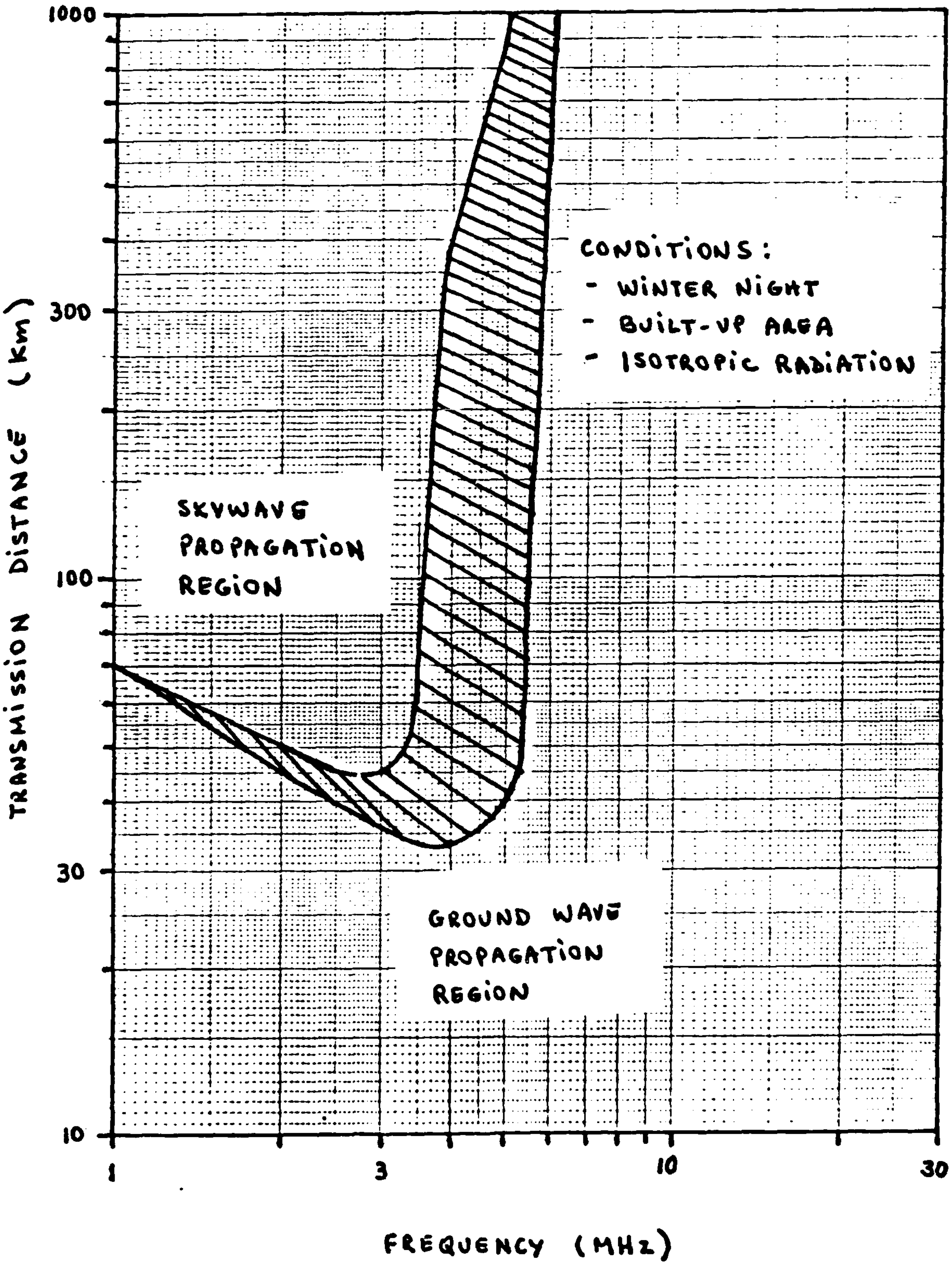

Fig. 2.8-2 Ground Wave and Skywave Propagation ranges in built-up areas vs. frequency for Winter night conditions

of the ground wave will be greatly diminished at frequencies between 5 and 15 MHz.

2.9 Basic Considerations in HF Antenna Selection:

Having discussed the various propagation modes involved in short and long haul HF transmission, we conclude the discussion of HF propagation by considering the implications of the propagation mode on the type of antenna needed. Because the ground wave and skywave are radiated and received at different elevation angles, care must be taken in selecting an antenna whose radiation pattern is such that the directive gain of the antenna is favorable at the desired elevation angle: 0^{o} for ground wave propagation and a somewhat higher elevation angle for skywave propagation. A general propagation chart [from a Collins Radio Co. Publ., 1978] which may be used to determine the elevation (take-off) angle of a skywave HF circuit for a given path length is shown in Figure 2.9-1. The range of elevation angles for skywave propagation is determined by drawing lines down from the minimum and maximum FOT (optimum operating frequency) scales for the desired path length (e.g., 800 km) and across the minimum and maximum reflection layer height scales as indicated in the example given along with the chart.

Because of the presence of the ground, the elevation patterns of simple omnidirectional antennas such as a horizontal and a vertical half-wave dipole or a quarter-wave monopole are modified and their efficiencies (gains) are reduced due to the finite conductivity of the ground. The elevation patterns of a horizontal dipole and a vertical dipole a half-wavelength above a ground of finite conductivity have been computed by Jordan [1950] and are shown in Fig. 2.9-2. The parameter

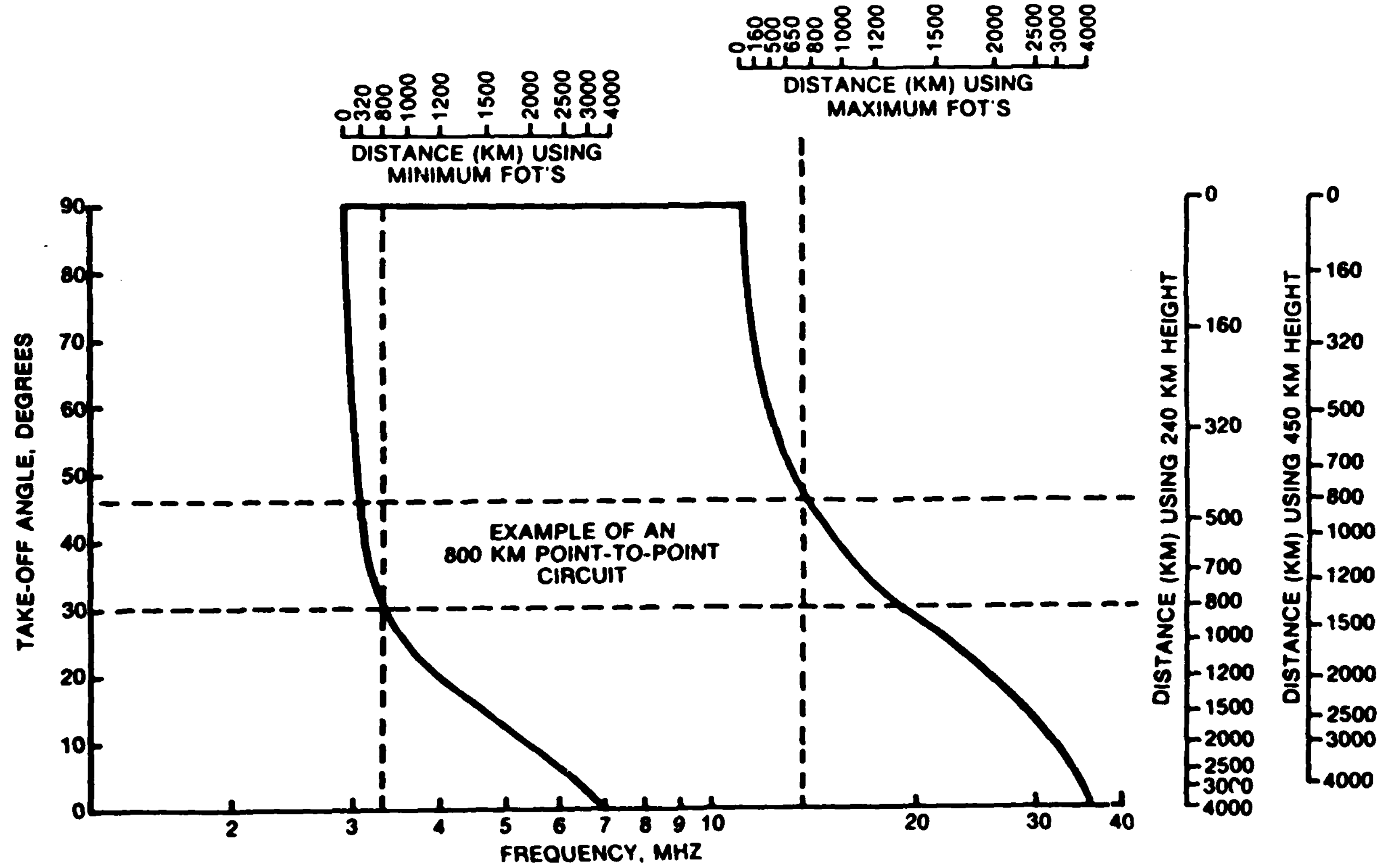

Fig. 2.9-1 General Propagation Chart with Example of 800-km Circuit (from Collins Radio, 1978)

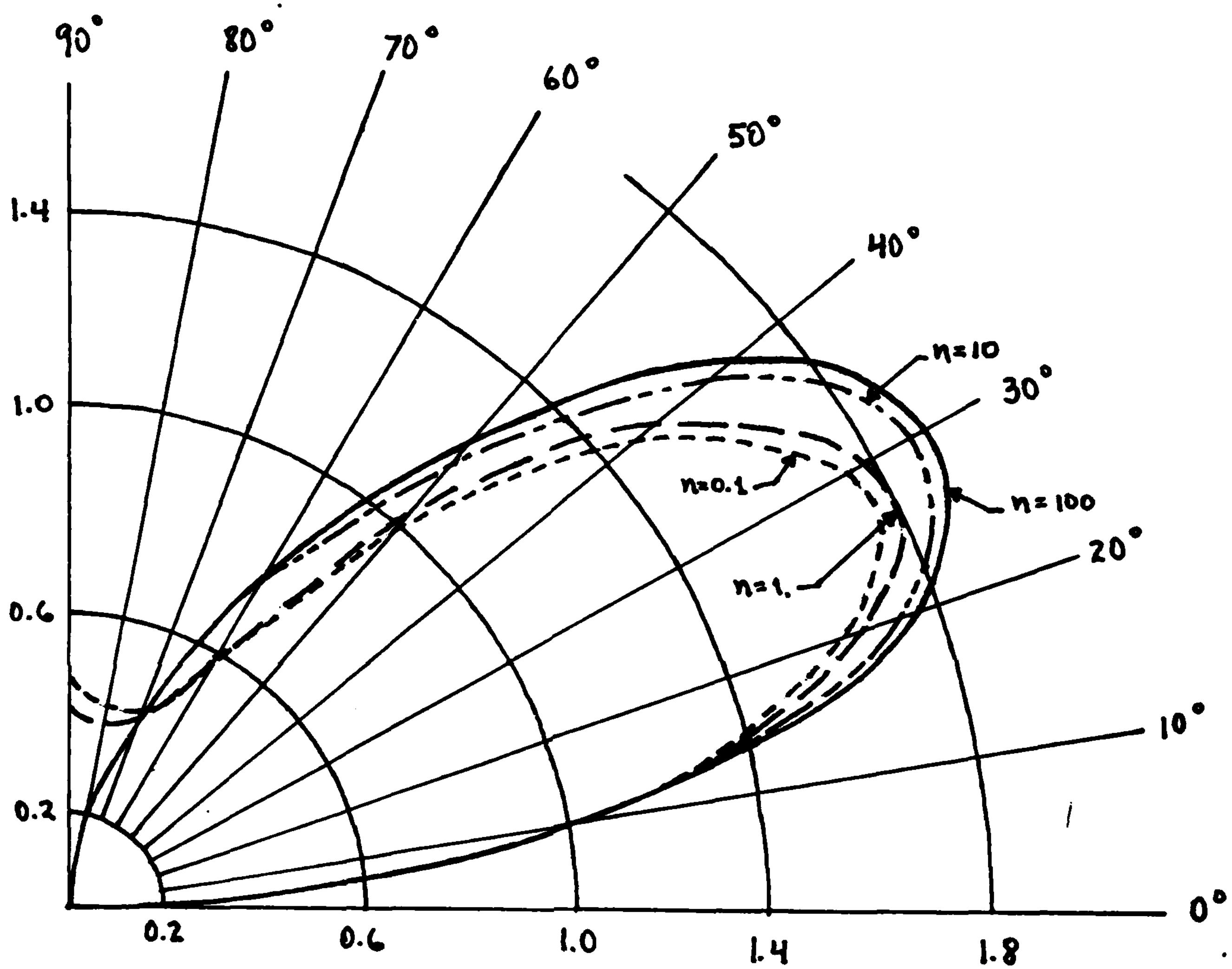

Fig. 2.9-2(a) Vertical Radiation Pattern (in the Plane Perpendicular to the Axis of the Dipole) of a Horizontal Dipole 1/2-Wavelength Above an Earth of Finite Conductivity (from Jordan, 1950)

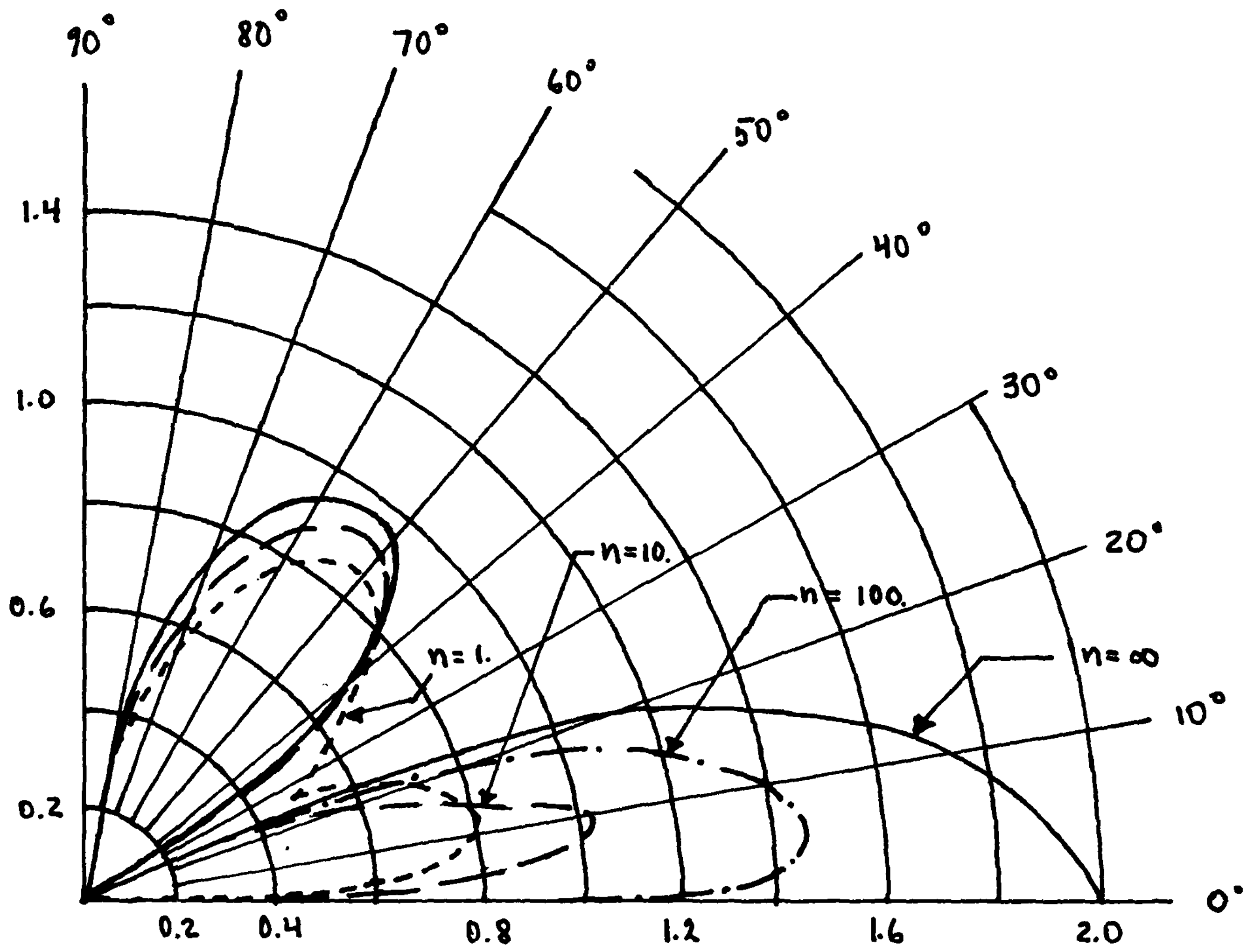

Fig. 2.9-2(b) Vertical Radiation Pattern of a Vertical Dipole 1/2-Wavelength Above an Earth of Finite Conductivity (from Jordan, 1950)

$n = x/\varepsilon_r$ where

ε_r = relative dialectric constant of earth

$$X = \frac{18 \times 10^3 \sigma}{f_{MHz}}$$

σ = conductivity of earth, mhos/m

$n = \infty$ corresponds to perfect ground.

The patterns of Figures 2.9-2(a) and (b) are voltage patterns. A value of 2.0 corresponds to a gain of 7.8 dB/isotropic. Note that while the gains of the vertical and horizontal dipole are the same over perfect ground, the horizontal dipole is much better over poor ground. The gain of a horizontal half-wave dipole at HF is between 6 and 8 dB above isotropic at beam maximum unless the ground is very poor or the antenna is unusually close to ground ($<\lambda/4$). The vertical plane patterns of vertical antennas are modified to a much greater extent by imperfect ground. Figure 2.9-3 shows the gain of a quarter-wave vertical monopole over good ground as well as the gain of the same monopole over a perfect ground plane. At a radiation angle along the ground(0^{o}), the vertical quarter-wave monopole over good ground has a gain of around -3 dB to -4 dB in the band between 3 to 30 MHz. A vertical quarter wave monopole over perfect ground has a gain of 5.15 dB. However, the gain of the vertical monopole over imperfect (good) ground is still higher than that of a horizontal dipole at 0^{o} elevation (Fig. 2.9-2). For skywave propagation at a radiation angle of 30^{o}, the gain of the quarter-wave monopole at 10 MHz is about +.5 dB over good ground and +3.3 dB over perfect ground. On the other hand, the gain of a horizontal half-wave dipole a half-wave above ground is 6 to 8 dB at the angle of maximum radiation (30^{o} from Fig. 2.9-2(a)). The advantage of the horizontal antenna is seen to be significant even if the vertical monopole is over perfect

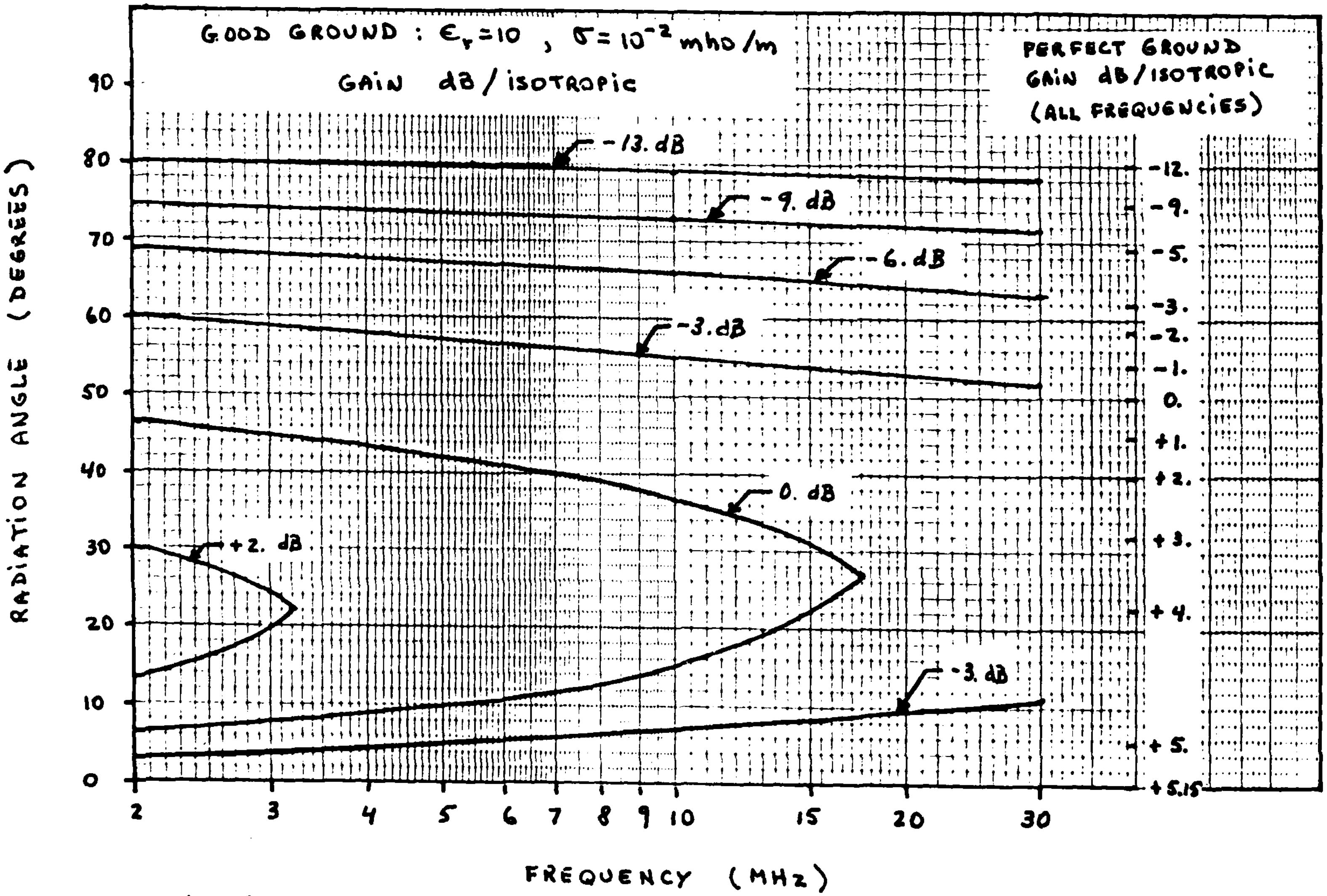

Fig. 2.9-3 Comparison of the Gain of a Perfect Quarter-Wave Vertical Monopole over Good Ground and over Perfect Ground (from Collins Radio, 1978)

ground. Of course raising a horizontal antenna to 49 ft. (half-wavelength at 10 MHz) might not be convenient, or the expense might not be justifiable. Raising the vertical antenna above ground would not help much. The gain of a vertical half-wave dipole a half-wavelength above good ground would be about +0.3 dB.

From these considerations and others we can then summarize the choice between vertical and horizontal polarization for HF circuits as follows.

Vertical polarization is the obvious choice in the following situations:

(1) For surface or ground wave propagation.

(2) Where a simple broadband omnidirectional radiator is required.

(3) Where long distances are to be covered by skywave and a horizontal antenna for some reason cannot be raised to a sufficient height.

(4) Where radiation near the horizon and a broad elevation pattern are required.

Horizontal polarization is preferable in the following situations:

(1) Where a rotatable omnidirectional antenna is required.

(2) On most short-range near-vertical-incidence skywave (NVIS) propagation circuits (0-300 miles) due to lower noise and higher gain at radiation angles near the zenith, unless terrain is favorable for surface-wave propagation.

(3) Where man-made noise propagated by surface waves may be a problem (near cities)

(4) In the common situation where high gain is required and the horizontal antenna can be raised to the optimum height for the required radiation angle (the horizontal antenna has higher directivity gain over ground than the corresponding vertical antenna although its efficiency may be lower if the optimum height is too close to the ground, i.e., less than a quarter wavelength).

The last situation exists in many land-based HF skywave circuits and accounts for the general use of horizontal polarization on such circuits, unless omnidirectional requirements or mechanical convenience dictates the use of a simple vertical radiator.

REFERENCES FOR SECTION 2

Barghausen, A.F., J.W. Finney, L.L. Proctor, and L.D. Schultz (1969), "Predicting Long Term Operational Parameters of HF Sky-wave Telecommunication Systems", ESSA Technical Report, ERL 110-ITS 78.

Barrick, D.E. (1971), "Theory of HF and VHF propagation across the rough sea, 1; The effective surface impedance for a slightly rough highly conducting medium at grazing incidence", Radio Science, V6, pp 517-526.

Beckmann, P. (1967), <u>Probability in Communication Engineering</u>, Harcourt, Brace & World, Inc., New York

Causebrook, J.H. (1977), "Ground-wave propagation at medium frequencies in built-up areas", BBC Research Dep. Report No RD 1977/25.

Causebrook, J.H. (1978), "Surface Waves in built-up areas, Re-examined by measurement and theory", IEEE Conference Publication No. 169, Pt 2 Propagation, pp 21-25

Crain, C.M. (1975), "Low Data rate ground wave communications over land", The Rand Corporation technical report DNA 3662T.

Ehrman, L. and S. Parl (1977), "Communications Data base analysis for military operations in a built-up area", SIGNATRON technical report 15068.1.

Feinberg, E.L. (1944), "On the propagation of radio waves along an imperfect surface", T. Phys. USSR (in Russian), 8, pp 317-330.

Halpern, S.W. (1977), "A study of environmental constraints in the coastal harbor radio-telephone system", IEEE Trans. Veh. Tech., VT 26, pp. 226-238.

Haydon, G.W., M. Leftin, and R. Rosich (1976), "Predicting the performance of HF sky wave telecommunication system (the use of the HFMUFES 4 Program)", ITS Report OTR 76-102.

Hufford, G.A. (1952), "An integral equation approach to the problem of wave propagation over irregular terrain", Quart. J. Appl. Math., 9, pp 341-404.

Jasik, H. (1961), Antenna Engineering Handbook, Ch. 33, McGraw Hill, New York.

Jordan, E.C. (1950), Electromagnetic Waves and Radiating Systems, Ch. 16, Prentice-Hall, New York

King, R.J. (1969), "Electromagnetic wave propagation over a constant impedance plane", Radio Science, Vol. 4, pp 255-268.

Malaga, A. and R.E. McIntosh (1978), "Delay and Doppler Power spectra of a fading ionospheric reflection channel", Radio Science, Vol. 13, pp. 859-872.

Monteath, G.D. (1978), "Computation of ground wave attenuation over irregular and inhomogeneous ground at low and medium frequencies", BBC Research Dept, Report No. RD 1978/7.

Norton, K.A. (1937), "The propagation of radio waves over the surface of the earth and in the upper atmosphere, 2", Proc. IRE, 25, pp. 1206-1236.

Norton, K.A. (1941), "The ground wave field intensity over a finitely conducting spherical earth", Proc. IRE, 29, pp 623-639.

Ott, R.H. (1971), "An alternative integral equation for propagation over irregular terrain, 2", Radio Science, Vol. 6, pp. 429-435.

Shaver, H.N., B.C. Tupper, and J.B. Lomax (1967), "Evaluation of a Gaussian HF channel model", IEEE Trans. Commun. Tech., V COM-15, pp. 79-88.

Sykes, C.B. and R.G. Robertson (1975), "Long-range sensor communications", Atlantic Research Corp. report RADC-TR-75-116.

Wait, J.R. (1959), "Guiding of electromagnetic waves by uniformly rough surfaces, parts 1 and 2", IRE Trans. Antenna Prop., 7S, pp 154-168.

SECTION 3

AM, SSB and DIGITAL MODULATION SYSTEM PERFORMANCE

3.0 Introduction

In this section, we discuss the performance of the analog and digital modulation techniques most commonly used for HF communications by the military. The performance of AM (also referred to as DSB-AM) and SSB-AM radios is discussed in Section 3.1 in terms of the signal-to-noise ratio. The discussion of digital modulation techniques is limited to binary non-coherent frequency shift keying (NCFSK) as this is the technique most commonly used to transmit low data rates with Army HF radios. The performance of NCFSK systems is considered in Section 3.2 We use as a measure of performance, the bit or element error probability as a function of signal-to-noise ratio. Non-fading, flat-fading and frequency selective fading conditions are considered in the discussion of AM, SSB-AM and NCFSK.

3.1 AM and SSB System Performance

Amplitude modulation (AM) and single-sideband (SSB) modulation are commonly used in voice radio communications at high frequencies (HF) and also in the broadcast frequency range (300 kHz to 3 MHz) for two primary reasons. First, because they are inherently narrowband, they are more spectrally efficient than other analog modulation formats such as FM, thus allowing a greater number of channels (users) in a given frequency band. Second, being narrowband systems, they are less susceptible to frequency selective fading than wider band modulation formats. Since AM and SSB are CW (analog) systems, their performance is usually given in terms of the

signal-to-noise ratio at the receiver input and output. Thus, in this section we will determine the output signal-to-noise ratio of AM and SSB systems in the presence of narrowband Gaussian noise and also in the presence of flat-fading and selective fading.

3.1.1 Non-Fading AM Performance

The AM signal at the output of the IF amplifier in an AM receiver, in the absence of fading, consists of an amplitude modulated carrier and noise:

$$x(t) = A_c[1+mf(t)] \cos \omega_o t + n(t) \tag{3.1-1}$$

where

A_c = carrier amplitude
$f(t)$ = information carrying signal ($|f(t)| \leq 1$)
m = modulation index ($m \leq 1$)
$n(t)$ = bandpass Gaussian noise

The information signal f(t) is recovered by passing x(t) through a detector and an audio filter to remove the frequency components above the information (baseband) bandwidth, B, as well as DC components. Most AM detectors are non-linear devices (e.g., square-law devices) and for this reason the noise at the output of the detector is greater than at the input.

The output SNR of a square-law envelope detector followed by a baseband filter (Audio) is given by [Schwartz, Bennet and Stein, 1966]

$$SNR_o = \frac{m^2 A_c^2}{2N\left(1+\frac{3N}{4A_c^2}\right)} \tag{3.1-2}$$

where N is the noise power in the IF (or RF) bandwidth W. Since the IF bandwidth of AM receivers is twice the baseband

bandwidth, then the noise power may be expressed in terms of the baseband bandwidth, B, and the noise density, η, as

$$N = 2\eta B \tag{3.1-3}$$

The carrier-to-noise ratio at the input of the detector is given by:

$$\rho = \frac{A_c^2}{2N} \tag{3.1-4}$$

Thus, the output SNR of an AM radio for large and small carrier-to-noise ratios is:

$$SNR_o \simeq m^2\rho \quad , \quad \rho>>1 \tag{3.1-5}$$

$$SNR_o \simeq \frac{8m^2\rho^2}{3} \quad , \quad \rho<<1 \tag{3.1-6}$$

which shows that the output of an AM receiver is linearly proportional to the input for large carrier-to-noise ratio and quadratic for small ρ. The signal suppression for small ρ results from the carrier sinking below the rms noise level $\sqrt{N}$.

The output SNR of an AM system is independent of the AM bandwidth as opposed to FM. Widening the AM bandwidth leads to additional noise and the possibility of interference from adjacent channels. The bandwidth is thus chosen as large as necessary to accommodate the signals transmitted and no larger. Thus, if the bandwidth of the information signal f(t) is B Hz, then the bandwidth of the AM signal W is 2B Hz centered around the carrier frequency. The RF and IF filters in the AM receiver must have a passband of 2B Hz which restricts the frequency separation between channels to be greater than

this bandwidth.

3.1.2 Non-Fading SSB Performance

The RF spectrum of an AM waveform is symmetric about the carrier frequency and its bandwidth is twice the baseband (information) bandwidth B. Each portion of the spectrum above and below the carrier is called a sideband and, since each sideband has the same spectral shape, then it must contain the same information. Thus, it is possible to design an AM transmitter that transmits a single sideband in order to save RF bandwidth at the expense of complexity. A single sideband (SSB) AM transmitter generates a waveform of the form

$$s(t) = A\,\{f(t)\cos\omega_o t - \hat{f}(t)\,\sin\omega_o t\} \qquad (3.1\text{-}7)$$

where

A = is the signal peak amplitude
$f(t)$ = information carrying signal ($|f(t)|\leq 1$)
$\hat{f}(t)$ = Hilbert transform of $f(t)$

The envelope of a single-sideband signal is a non-linear function of the information and for this reason cannot be detected using envelope detectors as in the case of simple AM. Instead SSB signals are normally detected using coherent receivers (homodyne). If the homodyne (demodulator) carrier does not have the correct frequency and phase, the recovered signal waveform will be distorted.

A detected SSB signal with frequency and phase errors in the presence of noise is of the form:

$$s_d(t) = A\,f(t)\cos(\omega_d t+\phi) + A\,\hat{f}(t)\sin(\omega_d t+\phi) + n_c(t) \qquad (3.1\text{-}8)$$

where ω_d is the frequency offset, θ is the phase error and $n_c(t)$ is the in-phase component of the noise. In the absence of any frequency or phase errors, the baseband peak signal-to-noise ratio is given by:

$$SNR_o = \frac{A^2}{2N} \qquad (3.1\text{-}9)$$

where $N=\overline{n_c^2}$. The effect of the phase and frequency error is to introduce a component proportional to the Hilbert transform of the signal. Some types of signals such as speech tolerate this form of distortion up to several Hertz frequency error. Others such as television or data transmission systems can be severely degraded by small frequency errors. When only a phase error is present, the desired output f(t) is reduced as the phase error θ increases from 0, while the distortion term $\hat{f}(t)$ increases. If $\theta=\pi/2$, in particular, only $\hat{f}(t)$ appears at the output. Interestingly, the human ear is insensitive to phase changes in signals ($\hat{f}(t)$ is a 90^o phase shifted version of f(t)). However, phase distortion becomes quite noticeable in TV and other signals (digital) when the phase shift θ approaches $\pi/2$. SSB receivers must thus be synchronized in frequency and phase.

Various methods of synchronizing the local carrier exist. Typically, a small amount of unmodulated carrier energy is sent as a pilot signal and, after extraction at the receiver, is used to provide the necessary synchronization.

In order to compare SSB with AM, it is convenient to express the noise power in terms of a noise power density η and the RF (i.e., IF) bandwidth W. Thus, letting $N=\eta W$ and recalling that the SSB (IF) bandwidth equals the baseband (audio) bandwidth, B, while the AM (IF) bandwidth is twice the baseband bandwidth we find from (3.1-5) and (3.1-9) that the audio speech signal-to-noise ratio is given by:

$$SNR_o = \begin{cases} \dfrac{m^2 A_c^2}{4\eta B} & , \text{ AM} \\ \dfrac{A^2}{2\eta B} & , \text{ SSB} \end{cases} \qquad (3.1\text{-}10)$$

If we define the AM carrier-to-noise density ratio as

$$\rho_{AM} = \frac{A_c^{\,2}}{2\eta} \qquad (3.1\text{-}11)$$

and the SSB RF PEP (peak envelope power) signal-to-noise density ratio as:

$$\rho_{SSB} = \frac{A^2}{2\eta} \qquad (3.1\text{-}12)$$

we see that ρ_{SSB} can be 3 dB lower than ρ_{AM} if the speech-to-noise ratio of a SSB signal is equal to that of a 100% (m=1) modulated AM signal.

Equations (3.1-10) through (3.1-12) provide us with a means for estimating the required signal-to-noise ratio for SSB systems as well as AM systems from test results made on either system. However, it should be kept in mind that in deriving the expression for SSB signals, complete carrier suppression has been assumed. The RF signal-to-noise density ratio for an actual SSB signal (with a reduced carrier) must be higher than that for a conceptual SSB signal without carrier by a correction factor that depends on the carrier reduction. Akima, et al., [1969] quote correction factors of 6.0 dB, 1.5 dB, .9 dB, .4 dB and .2 dB for SSB systems with carriers emitted at power levels of 6 dB, 16 dB, 20 dB, 26 dB, 32 dB and 40 dB below the peak envelope power.

Various criteria for estimating the required signal-to-noise ratio for a voice signal of just usable quality have been quoted in the literature. Some of these criteria are:

60% phonetically balanced (PB) word articulation
90% sentence intelligibility
An articulation index of 0.3

No one criterion has been proved superior to the others. Differences of several dB in required signal-to-noise ratio result from the adoption of several criteria. Even if a single criterion is used, several values of the required SNR (for a given criterion) have been reported by different investigators. Akima, et al., [1969] have used the criterion of 90% sentence intelligibility to determine the required signal-to-noise (SNR) ratios and signal-to-noise density (ρ_{AM} and ρ_{SSB}) ratios for SSB and 100% modulation AM from tests conducted by various investigators. These values are reproduced in Table 3.1. The tests of PB word articulation versus carrier-to-noise density ratio used by Akima are also listed in the table.

The required signal-to-noise ratios listed in Table 3.1 are distributed in a range as wide as 16 dB. Average values and standard deviations are given at the bottom of the tables. Since no one criterion has been found to be better than the other, Akima, et al., [1969] suggest that the values of 50 dB and 47 dB be used as the values of required signal-to-noise density ratio for voice signal of just usable quality for AM (i.e., double sideband DSB-AM) and SSB systems, respectively. These values correspond to a 12 dB signal-to-noise ratio in a 6 kHz RF bandwidth for AM and 3 kHz RF bandwidth for SSB. For voice communications of good commercial quality, an additional 17 dB in SNR is required for both DSB-AM and SSB systems. If the uncertainty associated with the adoption of the criterion

TABLE 3.1

Values of Required Signal-to-Noise Ratio for Voice Communication of 90-Percent Sentence Intelligibility Taken From Various Sources

Required Signal-to-Noise Ratio in dB				Data Source References		
DSB-AM		SSB-AM		Articulation test by	Conversion from word articulation to sentence intelligibility by	Articulation index based on voice spectrum given by
Carrier-to-noise (6 kHz) ratio $\frac{A_c^2}{4\eta B}$	Carrier-to-noise-density ratio $\frac{A_c^2}{2\eta}$	PEP-to-noise (3 kHz) ratio $\frac{A^2}{2\eta B}$	PEP-to-noise-density ratio $\frac{A^2}{2\eta}$			
11	49	11	46	Cunningham et al. (1947)		---
17	55	17	52	Licklider & Goffard (1947)	Licklider & Goffard (1947)	---
9	47	11	46	Craiglow et al. (1961)		---
20	58	20	55	Ewing & Huddy (1966)		---
6	44	6	41	Cunningham et al. (1947)		---
11	49	11	46	Licklider & Goffard (1947)	Kryter (1962a)	---
4	42	6	41	Craiglow et al. (1961)		---
14	52	14	49	Ewing and Huddy (1966)		---
10	48	10	45	Griffiths (1968)	Griffiths (1968)	---
12	50	12	47	---	---	Beranek (1947)
16	54	16	51	---	---	Kryter (1962a)
11.8	49.8	12.0	47.0	Mean value		
4.5	4.5	4.4	4.4	Standard deviation		

PEP stands for peak envelope power.

for just usable voice quality is also taken into account, the estimated dispersion associated with the values of required signal-to-noise density ratio is quoted by Akima [1969] as 5 dB.

The values of required SNR listed in Table 3.1 are applicable when the noise is Gaussian. On HF channels, however, the noise is mostly atmospheric and man-made noise which are impulsive in nature. Tests carried by Licklider and Goffard (1947) with DSB-AM signals in impulsive noise consisting of irregularly spaced pulses indicate that, if no noise limiter is used, the required carrier-to-noise ratio can be 5 to 10 dB lower than that required for Gaussian noise. Thus, the values of required SNR given in Table 3.1 are pessimistic for non-fading conditions. However, they have no allowance for noise due to fading.

3.1.3 Frequency-Flat Fading AM and SSB Performance

When a radio wave modulated by a voice signal is fading at a high rate, on the order of several Hertz or higher, or when the fading is frequency selective, i.e., when different portions of the spectrum of the signal are fading differently, the voice signal suffers severe degradation. When the fading is slow (below 1 Hz) and flat, the subjective effect on a listener may not be too bad as the fading results in intermittent attenuation of the voice signal. We may estimate the distortion of AM and SSB signals due to fading by calculating the signal suppression noise as follows. When the modulation bandwidth, B, is much smaller than the coherence bandwidth, the fading is frequency flat over the signal band. Then the output of an AM envelope detector (in the region above threshold) is:

$$v(t) = A(t)\,\{1 + mf(t)\} + n_c(t) \qquad (3.1\text{-}13)$$

where $f(t)$ is the information signal, m is the modulation index ($m=1$ for 100% modulation), $A(t)$ is the fading imposed by the medium and $n_c(t)$ is the low pass in-phase component of the noise. Similarly, the output of SSB coherent detector is:

$$S_d(t) = A(t)\ [f(t)\cos\theta + \hat{f}(t)\sin\theta] + n_c(t) \qquad (3.1\text{-}14)$$

where θ is the phase fluctuation introduced by the medium and it varies at the fade rate, $A(t)$ is the amplitude fluctuation, and $\hat{f}(t)$ is the Hilbert transform of the information signal $f(t)$.

(a) Slow-Fading Performance

If the fading is very slow (less than 1 Hz) its effect is merely the intermittent attenuation of the voice signal. Therefore, the mean (average) signal-to-noise ratio of an AM envelope detector is

$$SNR = \frac{m^2 \langle A^2 \rangle}{4\eta B} \qquad (3.1\text{-}15)$$

where η is the noise density (noise power per Hertz). This expression is similar to that for steady conditions (3.1-10) except that the mean carrier power is now averaged over the fading.

Equation (3.1-15) indicates that the output SNR depends on the statistics of the fading. As mentioned in Section 2, there are no statistics available for short range (ground wave) HF propagation in urban areas. From purely theoretical considerations, the surface wave component of the ground wave may be considered as a specular component while the space (or diffraction) field due to antenna elevation will result in a Rayleigh fading component. On the other hand, if

the distances involved are very long, then propagation is via the skywave which exhibits Rayleigh fading.

For Rician fading (specular plus Rayleigh fading component), the average AM signal-to-noise ratio is given by

$$(SNR)_{AM} = \frac{m^2}{4\eta B} (A_o^2 + \alpha) \qquad (3.1\text{-}16)$$

where A_o is the amplitude of the specular component and α is the mean power in the Rayleigh component.

The average signal-to-noise ratio for SSB systems in the presence of very slow fading (which allows phase tracking, i.e., $\Theta=0$) is also similar to the no-fading case and is given by

$$(SNR)_{SSB} = \frac{\langle A^2 \rangle}{2\eta B} = \frac{A_o^2 + \alpha}{2\eta B} \qquad (3.1\text{-}17)$$

When the specular component is much greater than the Rayleigh fading component ($A_o^2 >> \alpha$), the average SNR for AM and SSB is identical to that for the no-fading case. The required SNR for just usable voice is the same as those listed in Table 3.1.

On the other hand when $\alpha >> A_o^2$, the performance of AM and SSB systems is degraded compared to that for the no-fading case as a higher mean carrier-to-noise density ratio ($\alpha/2\eta$) is required to attain the required PB word articulation. Akima [1969] has shown that the mean carrier-to-noise ratio for 60% PB word articulation (just usable voice) in Rayleigh fading must be 1 dB greater than that required under no-fading conditions when no diversity reception is used. This

AD-A082 354 SIGNATRON INC LEXINGTON MA F/G 17/2.1
HF MOBA COMMUNICATIONS STUDY.(U)
MAR 80 A MALAG, L EHRMAN DAAK80-79-C-0773
UNCLASSIFIED A257-I CORADCOM-79-0773-1 NL

2 OF 2
AD
A082354

END
DATE
FILMED
4-80
DTIC

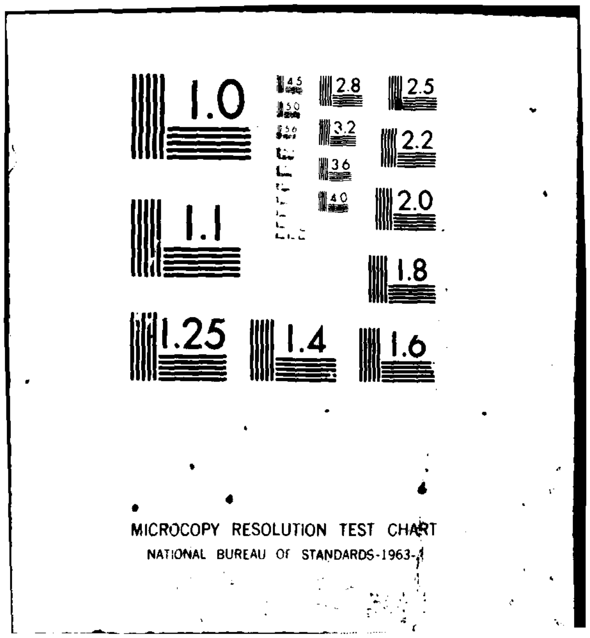
1.0
1.1
1.25
1.4
1.6
1.8
2.0
2.2
2.5
2.8
3.2
3.6
4.0
MICROCOPY RESOLUTION TEST CHART
NATIONAL BUREAU OF STANDARDS-1963-A

requirement may be improved by 3 dB if dual selection diversity reception is used. This value indicates that when dual selection diversity is used the mean carrier-to-noise density ratio ($\alpha/2\eta$) for Rayleigh fading signals can be 2 dB lower than for non-fading signals for an equal articulation score. These results are summarized in Table 3.2.

(b) Fast-Fading Performance

The previous results are valid as long as the fading is sufficiently slow. When individual syllables in a word or individual words in a sentence fade independently (fast fading), expressions (3.1-16) and (3.1-17) for the average signal-to-noise ratio are no longer valid. In this case, it is more appropriate to define the AM signal output as the average value $\bar{v}(t)$ of the detector output (since the noise is zero mean). The remainder of the output is zero mean and uncorrelated with $\bar{v}(t)$ and is defined as the noise, $n_c(t)$, plus signal-suppression noise, $n_v(t)$, due to fading. Hence, the output of an AM envelope detector may be expressed as [Jakes, 1974].

$$v(t) = \bar{v}(t) + n_v(t) + n_c(t) \qquad (3.1\text{-}18)$$

where

$$\bar{v}(t) = \langle A\rangle \, [1+mf(t)] \qquad (3.1\text{-}19)$$

$$n_v(t) = [A(t)-\langle A\rangle] \, [1+mf(t)] \qquad (3.1\text{-}20)$$

The signal-to-noise ratio is then given by:

$$(SNR)_{AM} = \frac{\langle|\bar{v}(t)|^2\rangle}{\langle|n_v|^2\rangle+\langle|n_c|^2\rangle} = \frac{m^2\langle A\rangle^2/2}{(1+\frac{m^2}{2})\,[\langle A^2\rangle-\langle A\rangle^2]+2\eta B} \qquad (3.1\text{-}21)$$

TABLE 3.2

Required Signal-to-Noise-Density Ratios for Various Voice Communication Systems

Type of Service		Required Signal-to-Noise-Density Ratio (dB)					
Emission designation	Description	Just usable quality			Good commercial quality		
		Stable condition	Fading condition		Stable condition	Fading condition	
			No diversity	Dual diversity		No diversity	Dual diversity
6A3	DSB-AM	50	51	48	67	75	70
3A3A	SSB-AM reduced carrier*	48	49	46	65	73	68
3A3J	SSB-AM suppressed carrier	47	48	45	64	72	67
6A3B	ISB-AM two voice channels	49	50	47	66	74	69
9A3B	ISB-AM three voice channels	49	50	47	66	74	69
12A3B	ISB-AM four voice channels	50	51	48	67	75	70

Signal-to-noise-density ratio is the ratio of carrier power to average noise power contained in a 1-Hz bandwidth for 6A3 emissions and is the ratio of signal peak envelope power to average noise power in a 1-Hz bandwidth for other types of emissions. For fading conditions carrier and signal peak envelope powers should be interpreted as median values.

*Carrier emitted at a level 20 dB below the peak envelope power.

where the brackets <.> denote ensemble averaging over all random variables. The baseband (output) SNR is again seen to depend on the statistics of the fading and in particular on the mean and mean-squared values of the carrier amplitude A.

From (3.1-21), it is clear that when the signal-suppression noise, $n_v(t)$, is greater than the thermal (or ambient noise), the baseband SNR is approximately given by the signal-to-signal-suppression noise ratio (maximum effective SNR):

$$(\gamma)_{AM} = \frac{\langle|\bar{v}(t)|^2\rangle}{\langle|n_v(t)|^2\rangle} = \frac{m^2}{2+m^2}\;\frac{\langle A\rangle^2}{\langle A^2\rangle-\langle A\rangle^2} \tag{3.1-22}$$

When the fading is Rician distributed, the mean and mean-squared values of the carrier are given by:

$$\langle A\rangle = \frac{\sqrt{\pi\alpha}}{2}\, e^{-A_o^2/\alpha}\;{}_1F_1\left(\frac{3}{2};1;\frac{A_o^2}{\alpha}\right) \tag{3.1-23a}$$

$$\langle A^2\rangle = A_o^2 + \alpha \tag{3.1-23b}$$

where A_o is the amplitude of the specular component, α is the mean power in the Rayleigh fading component and ${}_1F_1$ is the confluent hypergeometric function. Using asymptotic expansions of the hypergeometric function for the cases of a weak Rayleigh fading component ($A_o^2 >> \alpha$) and weak specular component ($A_o^2 << \alpha$), it can be shown that

$$\frac{\langle|\bar{v}(t)|^2\rangle}{\langle|n_v(t)|^2\rangle} \simeq \begin{cases} \dfrac{m^2}{2+m^2}\;\dfrac{\pi}{4-\pi}\;, & A_o^2 << \alpha \\[2ex] \dfrac{m^2}{2+m^2}\left(1+\dfrac{A_o^2}{2\alpha}\right), & A_o^2 >> \alpha \end{cases} \tag{3.1-24}$$

Thus, the signal-suppression noise is only significant when the specular component is weak ($A_o^2 << \alpha$) which corresponds to near-Rayleigh fading situation. The signal-to-signal suppression-noise ratio is greatest when the modulation index is unity, and even in this case it is in the order of 0 dB which is well below the required 12 dB (in a 6 kHz IF bandwidth) for just usable voice (Table 3.1). Typically, the modulation index is in the order of .4 to .5 in order to avoid overmodulation (distortion due to saturation) of the RF amplifier, and in this case the signal suppression noise is in the order of 3 times the signal.

Some improvement can be achieved by using diversity reception. In this case, Jakes [1974] has shown that the signal-to-signal-suppression noise in pure Rayleigh fading (A_o=0) is given by:

$$\gamma = \frac{\langle |v(t)|^2 \rangle}{\langle |n_v(t)|^2 \rangle} = \frac{m^2}{2+m^2} \frac{\pi \left(\sum_{k=1}^{M} \sqrt{\alpha_k} \right)^2}{(4-\pi) \sum_{k=1}^{M} \alpha_k} \tag{3.1-25}$$

where M is the number of diversity branches and α_k is the mean signal power in each diversity branch. If all the signals are of equal average strength ($\alpha_k = \alpha$), then

$$\gamma = \frac{m^2}{2+m^2} \frac{\pi M}{4-\pi} \tag{3.1-26}$$

which implies a prohibitively large order of diversity to increase the signal-to-signal-suppression-noise ratio in pure Rayleigh fading by a reasonable amount. The maximum effective baseband SNR (γ) as a function of the order of diversity is shown in Fig. 3.1-1 for a modulation index $S=m^2/2=0.1$.

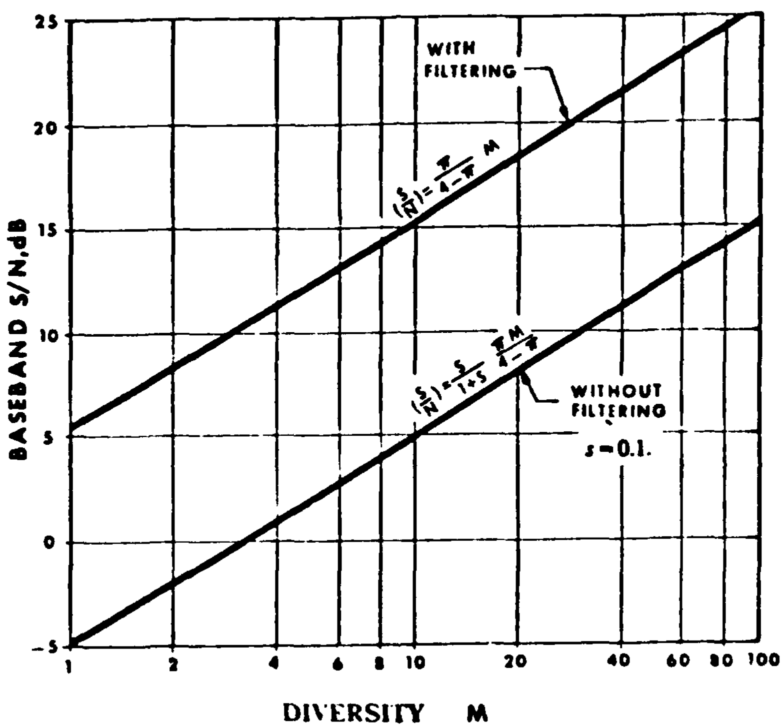

Fig. 3.1-1 Signal-To-Signal-Suppression-Noise Ratio in AM Systems With and Without Filtering vs. Diversity Order.
(from Jakes, 1974)

When the fading rate, f_m, is lower than the lowest baseband frequency (~150 Hz), then the fading noise can be considerably reduced by filtering. In this case, the noise is associated with the broadening of the modulation spectrum, the component due to the carrier fading is suppressed, leaving as the signal-suppression-noise

$$r_v(t) \simeq mf(t) \sum_{k=1}^{M} [A_k(t) - \langle A_k \rangle] \tag{3.1-27}$$

The signal-suppression-noise power can be calculated as before so that the signal-to-signal-suppression noise ratio with filtering, γ_f, in pure Rayleigh fading (worst case) becomes (assuming equal α_K)

$$\gamma_f = \frac{\pi}{4-\pi} M \tag{3.1-28}$$

The maximum effective baseband SNR (γ_f) is thus improved over the unfiltered case (Eq. (3.1-26)) by a factor of $1+2/m^2=1+1/S$. Furthermore, the baseband SNR with filtering is independent of the modulation index and is also plotted in Fig. 3.1-1 as a function of the order of diversity. This curve shows that fifth (M=5) order diversity as well as filtering must be used in order to achieve the required SNR (~12 dB) for just usable voice.

The signal-to-signal-suppression-noise ratio for SSB transmission is similar to that for AM with filtering (SSB does not have a carrier) provided that the fading is slow enough that phase-tracking is possible. In this case, the signal-to-signal-suppression-noise in arbitrary fading, is:

$$(\gamma)_{SSB} = \frac{\left(\sum_{k=1}^{M} \langle A_k \rangle\right)^2}{\left\langle \sum_{k=1}^{M} [A_k - \langle A_k \rangle]^2 \right\rangle} \tag{3.1-29a}$$

where we have assumed that Mth order diversity is used. When all the diversity signals are identically distributed, this equation reduces to

$$(\gamma)_{SSB} = \frac{\langle A\rangle^2 M}{\langle A^2\rangle - \langle A\rangle^2} \qquad (3.1\text{-}29b)$$

Equation (3.1-29b) is plotted in Fig. 3.1-2 for the case of Rician fading as a function of the specular-to-Rayleigh component power, A_o^2/α, for the dual (M=2) and no-diversity (M=1) cases. For comparison purposes, we have also plotted the corresponding ratio for DSB-AM (Eq. (3.1-22)) with 100% modulation (m=1). From these curves, we see that when $A_o^2/\alpha < .5$, the signal-to-signal-suppression noise ratio is identical to that for pure Rayleigh fading (see Eq. (3.1-24)). In this case, the fading has a disastrous effect on both AM and SSB and large orders of diversity are required to bring the SNR to a just usable voice level (γ~12 dB) and even greater to a level for good quality voice (γ~30 dB). When the specular-to-Rayleigh component power is greater than unity, the signal-to-signal-suppression noise in dB increases linearly with A_o^2/α so that the effect of fading is less severe and lower orders of diversity are necessary to bring γ to an acceptable level. In fact, when $A_o^2/\alpha > 7$, no diversity is necessary for SSB while the equivalent threshold for DSB-AM is $A_o^2/\alpha > 24$.

When the specular-to-Rayleigh component ratio is too low, further improvement in the signal-to-signal suppression-noise ratio (maximum effective SNR) for sufficiently slow fading (f_m<150 Hz) may be obtained by the proper application of automatic gain control (AGC).

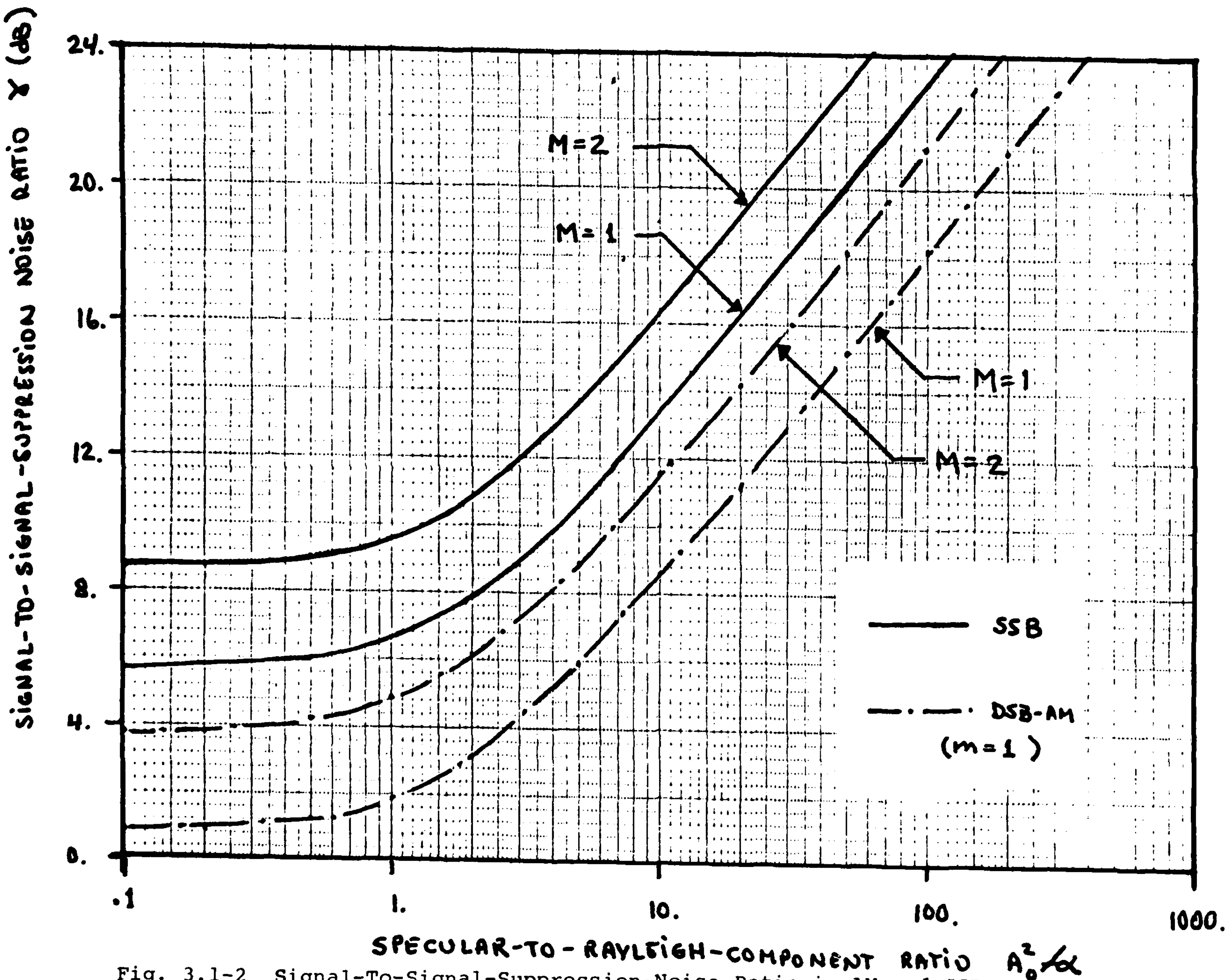

Fig. 3.1-2 Signal-To-Signal-Suppression-Noise Ratio in AM and SSB Systems Versus Specular-to-Rayleigh Component Ratio for Single and Dual Diversity Reception

3.1.4 Frequency-Flat Fading AM and SSB Performance with AGC

One method of correcting the real or complex envelope fading of AM and SSB is to transmit a pilot or carrier that is used for gain and/or phase control at the receiver. The pilot must be separated sufficiently in time or frequency to avoid overlapping the signal due to multipath delay spread or Doppler frequency spread. However, as the separation is increased, error is introduced in estimating the envelope correction required [Jakes, 1974].

Another method employs an AGC loop detector filter to separate the channel fluctuations (say $f < 150$ Hz) from the modulation (300 Hz $< f < 3$ kHz) and to correct the envelope fluctuations of the received signal [Ohlson, 1974]. The advantage of using this method is that it doesn't require the transmission of a special signal (pilot tone).

In either case, the signal component at the output of an AM envelope detector is of the form

$$v(t) = \frac{A(t)}{A_p(t)} [1+mf(t)] \tag{3.1-30}$$

where $A_p(t)$ is the envelope of the pilot when a special carrier is used. If an AGC loop filter is used, then A_p is given by [Ohlson, 1974]

$$A_p(t) = \frac{1}{b} h(t)*A(t) \ [1+mf(t)] \tag{3.1-31}$$

where $h(t)$ is the impulse response of the AGC loop, which in most systems is a simple low pass RC filter, and b is a voltage reference bias.

The gain controlled voltage, A_p, is seen to fade at the same rate as $A(t)$ but with correlation less than one due to

either non-zero delay in the AGC loop or frequency separation between the pilot and the AM carrier. Hence, if A(t) is Rayleigh fading (worst case) so is $A_p(t)$, and the probability density of the amplitude ratio $r(t)=A(t)/A_p(t)$ is [Jakes, 1974]

$$p_r(R) = \frac{2R(1-\lambda^2)(1+R^2)}{[(1+R^2)^2-4\lambda^2R^2]^{3/2}} \tag{3.1-32}$$

where λ is the correlation between A(t) and $A_p(t)$.

Since the gain controlled amplifiers saturate at some maximum gain value, $g_{max}=1/A_{min}$, the detector output of an AM receiver with limited AGC is more realistically given by

$$v(t) = r_L(t)\ [1+mf(t)] \tag{3.1-33}$$

where

$$r_L(t) = \begin{cases} \dfrac{A(t)}{A_{min}} = g_{max}A(t) & \text{if } A_p(t)<A_{min} \\ \dfrac{A(t)}{A_p(t)} & \text{if } A_p(t)>A_{min} \end{cases} \tag{3.1-34}$$

and the signal-to-signal suppression noise ratio is given by

$$\frac{\langle|\bar{v}(t)|^2\rangle}{\langle|n_v(t)|^2\rangle} = \frac{m^2}{2+m^2}\ \frac{\langle r_L\rangle^2}{\langle r_L^2\rangle-\langle r_L\rangle^2} \tag{3.1-35}$$

This ratio has been calculated by Jakes [1974] for the case of Rayleigh fading and his results are reproduced in Fig. 3.1-3 where (3.1-35) is plotted for $S=m^2/2=.1$ and various correlation amplitudes, λ , versus the limiting gain of the AGC nor-

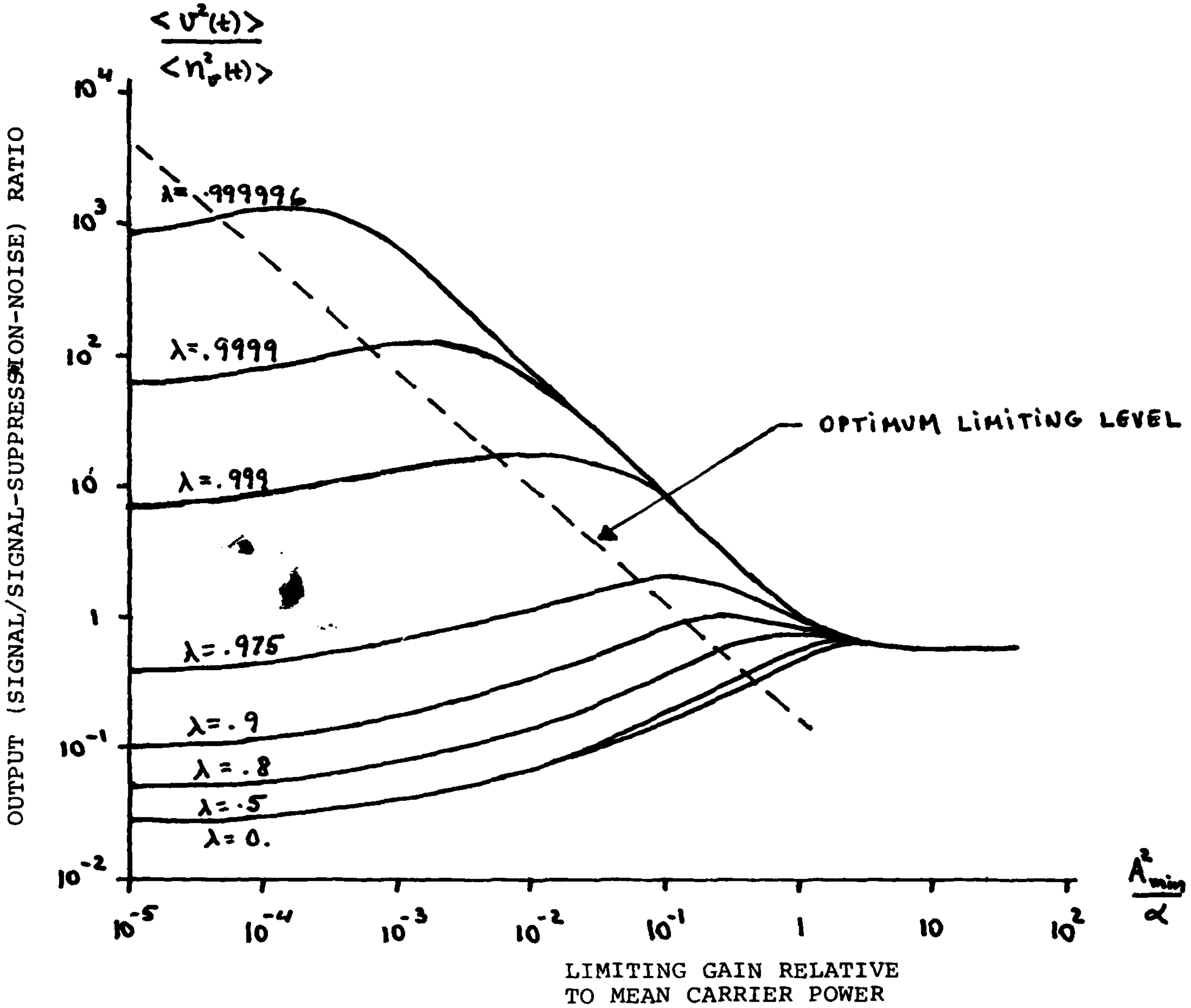

Fig. 3.1-3 Limiting Gain Relative to Mean Carrier Power (from Jakes, 1974)

malized to mean carrier power, α/A_{min}^2. As seen from these curves, there is an optimum level at which to limit the AGC for each correlation amplitude, λ, as indicated by the dashed curve (the optimum is rather broad though). On the other hand, when $A_{min}^2/\alpha > 1$, the signal-to-signal suppression noise ratio is equal to that in the absence of AGC (i.e., Eq. 3.1-24).

The correlation between the gain control voltage, $A_p(t)$, and the fading envelope, $A(t)$, is very close to unity when the frequency separation between the pilot and the carrier is minimal, or when the AGC loop time constant, τ, satisfies the constraint [Ohlson, 1974]

$$f_m\tau << 1 << 0.1\ B\tau \qquad (3.1\text{-}36)$$

Since the AGC loop filter bandwidth is in the order of $1/2\pi\tau$, Eq. (3.1-36) requires that the AGC bandwidth be greater than the fading rate, f_m, but smaller than the lowest modulation frequency, 0.1B. Obviously, these two constraints can only be satisfied if the fading rate is slower than the lowest modulation frequency to begin with. If it is not, a pilot tone AGC must be used.

When the amplitude correlation is very close to unity, an optimum signal-to-signal suppression noise ratio of 30 dB can be achieved when the limiting gain is such that $\alpha g_{max}^2 = \alpha/A_{min}^2 \sim 10^3$ to 10^5.

These results also apply to SSB where the format of the detector signal output is different from that of a DSB-AM system, but the AGC concept is similar. In this case, the signal-to-signal suppression noise is greater by a factor of $1+2/m^2$ where m is the modulation index of DSB-AM system which is being compared with SSB.

3.1.5 Frequency-Selective Fading AM and SSB Performance

When the coherence bandwidth of the transmission medium is smaller than the modulation bandwidth, B, the fading introduced by the medium is frequency selective. This type of fading is caused by multipath propagation when the multipath delay spread is greater than the inverse of the modulation bandwidth, B, since the coherence bandwidth is approximately equal to the inverse of the delay spread. At HF this situation arises when energy propagates via both the ground wave and skywave or when skywave propagation predominates and the skywave field consists of many returns whose delay spread is greater than .3 msec (for a 3 kHz modulation bandwidth).

We may estimate the distortion of AM and SSB systems by calculating the effective signal-to-noise ratio as before. This may be done by representing the impulse response of the frequency-selective transmission medium as

$$h(t) = A_o \delta(t) + \sum_{k=1}^{L} A_k e^{j\Theta_k} \delta(t-t_k) \qquad (3.1\text{-}37)$$

where the A_k are the gains (attenuations) of each path (return), the Θ_k are the relative phases, the t_k are the relative delays, and L is the total number of echoes.

Since frequency-selective fading is caused by signal energy arriving from many directions and at different times, it is more appropriate to deal with instantaneous power rather than time averaged power. In particular, the received signal at a particular time t_o is given by

$$y(t_o) = A_o x(t_o) + \sum_{k=1}^{L} A_k \ell^{j\Theta k} x(t_o - t_k) + n(t_o) \qquad (3.1\text{-}38)$$

where the first term is the desired signal, the second term is the multipath interference, and the third term is the receiver or ambient noise. The (ensemble) average signal-to-noise ratio at time t_o is thus (assuming the individual returns are statistically independent)

$$\mathrm{SNR} = \frac{\langle A_o^2 \rangle R_x(0)}{R_n(0) + \sum_{i=1}^{L} \langle A_k^2 \rangle R_x(0)} \tag{3.1-39}$$

where $R_x(0)$ is the average transmitted power (which is assumed to be independent of time (i.e., stationary) and $R_n(0)$ is the average noise power (in the RF bandwidth of interest). Note that the interference power is directly proportional to the transmitted power.

When the transmitted signal is an AM waveform, $R_x(\tau) = A_c^2 \cos \omega_o \; [1+m^2 R_f(\tau)]$, where $R_x(\tau)$ is the autocorrelation of the AM waveform, $R_f(\tau)$ is the autocorrelation of the modulation (for speech we have assumed in previous sections that $R_f(\tau) \approx .5\delta(\tau)$). The effective signal-to-noise ratio (prior to detection) is then

$$(\mathrm{SNR})_{AM} = \frac{A_c^2 \; m^2 \; R_f(0) \; \langle A_0^2 \rangle}{2\eta B + A_c^2 [1+m^2 R_f(0)] \sum_{K=1}^{L} \langle A_K^2 \rangle} \tag{3.1-40}$$

Letting $A_o^2 = 1$ and recalling that $A_c^2/4\eta B$ is the carrier-to-noise ratio for AM systems, we can rewrite (3.1-40) as:

$$(SNR)_{AM} = \frac{m^2 \rho_o}{1+\rho_o(2+m^2)\ \varepsilon^2} \qquad (3.1\text{-}41)$$

where ρ_o is the AM carrier-to-noise ratio and ε^2 is the interference-to-signal power ratio defined as:

$$\varepsilon^2 = \frac{\Sigma \langle A_K^2 \rangle}{\langle A_o^2 \rangle} = \sum_{K=1}^{L} \langle A_K^2 \rangle \qquad (3.1\text{-}42)$$

Equation (3.1-41) shows that when the carrier-to-noise ratio is greater than the signal-to-interference ratio ($\rho_o >> \varepsilon^{-2}$), the average signal-to-noise ratio is dominated by the signal-to-interference ratio. Furthermore, if the interference power is in the order of the direct signal power or greater, ($\varepsilon \geq 1$), the signal-to-noise ratio will be well below the levels required for just usable voice quality (at least 15 dB below).

When the transmitted signal is a SSB waveform, $R_x(\tau) = A^2[R_f(\tau) \cos \omega_o \tau - \hat{R}_f(\tau) \sin \omega_o \tau]$ where $\hat{R}_f(\tau)$ is the Hilbert transform of $R_f(\tau)$. Thus for speech, the effective signal-to-noise ratio for SSB transmission is (assuming $\langle A_o^2 \rangle = 1$)

$$(SNR)_{SSB} = \frac{A^2}{2\eta B + A^2 \varepsilon^2} \qquad (3.1\text{-}43)$$

which for large $A^2/2\eta B$ reduces to $(SNR)_{SSB} \sim \varepsilon^{-2}$. Thus, the signal-to-noise ratio of SSB is greater than that of DSB-AM

by a factor of $1+2/m^2$ where m is the modulation index of the DSB-AM signal.

In order to determine the maximum acceptable level of interference-to-signal power ratio, ε^2, we have plotted (3.1-43) and (3.1-41) in Fig. 3.1-4 for two values of the SNR in the absence of selective fading. It is seen that when the signal-to-noise ratio in the absence of fading is 30 dB (good quality voice), the effective SNR in selective fading falls below acceptable levels (12 dB) when the interference-to-signal power exceeds .08 (-11 dB) for SSB transmission and .04 (-14 dB) for DSB-AM transmission. When the SNR in the absence of fading is just acceptable (12 dB), the effective SNR drops below acceptable levels when the interference-to-signal power ratio is greater than .003 (-25 dB) for both AM and SSB.

These results (3.1-41 and 3.1-43) show that frequency selective fading has a disastrous effect on AM and SSB transmission which cannot be compensated for by increasing the signal power. However, when the interference is such that

$$\sum_{K=1}^{L} |A_K| < |A_O| \tag{3.1-44}$$

an adaptive multipath cancellation technique using transversal filters [Morgan, 1978] may be used to reduce ε to acceptable levels. If the constraint (3.1-44) is not satisfied then non-linear processing techniques such as Cepstrum analysis can be used [Kemerait and Childens, 1972]. Both of these techniques result in a more complex receiver structure.

3.2 Digital Modulation System Performance

Most Army HF Radios have the capability to transmit narrowband digital data at low data rates. The data is binary

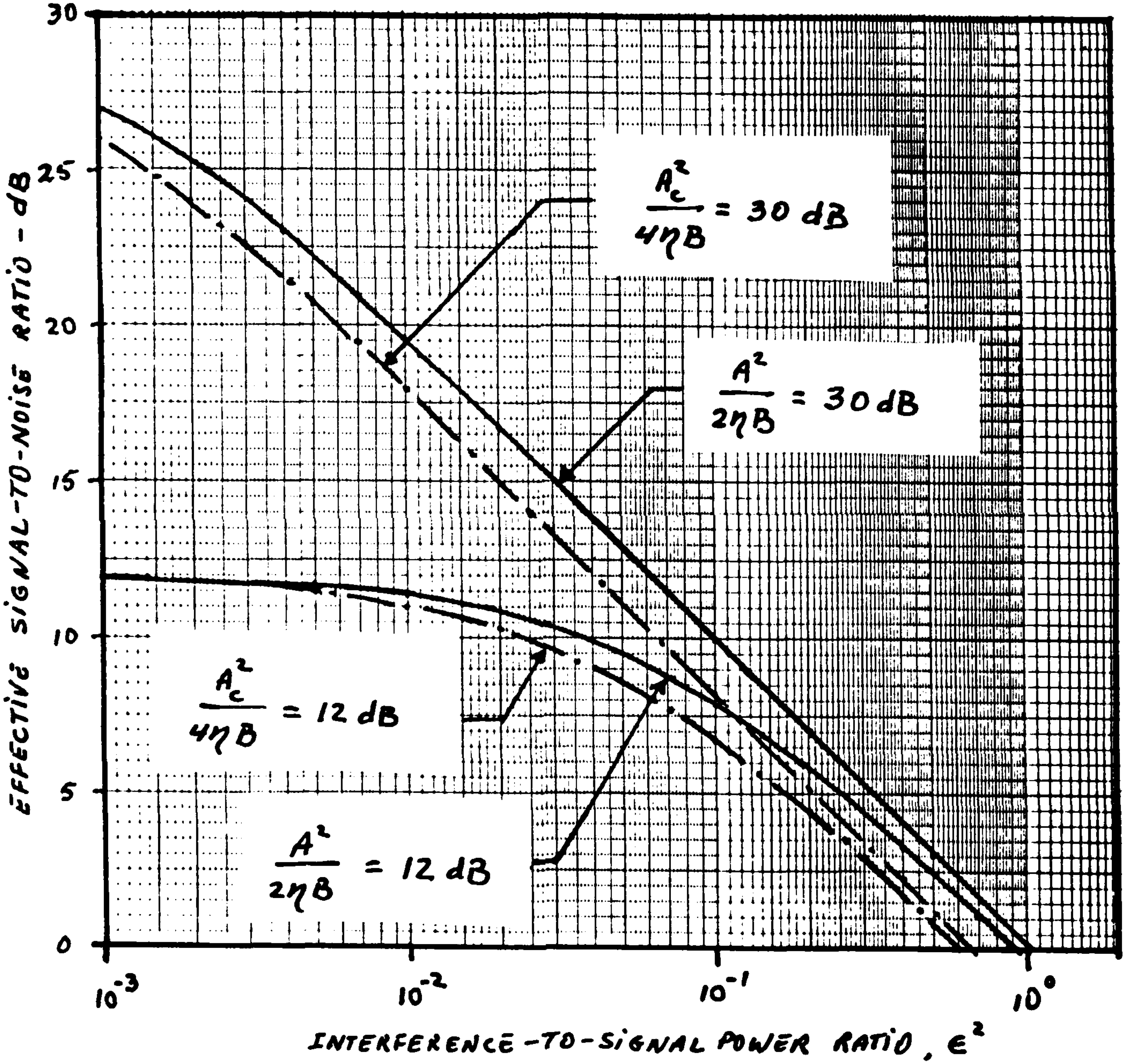

Fig. 3.1-4 Effective SNR versus interference-to-signal power ratio for AM and SSB in the presence of frequency selective fading

teletype data and typical data rates are 75 baud (bits per second) for single-channel transmission and 2400 baud for four-channel time-division-multiplexed transmissions or encrypted single-channel data. The teletype data is transmitted using binary non-coherent-frequency-shift-keying (NCFSK). A binary NCFSK system is characterized by its modulation (data) rate and the frequency shift used. The modulation rate is defined as the reciprocal of the signalling unit interval (1/T) measured in seconds and is expressed in baud. The frequency shift, f_s, is the difference between the frequencies corresponding to the "mark" and "space" elements. The ratio of the frequency shift to the modulation rate is often called the modulation index, f_sT, which is usually greater than unity.

A noncoherent FSK signal can be demodulated by either a limiter-discriminator demodulator or a dual-filter followed by envelope detection demodulator. When the IF filter bandwidth in a limiter-discriminator demodulator is equal to twice the bandwidth of the "mark" and "space" filters in a dual-filter demodulator, the performance (in terms of bit error probability) for both systems is nearly identical [Schwartz, Bennet and Stein, 1966].

When several teletypewriter signals are to be transmitted simultaneously, either a time-division multiplexing (TDM) or frequency-division multiplexing (FDM) technique is used. In a TDM-NCFSK system, a number of teletypewriter signals are time-division multiplexed first, and the multiplexed signal is used to frequency-shift-key the RF carrier. The modulation rate is equal to the number of teletypewriter signals times the modulation rate of a single channel system. The type of emission is the same as that of a single-channel system also, the modulated RF wave has constant amplitude, and its performance can be analyzed in exactly the same manner as that of a single-channel system.

In an FDM-NCFSK system, a number of subcarriers or tones uniformly spaced in frequency, usually in a 3 kHz bandwidth, are used. Each subcarrier is frequency-shift keyed by one teletypewriter signal and the composite baseband signal of all the tones is transmitted as a sideband signal of a SSB or ISB-AM system. The modulation rate in each subchannel of an FDM-NCFSK system is the same as that of a single-channel system. The type of emission for this system is different from that of a single-channel or a TDM-NCFSK system, and the amplitude of the modulated RF wave is not constant. The performance of a single subchannel in an FDM-NCFSK system is analyzed in the same way as a single-channel NCFSK system. To obtain the required signal-to-noise ratio for an FDM-NCFSK system we have to multiply the required ratio for a single channel system not only by the number of subchannels, but also by a factor corresponding to the ratio of the peak envelope power to the average power of the RF signal.

Basically, there are two teletypewriter systems: start-stop and synchronous systems. The two systems are significantly different in two aspects: (a) the relation between teletypewriter speed and modulation rate; and (b) the relation between character error probability and binary element or bit error probability.

Akima, et al., [1969], have determined the relation between the start-stop and synchronous teletypewriter systems (in words per minute per channel) and the modulation rate in baud (bits per seconds). Table 3.3 shows the modulation rates derived by Akima corresponding to some typical teletypewriter speeds for various multiplexing techniques.

The quality of teletypewriter transmissions is usually specified in terms of character error probability, while the basic quantity that is theoretically calculated is the bit or

Table 3.3

Relation Between Teletypewriter Speed and Modulation Rate in 5-Unit Teletypewriter Systems

Channel Multiplexing	Teletypewriter System	Teletypewriter Speed (w/m/ch)	Modulation Rate (bauds)
Single-channel	Start-Stop	60	45
		100	75
	Synchronous	60	36
		100	60
Frequency-division-multiplexing	Start-Stop	60	45
		100	75
Two-channel time-division-multiplexing	Synchronous	60	72
		100	120
Four-channel time-division-multiplexing	Synchronous	60	144
		100	240

element error probability. When binary element errors occur independently of each other, the character error probability P_c is given as a function of the element error probability P_e by

$$P_c = 1 - (1-P_e)^{17} \simeq 17\ P_c \qquad (3.2\text{-}1)$$

for a start-stop system, and by

$$P_e = 1 - (1-P_e)^{5} \approx 5\ P_e \qquad (3.2\text{-}2)$$

for a synchronous system [Watt, et al., 1958].

Since the character error probability is directly proportional to the bit or element error probability, we will give the performance of NCFSK in terms of P_e. The required bit or element error probabilities, P_e, for typical character error probabilities are listed in Table 3.4. In the remainder of this section, we discuss the relationship between the element error probability and the average detected signal-to-noise ratio under nonfading conditions, slow flat-fading conditions, fast flat-fading conditions and frequency selective-fading conditions.

3.2.1 Nonfading NCFSK System Performance

The performance of NCFSK in pure Gaussian noise is well known and is given by [Schwartz, Bennet and Stein, 1966]

$$P_e = 1/2\ e^{-\gamma/2} \qquad (3.2\text{-}3)$$

where γ is the ratio of the average signal power in one filter to average noise power in one filter of bandwidth $2B=1/T$ where T is the element or bit duration. Thus,

Table 3.4

Values of Element Error Probability P_e Corresponding to Some Typical Values of Character Error Probability P_c in 5-Unit Teletypewriter Systems

Teletypewriter System	P_c (%)	P_e (%)
Start-Stop	1	0.059
	0.1	0.0059
	0.01	0.00059
Synchronous	1	0.2
	0.1	0.02
	0.01	0.002

$$\gamma = \frac{A^2T}{2N_o} \tag{3.2-4}$$

where A is the amplitude (envelope) of the received signal, N_o is the noise density which is assumed to be flat over the filter of bandwidth 1/T.

The element error probability for NCFSK is shown in Fig. 3.2-1 as a function of the signal-to-noise ratio, γ, along with that for other binary signalling schemes. From the curve for NCFSK we can see that in order to achieve a character error probability $P_c=10^{-2}$ with a start-stop teletypewriter system ($P_e \sim 6x10^{-4}$), the signal-to-noise ratio in pure Gaussian noise must be 11.5 dB. The required signal-to-noise ratio for synchronous teletypewriter system ($P_e \sim 2x10^{-3}$) is 10.5 dB. The required signal-to-noise ratios for smaller character error probabilities are greater and may be read directly from the graph.

The curves of Fig. 3.2-1 have been obtained for the case in which the noise has Gaussian statistics. However, HF noise is atmospheric, and in general does not have Gaussian statistics. In this case, the element error probability is one-half the amplitude probability distribution (APD) of the noise corresponding to the level of the received signal. The APD of atmospheric noise can be represented sufficiently accurately for most applications by an appropriate curve chosen out of a family of idealized curves. The ratio of the rms to average of the envelope of the noise, denoted V_d (in dB), is used to specify the curve that can be used to represent the noise envelope distribution [CCIR, 1964]. For Gaussian noise V_d=1.049 dB. For atmospheric noise V_d is usually greater than this value. Curves of the element error probability in atmospheric noise as a function of the signal-to-noise ratio

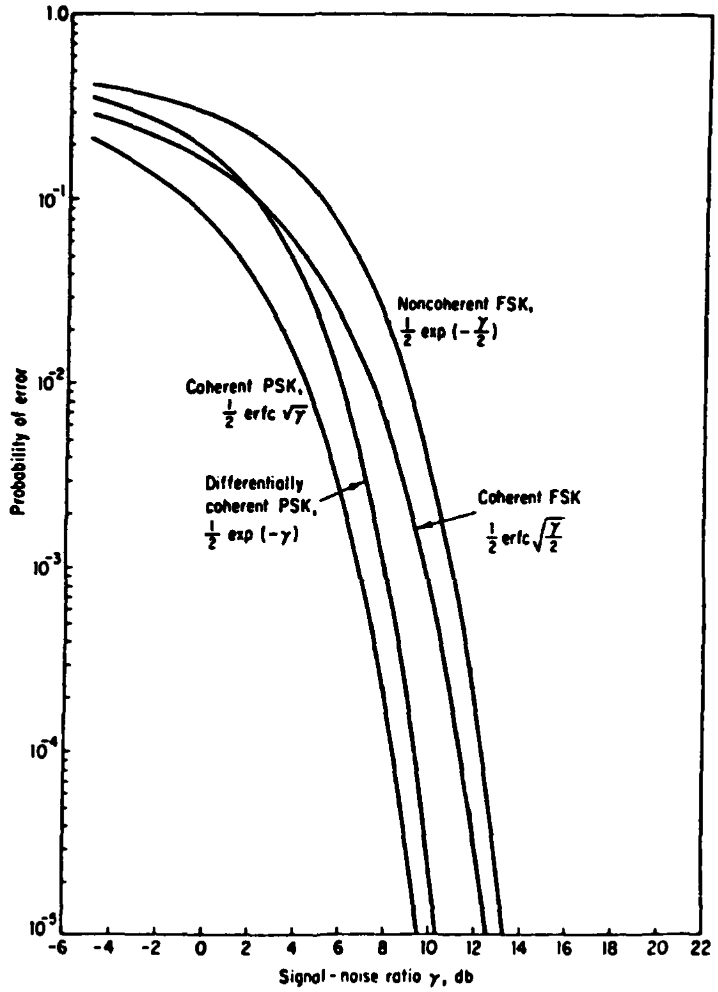

Fig. 3.2-1 Bit (element) error probability versus signal-to-noise ratio (from Schwartz, Bennet and Stein, 1967)

and the noise parameter V_d are given by [Akima, et al., 1969] and are reproduced in Fig. 3.2-2. The curve for V_d=1.049 dB corresponds to the curve for NCFSK in Gaussian noise. However, the signal-to-noise ratios of Fig. 3.2-2 for a given error probability are smaller by a factor of 2 (3 dB) than those of Fig. 3.2-1 because the noise is in a bandwidth equivalent to the sum of the bandwidths of the "mark" and "space" filters. Thus, in Fig. 3.2-1 the signal-to-noise ratio is defined as $\gamma'=A^2T/4N_o$.

The parameter V_d depends largely on the season, the local time of day, the operating frequency, and the receiver bandwidth [CCIR, 1964]. In the lower region of the HF band, it is almost independent of the season and local time. When the two-filter bandwidth $2/T \sim 200$ Hz, it is around 6 dB. Thus, the required signal-to-noise ratio $\gamma=A^2T/2N_o$ for a character error probability of 10^{-2} is 22.6 dB for a start-stop teletypewriter system ($P_e \sim 6\times10^{-4}$) and 18.7 dB for a synchronous teletypewriter system ($P_e \sim 2\times10^{-3}$).

3.2.2 Frequency-Flat Fading NCFSK Performance

Most of the studies on the performance of NCFSK systems under fading conditions have been limited to the case in which the noise is Gaussian except for [Bello, 1965] in which approximate results for the case of slow flat-fading conditions and atmospheric noise are given. Thus, in this section we will consider the effects of flat fading and frequency selective fading in the presence of Gaussian noise only. The effects of atmospheric noise will only be considered in the case of slow flat-fading conditions.

a. Slow Fading Conditions

When the fading rate is sufficiently slow such that changes over a few pulse intervals can be disregarded,

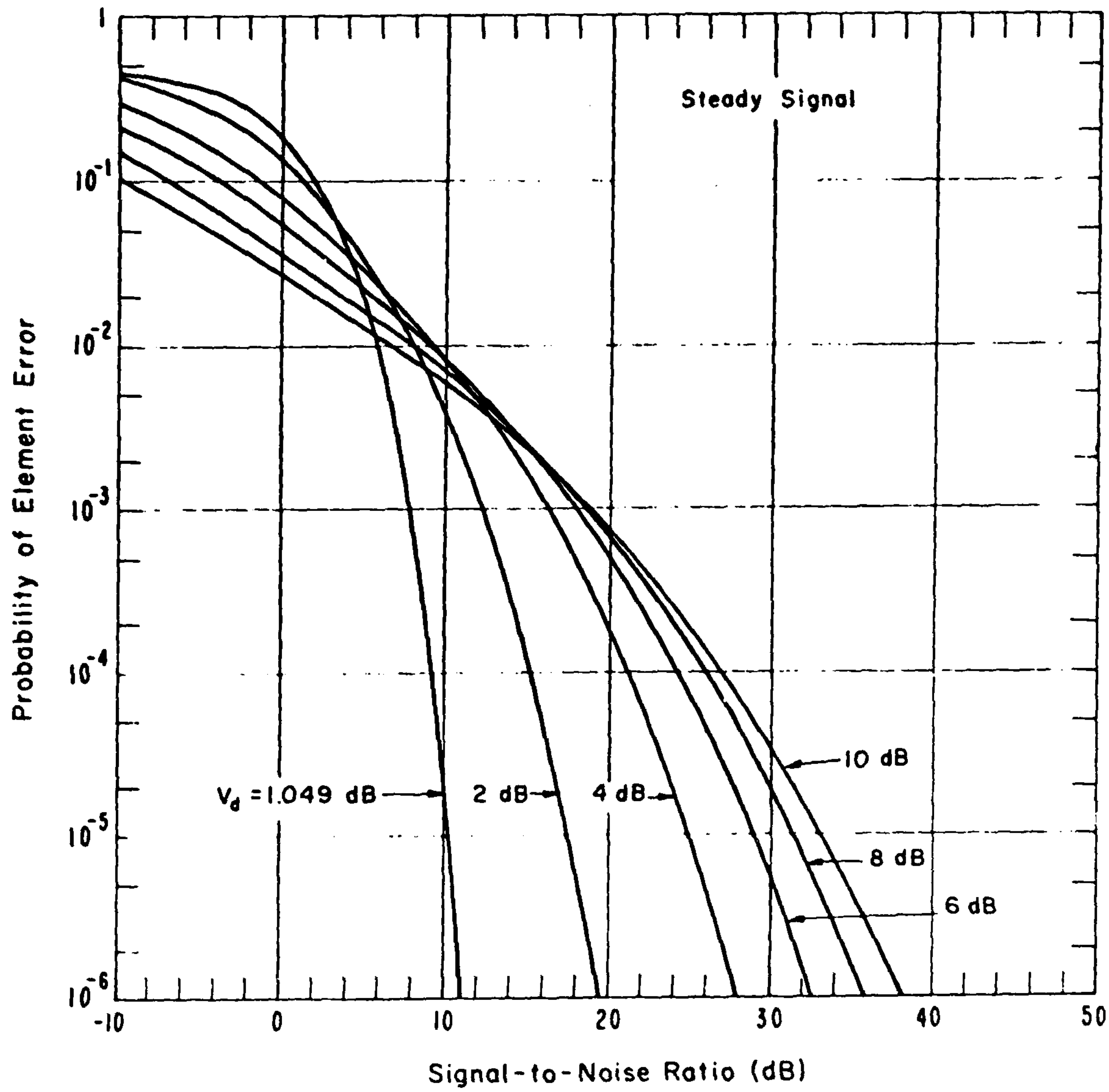

Fig. 3.2-2 Element error probabilities in a single-channel NCFSK system under stable conditions. (Signal-to-noise ratio is the ratio of signal power to average noise power, and V_d is the ratio of rms to average of the noise envelope voltage, both measured at the input to the limiter in a limiter-discriminator demodulator, and measured in a bandwidth equivalent to the sum of the bandwidths of the two filters in a dual-filter demodulator. Modulation index is assumed to be not less than unity, and no low-pass filter is used before the decision-making circuit.)
(from Akima, et al., 1969)

the element error probability is equal to the error probability in the absence of fading, averaged over the fading statistics [Schwartz, Bennet and Stein, 1966]:

$$\hat{P}_e = \int_0^\infty P_e(\gamma)\, p(\gamma)\, d\gamma \qquad (3.2\text{-}5)$$

where $P_e(\gamma)$ is the element error probability due to Gaussian or atmospheric noise only, and $p(\gamma)$ is the density function of the normalized square of the envelope of the received signal (Eq. 3.2-4) which completely describes the statistics of the fading.

Pierce [1958] has determined the element error probability, P_e, for NCFSK for the case of slow Rayleigh fading and additive Gaussian noise with diversity reception. His results show that when Mth order diversity is used, the element error probability is given by

$$\hat{P}_e = \left[\frac{1}{2+\gamma_o}\right]^M \sum_{m=0}^{M} \frac{(m+M-1)!}{m!\,(M-1)!} \left[\frac{1+\gamma_o}{2+\gamma_o}\right]^m \qquad (3.2\text{-}6)$$

where γ_o is the mean signal-to-noise ratio, i.e.,

$$\gamma_o = \frac{\langle A^2 \rangle T}{2N_o} = \frac{\alpha T}{2N_o} \qquad (3.2\text{-}7)$$

The parameter α is equal to $2S_o$ where S_o is the long-time average received power defined by Pierce [1958].

Equation (3.2-6) for M=1 (no diversity) is shown in Fig. 3.2-3 as a function of γ_o along with similar curves for other types of signalling schemes. The curve for NCFSK shows that a single channel subject to slow flat-Rayleigh

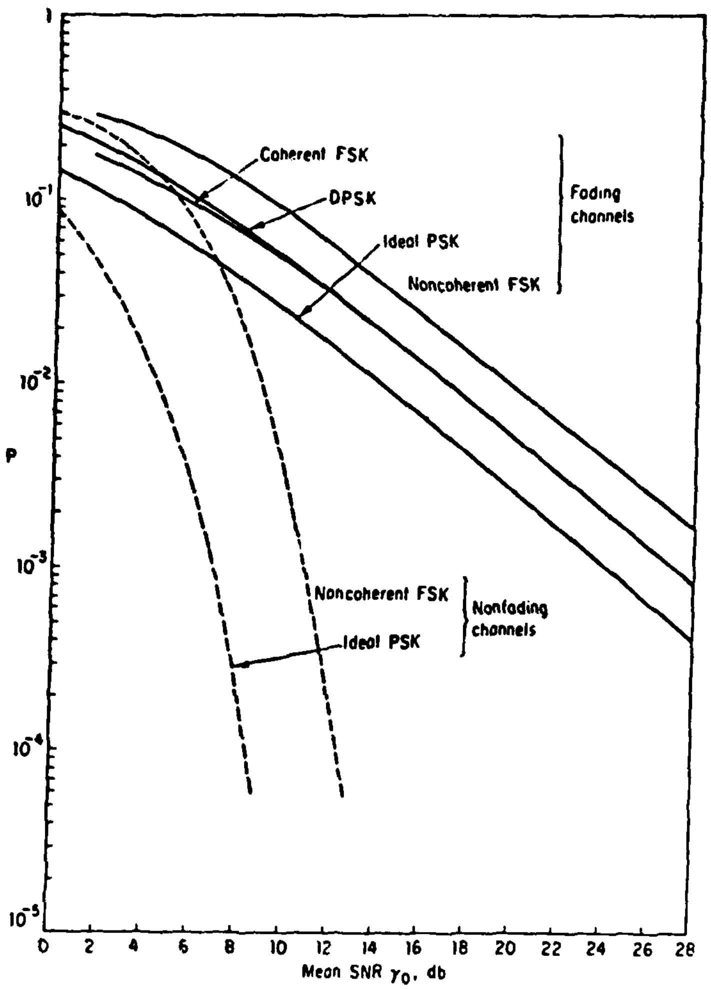

Fig. 3.2-3 Probability of error for several systems in Rayleigh fading (from Schwartz, Bennet, and Stein, 1967)

fading requires additional system margins (mean SNR required in fading as compared with SNR required in the absence of fading) of the order of 18 dB for element error rates of 10^{-3} with approximately an additional 10 dB for every order of magnitude (factor of 10) further decrease in allowed system error rate.

The additional system margin required in Rayleigh fading can be reduced substantially if diversity reception is used. Curves of bit error probability as a function of average signal-to-noise ratio for various orders of diversity may be found in [Pierce, 1958 - Fig. 1].

The error probabilities derived by Pierce are only valid for the case in which the fading is Rayleigh distributed and the noise is Gaussian. Lindsay [1964] has derived the element error probabilities for NCFSK for the case of Mth order diversity and Rician fading in Gaussian noise. In this case, the error probability is given by

$$\hat{P}_e(M) = \left[\frac{1}{2+\gamma_o}\right]^M \exp\left\{-\frac{\rho_o}{2+r_o}\right\}$$

$$\sum_{m=0}^{M-1} \frac{(m+M-1)!}{(M-1)!} \left(\frac{1+\gamma_o}{2+\gamma_o}\right)^m \frac{X^m}{m!} \tag{3.2-8}$$

where γ_o is given by (3.2-7) and

$$\rho_o = \frac{A_o^2 T}{2N_o} \tag{3.2-9}$$

$$X = \frac{\rho_o}{(1+\gamma_o)(2+\gamma_o)} \tag{3.2-10}$$

The ratio of specular-to-Rayleigh component is equal to

$$R = \frac{\rho_o}{\gamma_o} = \frac{A_o^2}{\alpha} \qquad (3.2\text{-}11)$$

Hence, when $\rho_o=0$, (3.2-8) reduces to the pure slow Rayleigh fading case derived by Pierce [1958]. When M=1, (3.2-8) reduces to

$$\hat{P}_e = \frac{1}{2+\gamma_o} \exp\left\{-\frac{\rho_o}{2+\gamma_o}\right\} \qquad (3.2\text{-}12)$$

From this expression we can see that when the Rayleigh fading component becomes negligible (γ_o=o), the element error probability approaches that of the steady NCFSK signal (no fading) in Gaussian noise (Eq. 3.2-3). On the other hand, when the specular component is negligible (ρ_o=o), (3.2-12) reduces to the case of a Rayleigh fading NCFSK signal in Gaussian noise (Eq. 3.2-7).

Plotted in Fig. 3.2-4 are the element error probabilities derived by Lindsay [1964] for various orders of diversity as a function of the average signal-to-noise ratio

$$\gamma_{AV} = (1+R)\ \gamma_o = \rho_o + \gamma_o \qquad (3.2\text{-}13)$$

for the cases R=0 (pure Rayleigh fading), R=∞ (no fading), R=8 and R=16. These curves show that as the ratio of specular-to-Rayleigh component increases, the additional margin in SNR (over the no-fading case) required to achieve a desired element-error probability decreases. Furthermore, even if the

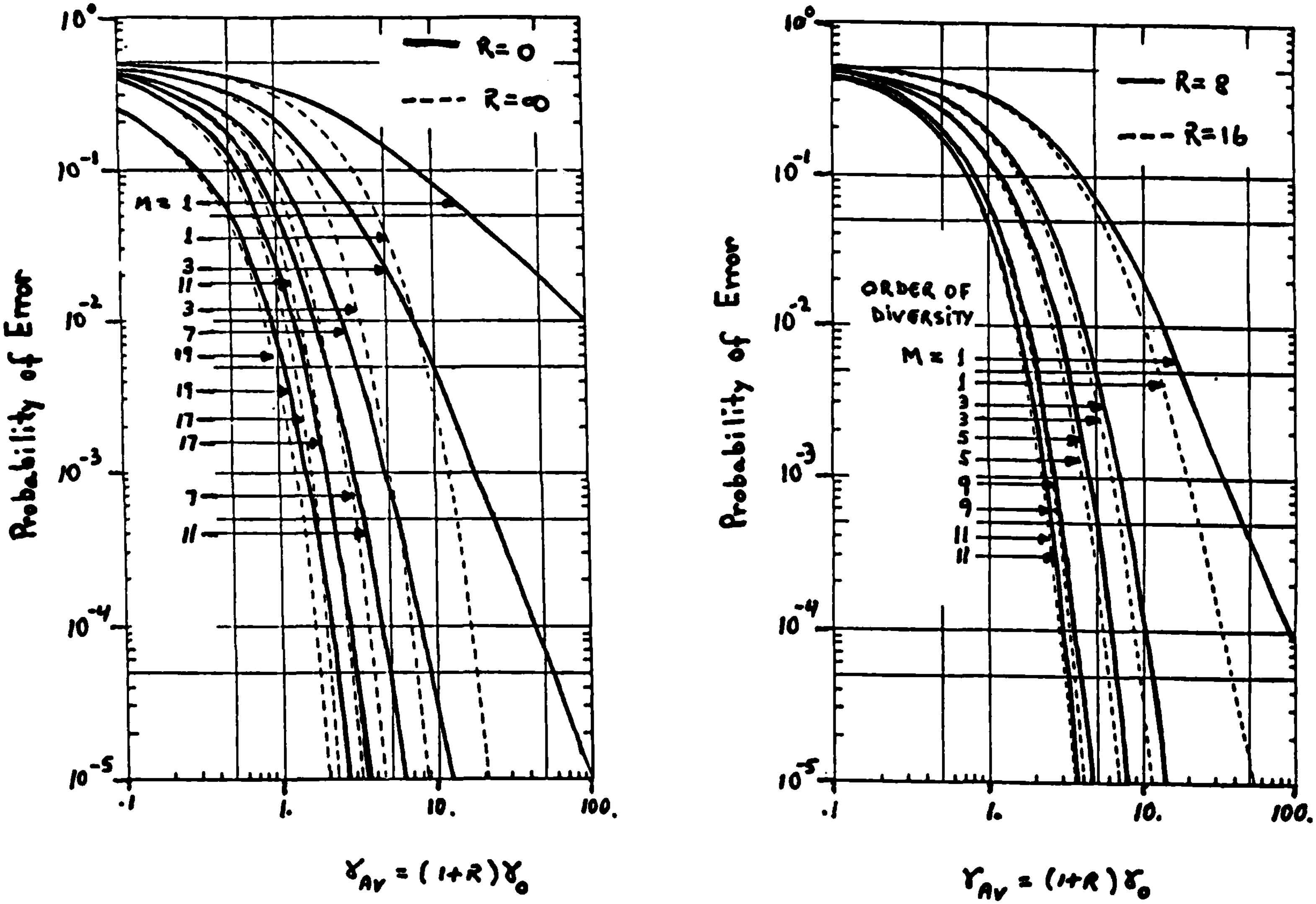

Fig. 3.2-4 Probability of error for NCFSK systems in Rician fading for various orders of diversity M. (from Lindsay, 1964)

specular component is 16 times greater (12 dB) than the Rayleigh fading component, an additional margin of 8.5 dB in SNR over the SNR required under no fading conditions (11.5 dB) is needed. However, if third order diversity (M=3) reception is used, no additional margin is required.

The error probabilities in flat (non-selective) Rayleigh and Rician fading discussed above have been derived assuming that the additive noise is Gaussian. Since the additive noise at HF is predominantly atmospheric, these results are not strictly valid although they provide us with an estimate of the additional margins required under slow fading conditions. Element error probabilities for flat Rayleigh fading NCFSK is the presence of atmospheric noise have been derived by Bello [1965] for the general case of Mth order diversity reception. He has found that when no diversity is used (M=1), the error probabilities due to atmospheric noise will be lower than those due to Gaussian noise while the opposite will be true when diversity is used. At high SNR's and nondiversity operation, the error probability is independent of the noise statistics. Thus, in the case of no diversity operation, the results of Pierce [1958] and Lindsay [1964] provide us with the necessary requirements. At high SNR and Mth order diversity, the SNR degradation (additional margin required) of system performance (in dB) with atmospheric noise as compared to Gaussian is given by [Bello, 1965].

$$(SNR)_{deg} = V_d(M-1) - \frac{10}{M}\log_{10}\frac{(2M-1)!}{M^M(M-1)!} \qquad (3.2\text{-}14)$$

where V_d is the noise parameter previously defined.

The effective signal-to-noise ratio required for a given error probability in atmospheric noise is

$$(\gamma_A)_{dB} = (\gamma_o)_{dB} + (SNR)_{deg} \qquad (3.2\text{-}15)$$

where γ_o is the average signal-to-noise ratio required in the presence of Gaussian noise (Eq. 3.2-7).

Table 3.5 summarizes the required signal-to-noise ratios for teletypewriter systems with character error probabilities, P_c, of 10^{-2}, 10^{-3} and 10^{-4} and no fading, slow flat-Rayleigh fading and flat-Rician fading and atmospheric noise. The value of the noise parameter V_d assumed in obtaining the values of required SNR is V_d=6 dB as recommended by Akima [1969].

b. Fast-Fading Conditions

The previous results were obtained assuming that the fading was slow enough so that changes over a few pulse intervals could be disregarded. When the fading rate is comparable to the data rate 1/T, a degradation in the system performance occurs resulting in an irreducible error probability. Bello and Nelin [1962] have derived the error probabilities for NCFSK in Rayleigh fading with Gaussian and exponential fading spectra and in the presence of additive Gaussian noise. The element error probability is again given by:

$$\hat{P}_e(M) = \left[\frac{1}{2+\gamma_e}\right]^M \sum_{m=0}^{M-1} \frac{(m+M-1)!}{m!\,(M-1)!} \left[\frac{1+\gamma_e}{2+\gamma_e}\right]^m \qquad (3.2\text{-}16)$$

which is identical to the expression obtained by Pierce [1958] for the zero-bandwidth fading spectrum except that γ_e is now an effective signal-to-noise ratio which depends on the shape of the fading spectrum and its half-power bandwidth, B (i.e., fading rate). When the fading rate is negligible compared to the data rate (B=o), γ_e is equal to γ_o (Eq. 3.2-7).

TABLE 3.5 Required Signal-To-Noise Ratios for Single Channel NCFSK System Over HF Paths With Atmospheric Noise Parameter $V_d = 6$ dB

Teletypewriter System	Character Error Probability P_c(%)	Required Average Signal-To-Noise Ratio (dB)*			
		No Fading	Slow Flat Rayleigh Fading		Slow Rician Fading $A_o^2/\alpha=8$ (9 dB)
			No Diversity	Dual Diversity	No Diversity
Start-Stop	1	17.	30.8	22.	24.5
	0.1	23.	41.	28.5	31.
	0.01	27.	51.	33.5	36.5
Synchronous	1	12.7	26.9	20.	21.
	0.1	19.5	37.0	27.	28.
	0.01	25.0	47.0	32.	34.

*The average noise power in a dual-filter demodulator system is measured at the output of a "mark" or "space" filter in a bandwidth of 1/T. The equivalent noise power in limiter-discriminator demodulator is measured at the input to the limiter in a bandwidth of half-the IF filter bandwidth. This is equivalent to the bandwidth of the "mark" or space filter in a dual filter system.

Bello and Nelin [1962] have derived exact and asymptotic expressions for the effective SNR, γ_e, for the case of a Gaussian fading spectrum and exponential fading spectrum. When the fading rate is smaller than the data rate (BT<1), the effective SNR for the case of "mark" and "space" waveforms separated by f_s Hz is given by

$$\gamma_e \simeq \frac{\gamma_o}{1+\frac{2BT}{\pi(f_sT)^2}\gamma_o}\left\{1-2\pi BT\left[\frac{1}{3}+\left(\frac{1}{\pi f_sT}\right)^2\right]\right\} \tag{3.2-17a}$$

for an exponential fading spectrum and by

$$\gamma_e \simeq \frac{\gamma_o}{1+\frac{(BT)^2\gamma_o}{2\ell n2(f_sT)^2}}\left\{1-\frac{(\pi BT)^2}{2\ell n2}\left[\frac{1}{3}-\left(\frac{1}{\pi f_sT}\right)^2\right]\right\} \tag{3.2-17b}$$

for a Gaussian fading spectrum.

From the equations for the effective SNR, we can see that even when the actual SNR, γ_o, becomes infinitely large ($\gamma_o \to \infty$), γ_e is finite. Thus, there exists an irreducible error probability (or if one wishes a maximum signal-to-noise ratio caused by the fading). The irreducible error probability depends on the fading bandwidth, shape of the fading spectrum and the frequency separation between the "mark" and "space" waveforms. Fig. 3.2-5 shows various curves for the irreducible error probability as a function of these parameters. From these curves, we can see that it increases as the relative fading bandwidth increases and that it decreases as

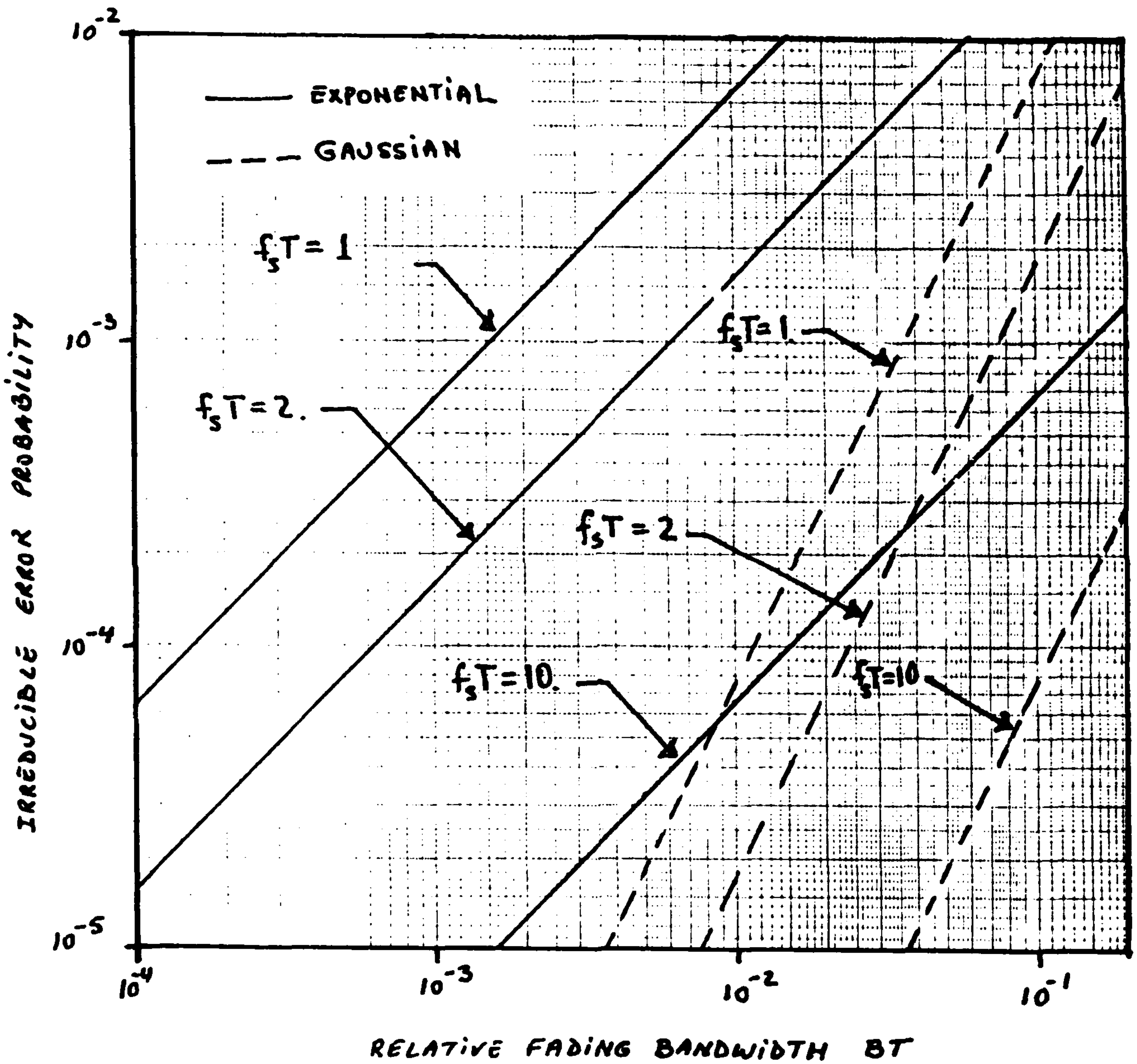

Fig. 3.2-5 Irreducible error probability vs. fading rate for NCFSK in Rayleigh fading

the separation between the tones increase, as expected. It can also be seen that the irreducible error probability for a fixed fading bandwidth, B, and tone separation, f_s, is higher when the spectrum is exponential rather than Gaussian.

When the required element error probability for a NCFSK system is an order of magnitude greater than the irreducible error probability at a given fading bandwidth, B, and tone spacing, f_s, relative to the data rate 1/T, then the mean SNR, γ_o, required to attain that error probability is practically the same as that required under slow flat Rayleigh fading conditions. However, if the desired error probability is of the same order of magnitude (but still greater) than the irreducible error probability, then the average SNR, γ_o, required to attain that error probability must be greater than the average SNR required under slow fading conditions (B=0) by an amount equal to the degradation factor, γ_o/γ_e, where γ_e is now equal to the required SNR when B=0. As the required element error probability approaches the irreducible error probability for a given fading bandwidth and tone separation, the degradation factor (additional margin) approaches infinity. This effect is clearly reflected by the curves of Fig. 3.2-6 where we have plotted the additional SNR (over that required when B=0) required to attain an element error probability $P_e=10^{-4}$ as a function of the relative fading bandwidth, BT, and the relative tone shift, f_sT.

The curves of Figs. 3.2-5 and 3.2-6 indicate that when the tone spacing of a NCFSK system is in the order of the data rate 1/T, fading rates in the order of 1% of the data rate or greater result in a significant degradation which limits the element error probability. The degradation can be reduced by increasing the tone separation (frequency shift) or modulation index, f_sT.

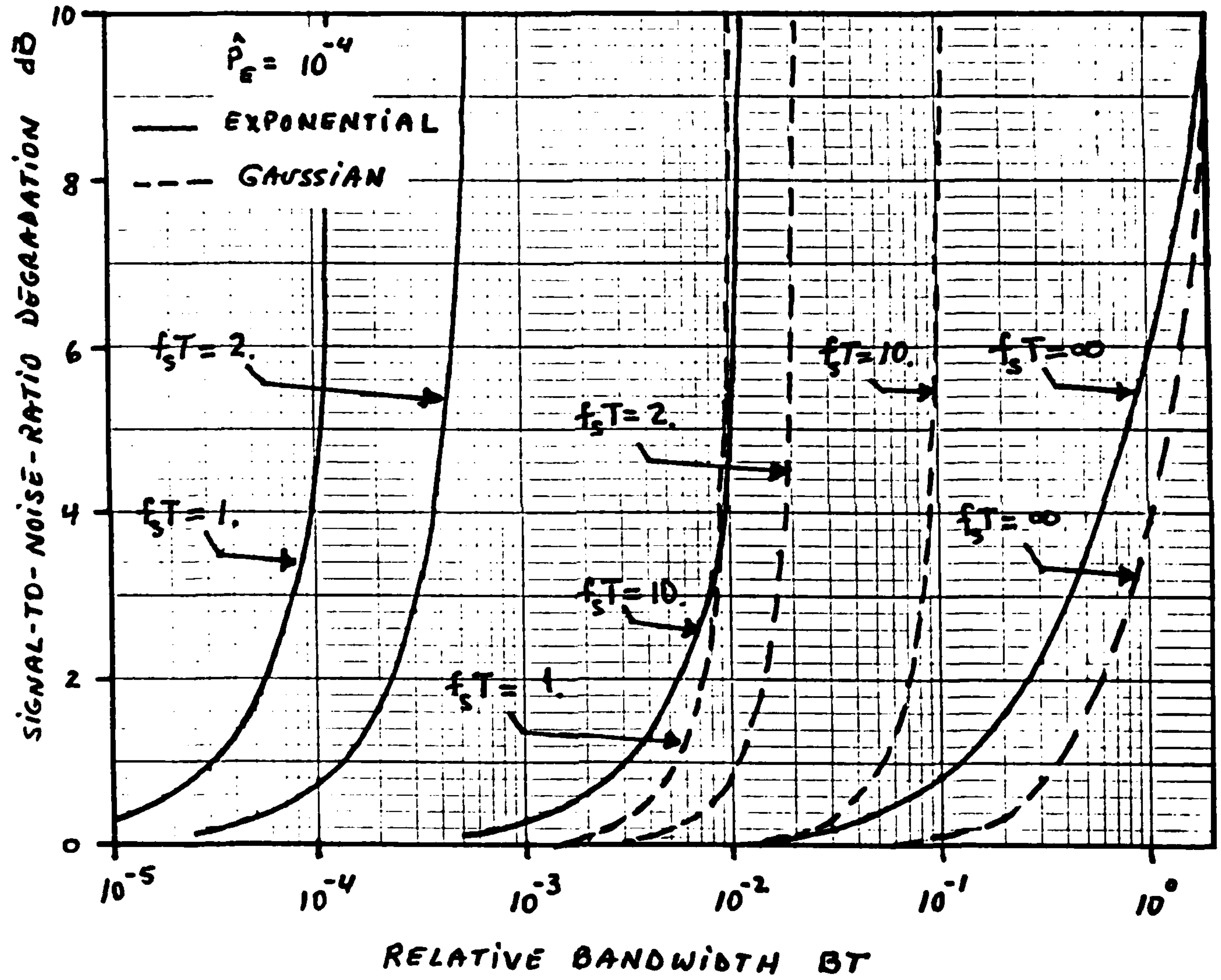

Fig. 3.2-6 Signal-to-noise ratio degradation vs. fading rate for NCFSK in Rayleigh fading

Typical fading rates in HF skywave propagation are in the order of 1 Hz at mid-latitudes and up to 10 Hz in the auroral oval. Hence, single-channel NCFSK teletypewriters which typically operate at rates of 75 baud in a bandwidth of 100 Hz (f_sT=1.33) will be limited to element error probabilities of $7x10^{-5}$ at mid-latitudes (assuming Gaussian fading spectrum) and $7x10^{-3}$ at northern latitudes. Multiplexed NCFSK systems which operate at higher data rates will be limited to similar error probabilities provided that the modulation index remains constant. The performance of these systems in built-up areas where the propagation mode is ground wave may not be deduced as readily as data regarding the statistics and fading rates for ground wave propagation in built-up areas is not available. If the statistics are Rician with a strong specular component (R=5), the irreducible error probabilities for relative fading rates as high as BT=.05 result in irreducible error probabilities in the order of 10^{-5} and lower [Hingorani, 1967] so that fast-fading effects are not as significant as for the case of Rayleigh fading.

3.2.3 Frequency-Selective Fading NCFSK Performance

The results of the previous section assumed that the fading was flat or equivalently, that the tone duration, T, in a NCFSK system was much greater than the multipath spread of the channel. When the multipath spread, M, of the channel is in the order of the tone duration, overlapping between adjacent symbols results in intersymbol interference. Errors due to this type of interference are also referred to as frequency selective fading because the coherence bandwidth of the channel $1/2\pi M$ is smaller than the data rate 1/T. The intersymbol interference (frequency-selective fading) results in an irreducible error probability (or maximum achievable signal-to-noise ratio if you will).

Expressions for the error probability for binary NCFSK in the presence of slow (B=0) frequency selective Rayleigh fading have been obtained by Bello and Nelin [1963] for the case in which the multipath is of the diffuse type with a Gaussian delay spectrum. The error probability expression for this situation is similar to that of (3.2-16) but where the effective SNR, γ_e, depends on the transmitted adjacent symbols. Curves for the irreducible error probability for NCFSK for dual and fourth order diversity may be found in [Bello and Nelin, 1963].

Expressions for the element error probability for NCFSK for the case of discrete multipath with two delayed Doppler shifted Rician fading components have been obtained by Hingorani [1967]. Plots of the irreducible error probability as a function of the normalized multipath spread, M/T, for various values of the relative Doppler shift between the two fading components, BT, and for various specular-to-Rayleigh component power ratios, R, are shown in Fig. 3.2-7. These curves show that for a given tolerable irreducible error probability there is a maximum tolerable multipath spread and/or Doppler spread. These maximum tolerable values increase as the ratio of specular-to-Rayleigh component increases as one might expect. When the fading rate is negligible ($B \simeq 0$), the maximum tolerable normalized multipath spread for a maximum irreducible error probability of 10^{-5} is 0.1 if the specular component is vanishingly small (R=0). The maximum tolerable multipath spread increases to 0.2 when the specular-to-Rayleigh ratio is 5 (7 dB). When the normalized (or relative) fading rate increases above a value of 0.01, the irreducible error probability is dominated by the fading bandwidth as long as the normalized multipath spread is below 0.1. From these considerations it may be concluded that the maximum tolerable pro-

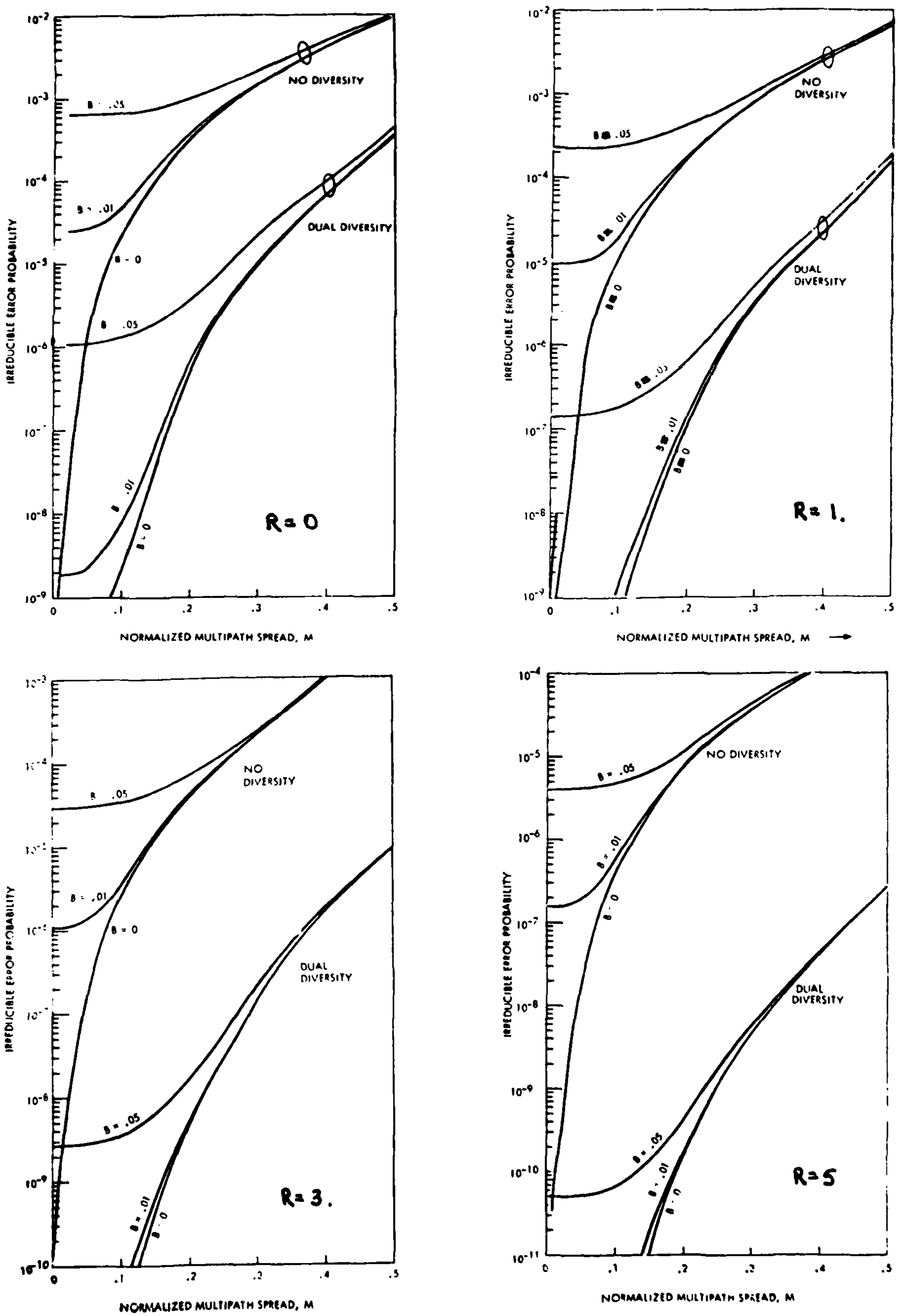

Fig. 3.2-7 Irreducible error probability vs. multipath spread and fade rate for NCFSK in the presence of two Rician discrete multipath components (from Hingorani, 1967)

duct of multipath and Doppler spread is around 0.001 in order for the irreducible error probability to remain below 10^{-5}. Typical values of multipath spread for skywave HF links are in the order of 0.1 to 2 msec, while the fade rates or Doppler spreads are in the order of 1 Hz at mid-latitudes so that the irreducible error probability for these circuits will be around 10^{-5}.

REFERENCES FOR SECTION 3

Akima, H., G.G. Ax and W.M. Beery (1969), "Required Signal-to-Noise Ratios for HF Communications Systems", ESSA Technical Report ERL 131-ITS 92, U.S. Dept. of Commerce, Boulder, Colorado.

Bello, P.A. and B.D. Nelin (1962), "The influence of Fading Spectrum on the Binary Error Probabilities of Incoherent and Differentially Coherent Matched Filter Receivers", IRE Trans. Commun. Syst., V. CS-10, pp. 160-168.

Bello, P.A. and B.D. Nelin (1963), "The Effect of Frequency Selective Fading on the Binary Error Probabilities of Incoherent and Differentially Coherent Matched Filter Receivers", IEEE Trans. Commun. Syst., V. CS-11, pp. 170-186.

Bello, P.A. (1965), "Error Probabilities Due to Atmospheric Noise and Flat Fading in HF Ionospheric Communication Systems", IEEE Trans. Commun. Technol. V. COM-13, pp. 266-279.

Beranek, L.L. (1947), "The Design of Speech Communication Systems", Proc. IRE, V. 35, pp. 880-890.

CCIR (1964), "World distribution and characteristics of atmospheric noise", Report 322, International Telecommunications Union (ITU), Geneva, Switzerland.

Craiglow, R.L., N.R. Getzin and R.A. Swanson (1961), "Power Requirements for Speech Communication Systems", IRE Trans. Audio, V. AU-9, pp. 186-190.

Cunningham, W.T., S.J. Goffard and J.C.R. Licklider (1947), "The influence of Amplitude Limiting and Frequency Selectivity upon the Performance of Radio Receivers in Noise", Proc. IRE, V. 35, pp. 1021-1025.

Ewing, G.D. and N.W. Huddy, Jr. (1966), "RF Clipping and Filtering to Improve the intelligibility of Speech in Noise", IEEE Trans. Audio Electroacoustics, V. AV-14, pp. 184-186.

Griffiths, J.D. (1968), "Optimum Linear Filter for Speech Transmission", J. Acoust. Soc. Am., V. 43, pp. 81-86.

Hingorani, G.D. (1967), "Error Rates for a Class of Binary Receivers", IEEE Trans. Commun. Tech, Vol. COM-15, pp. 209-215.

Jakes, W.C. (1974), Ed., Microwave Mobile Communications, Ch. 6, John Wiley & Sons, New York.

Kemerait, R.C. and D.G. Childers (1972), "Signal Detection and Extraction by Cepstrum Techniques", IEEE Trans. Information Theory, V. IT-18, pp. 745-759.

Kryter, K.D. (1962), "Methods for the Calculation and Use of the Articulation Index", J. Acoust. Soc. Am., V. 34, pp. 1689-1697.

Licklider, J.C.R. and S.J. Goffard (1947), "Effects of Impulsive Interference upon A-M Voice Communication", J. Acoust. Soc. Am., V. 19, pp. 653-663.

Lindsay, W.C. (1964), "Error Probabilities for Rician Fading Multichannel Reception of Binary and N-ary Signals", IEEE Trans. Inform. Theory, V. IT-10, pp. 339-350.

Morgan, D.R. (1978), "Adaptive Multipath Cancellation for Digital Data Communication", IEEE Trans. Commun., Vol. COM-26, pp. 1380-1390.

Ohlson, J.E. (1974), "Exact Dynamics of Automatic Gain Control", IEEE Trans. Commun., V. COM-22, pp. 72-75.

Pierce, J.N. (1958), "Theoretical Diversity Improvement in Frequency-Shift Keying", Proc. IRE, V. 46, pp. 903-910.

Schwartz, M., W.R. Bennett and S. Stein (1966), Communication Systems and Techniques, McGraw-Hill, New York.

Watt, A.D., R.M. Coon, E.L. Maxwell and R.W. Plush (1958), "Performance of some Radio Systems in the Presence of Thermal and Atmospheric Noise", Proc. IRE, V. 46, pp. 1914-1923.

SECTION 4

APPLICATION TO EXISTING HF RADIOS

4.0 Introduction

In this section, we examine the performance of six HF radios in both non-built-up (rural) and built-up (urban) environments. The radios are representative of current military HF equipment. Their characteristics and nomenclature are discussed in Section 4.1. Section 4.2 analyzes the performance of these radios using range coverage as a measure of effectiveness. It is shown that the presence of buildings and other obstacles reduces the range coverage of the radios by a significant amount which depends on frequency. Section 4.3 discusses the implications of the results of Section 4.2. It is pointed out that the lower HF band (3-10 MHz) will provide significantly greater coverage in built-up areas than lower VHF (30-80 MHz) all conditions being equal (i.e., equal transmitted power levels).

4.1 Radio Characteristics

In this section, we present the characteristics of typical military HF radios which could be used in MOBA communications. These are:

AN/PRC-104	Receiver/Transmitter
AN/PRC-70	Receiver/Transmitter
AN/GRC-106, 106A	Receiver/Transmitter
AN/GRC-122, 142, 142B	Radio Teletypewriter
AN/FRC-93	Receiver/Transmitter
AN/PRC-72A, B, C	Receiver/Transmitter

These radios cover a wide spectrum of designs and uses, as discussed in the following subsections.

4.1.1 AN/PRC-104

The AN/PRC-104 is currently under development by Hughes Aircraft Company for the U.S. Marine Corps, and is the most state-of-the-art of all the radios listed. Designed as an ultra-light (12.5 pounds) 20 watt manpack HF radio, it also can be interfaced with HPA's to make a 400 watt vehicular radio as well as a 100 watt portable radio. It contains an automatic antenna tuner which is supposed to tune to the correct frequency in 8 seconds maximum. The communications range of the PRC-104 is nominally 30 miles with a whip antenna and up to 300 miles using a dipole antenna. The radio tunes the entire 2 to 30 MHz HF band using a frequency synthesizer with 100 Hz increments. It is capable of CW, SSB, and coded data transmission, the latter using a TADIL-A. The specification operating life with its built-in 28 volt, 5 amp-hours, silver zinc battery pack is 16 hours, but CENCOMS tests show 10 hours to be more realistic. The 3 dB bandwidth of a single (not a tandem) radio is specified to be 500 to 3000 Hz, and is thus not PARKHILL compatible.

4.1.2 AN/PRC-70

The AN/PRC-70 is a lightweight (39 pounds) manpack radio designed for employment in the forward combat area. It tunes over the HF/VHF band, from 2 to 76 MHz, using a frequency synthesizer. It is capable of operating in FM at VHF, and AM/SSB/CW/FSK at HF. The transmitted power ranges from 20 to 40 watts, depending on the modulation employed. In the receiving mode the radio draws 7 watts, while in transmitting it varies from 50 to 160 watts. The radio contains an automatic antenna tuner, and comes with a two-section whip antenna, as well as with a doublet antenna. At HF, its nominal range with the whip is 25 miles, and with the doublet, up to 2500 miles. Secure voice operation is possible using the TSEC/KY-57 or TSEC/KY-38.

4.1.3 AN/GRC-106, 106A

The AN/GRC-106 and AN/GRC-106A are mobile (128 pounds) HF radios which are designed for deployment from division level through the COMMZ. The radios tune over the 2 to 30 MHz HF band using a frequency synthesizer, in 1 KHz increments for the GRC-106 and in 100 Hz increments for the GRC-106A. The two radios are identical in all other respects. The radios have $\pm$600 Hz vernier tuning capability on their receivers, and are capable of both transmitting and receiving USB voice, compatible AM, and CW, as well as receiving DSB AM. When interfaced with RTT terminal equipment, the GRC-106 also transmits and receives FSK and NFSK. The radio transmits 400 watts, and has a nominal range of 50 miles with a 15 foot whip antenna, and up to 1500 miles with a doublet antenna. Antenna tuning is manual. The GRC-106 does not have a secure voice capability.

4.1.4 AN/GRC-122, 142, 142B

The AN/GRC-122/142 is a family of vehicular mounted medium power HF SSB radios. While used primarily for teletype, they are also capable of AM and SSB voice, as well as CW operation. As with the AN/GRC-106, they are deployed from division level through COMMZ. The radios cover the 2-30 MHz band, are shelter mounted, and weigh in the order of 1800 pounds. The normal antennas for the radios are a 15 foot whip or an AN/GRA-50 doublet. The AN/GRC-122 family has a range of up to 2400 miles. The radio has no secure voice operation mode, although secure FSK is possible when used with the TSEC/KW-7. The normal transmitted power level is 200 watts for telegraphy, and 400 watts PEP for SSB. A 1 kW amplifier is added to the AN/GRC-122 when the long range capability is desired.

4.1.5 AN/FRC-93

The AN/FRC-93 is a military HF radio system based on the Collins KWM2 HF radio. It is deployed in base camps and field artillery units, has no official configuration and includes portable 100 and 1000 watt, mobile 100 watt, and fixed station 100 and 1000 watt configurations. The basic KWM-2 transceiver weighs 95 pounds, and covers the 3.4 to 5.0 MHz, and 6.5 to 30 MHz bands with the frequency selection being crystal controlled with 14 crystals in the KWM-2, and 28 in the KWM-2A. The operating bands are manually controlled and are 200 kHz wide about the crystal frequencies. No antenna tuning is provided, and the radios must operate with a 50 ohm load (VSWR less than 2.0 to 1) or destruction of the transmitter output stage will result. The only modulations available are SSB and CW, with the SSB 6 dB bandwidth being 300 to 2400 Hz. At 100 watts transmitted power it has a 50 mile ground wave range. Up to 1000 mile range is available with 1 kW transmitted power and a dipole antenna. The AN/FRC-93 does not have a secure voice mode.

4.1.6 AN/PRC-74A, B, C

The AN/PRC-74 is a low power HF radio designed for use by special forces, forward area patrols, and air assault divisions. The PRC-74 and -74A cover the 2 to 12 MHz range, while the -74B and -74C cover the 2-18 MHz range. All models of the -74 are frequency synthesizer controlled in 1 kHz channel spacings. The radios are low power, 15 watts PEP nominal, and weigh between 30 and 50 pounds, depending on the battery pack employed. The batteries are rated for a 24 hour life with a duty cycle of 9 minutes receiver/1 minute transmit. The range with the 10 foot whip antenna supplied with the radio is 25 miles nominal. Extended range operation requires the use of the dipole antenna supplied with the radio. The

tuning of the radio if manual, and there is no secure voice capability.

4.2 Radio Performance

In this section we evaluate the performance of the aforementioned radios in built-up (urban and suburban) and flat non-built-up (rural) areas. The performance is evaluated by determining the range of the various radios in the urban and rural environments. The range of the radios is determined from the minimum required signal-to-noise ratio (SNR) for the type of transmission (SSB, DSB-AM, FSK, etc.). As discussed in Section 3, the minimum required SNR varies upon whether the received signal is fading or not and the statistics of the fading. The nature (statistics) of the fading depends on whether the signal propagates from transmitter-to-receiver via ground wave or skywave. When propagation is via ground wave, the received signal exhibits no fading if the terrain is reasonably flat (rural). When the terrain is typical of a built-up area (urban and suburban), the received signal might exhibit Rician fading or Rayleigh fading (refer to Section 2.5) especially at the higher frequencies in the HF band. On the other hand, if the signal arrives via skywave propagation, it will exhibit slow Rayleigh fading under most conditions. Finally, if the signal arrives via both ground wave and sky-wave, it will exhibit slow Rician fading. Since we are mostly interested in short-range HF propagation, we will assume that the intended mode of propagation is via ground wave so that the radios are equipped with vertically polarized whips. Further-more, for lack of better data, we will also assume that the received signal is slowly fading when propagation is over built-up areas (urban and suburban) and that the fading is Ray-leigh distributed (worst case). When propagation is over smooth, flat (rural) ground, we will assume the signal is not

fading. Those cases where the assumptions might be violated due to the presence of skywave interference will be indicated.

From these considerations, the minimum required SNR for SSB (voice) transmissions in a 3 kHz bandwidth is assumed to be 13 dB (from Table 3.2) in built-up areas and 12 dB in non-built-up areas. Similarly, the minimum required SNR for start-stop teletype data with 1% character error probability is assumed to be 31 dB (from Table 3.5) in built-up areas and 17 dB in non-built-up areas.

The range of the various HF radios may now be determined by finding the transmitter-receiver separation at which the minimum required SNR is first exceeded. In general, when atmospheric or man-made noise levels are greater than receiver thermal noise the SNR at a given frequency and transmitter-receiver separation is given by

$$SNR = P_t + G_t + D_r - L(f,d) - F_{am}(f) - W + 204 \qquad (4.1)$$

where

SNR	=	pre-detection signal-to-noise power ratio for the specified bandwidth B
P_t	=	transmitter power delivered to antenna input (dBw) (PEP for SSB and average power for teletype data)
G_T	=	power gain of transmitting antenna (dB) in direction of propagation path relative to isotropic antenna in free space
D_r	=	directive gain of receiving antenna (dB) in direction of propagation path relative to isotropic antenna in free space
L	=	total attenuation (path loss) in the propagation path (dB) at the specified frequency, f, and range d
F_{am}	=	median of the hourly values of atmospheric or man-made noise power in dB above kTB
W	=	$10 \log_{10} B$ where B is the effective receiver bandwidth in Hz

Since the path loss increases with distance, the SNR decreases with distance. Hence, the range of the radio is found by determining the value of the path loss for which the SNR equals the minimum required SNR. The range is seen to vary with frequency, transmitted power, noise level and antenna gain. Typical noise levels at a given frequency may be determined from Fig. 2.7-1. The transmitted power levels vary from one radio to another as discussed in Section 4.1. The antenna gains vary with length and frequency and need to be determined prior to calculating the range of the radios.

a. Antenna Gain

The antenna gain in the direction of propagation is defined as the product of the directivity (directive gain) of the antenna in the direction of propagation and the efficiency of the antenna [Jasik, 1961]. The directivity is the ratio of the radiation intensity in the direction of propagation to the average radiation intensity. The efficiency of the antenna accounts for copper, dielectric, ground or mismatch losses and is equal to one if these losses are negligible. Thus, the directivity is the gain of a lossless antenna.

Since we are concerned with ground wave propagation mainly, the directive gain (directivity) is the gain of a lossless vertical whip (typical length for MOBA use in 9 feet) near zero elevation angle and over imperfect ground. Vertical directive gain patterns for monopoles (vertical whips) found in the literature are usually based upon the antenna being placed over perfect ground. Fortunately, the directive gain at near grazing (zero) elevation angles for a whip placed over imperfect ground is the same as that of a whip placed over perfect ground [Jordan, 1950] when used to excite surface waves. This means that the directive gain of a vertical whip antenna used for ground wave propagation is 5.15 dB if the whip

is exactly a quarter-wavelength long and 4.76 dB if the whip is much shorter than a quarter-wavelength long [Jasik, 1961]. Thus, a 9 foot whip used for radiating at the horizontal level has a directive gain of 4.76 dB at frequencies below 15 MHz and a directive gain between 4.76 dB and 5.15 dB at frequencies between 15 MHz and 30 MHz. This gain is reduced by the efficiency of the antenna.

The efficiency of an antenna is limited by two factors: near field losses in the ground and losses which result from matching the impedance of the antenna to the radio. The factor which accounts for near field losses is referred to here as the radiation efficiency of the antenna. The radiation efficiency for a short monopole (whip) antenna over average imperfect ground is given by the empirical formula [Barghausen, et al., 1969]

$$E_{ff}(\mathrm{dB}) = -25.646 + 364.817\left(\frac{H}{\lambda}\right) - 2179.89\left(\frac{H}{\lambda}\right)^2 + 6091.33\left(\frac{H}{\lambda}\right)^3 - 6416.702\left(\frac{H}{\lambda}\right)^4 \qquad (4.2)$$

valid for $.02 < (H/\lambda) < 0.3$ where H is the length of the monopole and λ is the wavelength. This formula is shown in Fig. 4.1 as a function of the electrical length, H/λ, of the whip antenna. This curve shows that the radiation efficiency of a 9 foot whip varies from -17 dB at 3 MHz to -6 dB at 10 MHz and to 0 dB at 30 MHz.

Mismatch (tuning) losses depend on the type of matching network used and in particular on the Q of the matching network. For the purpose of this study, we will assume that mismatch (or tuning) losses are negligible in comparison to the ground losses. However it should be pointed out that in some cases, for the (electrically) short antennas used with Army HF radios, tuning losses can be substantial and reduce antenna efficiency significantly, in particular at the lower end of the HF band.

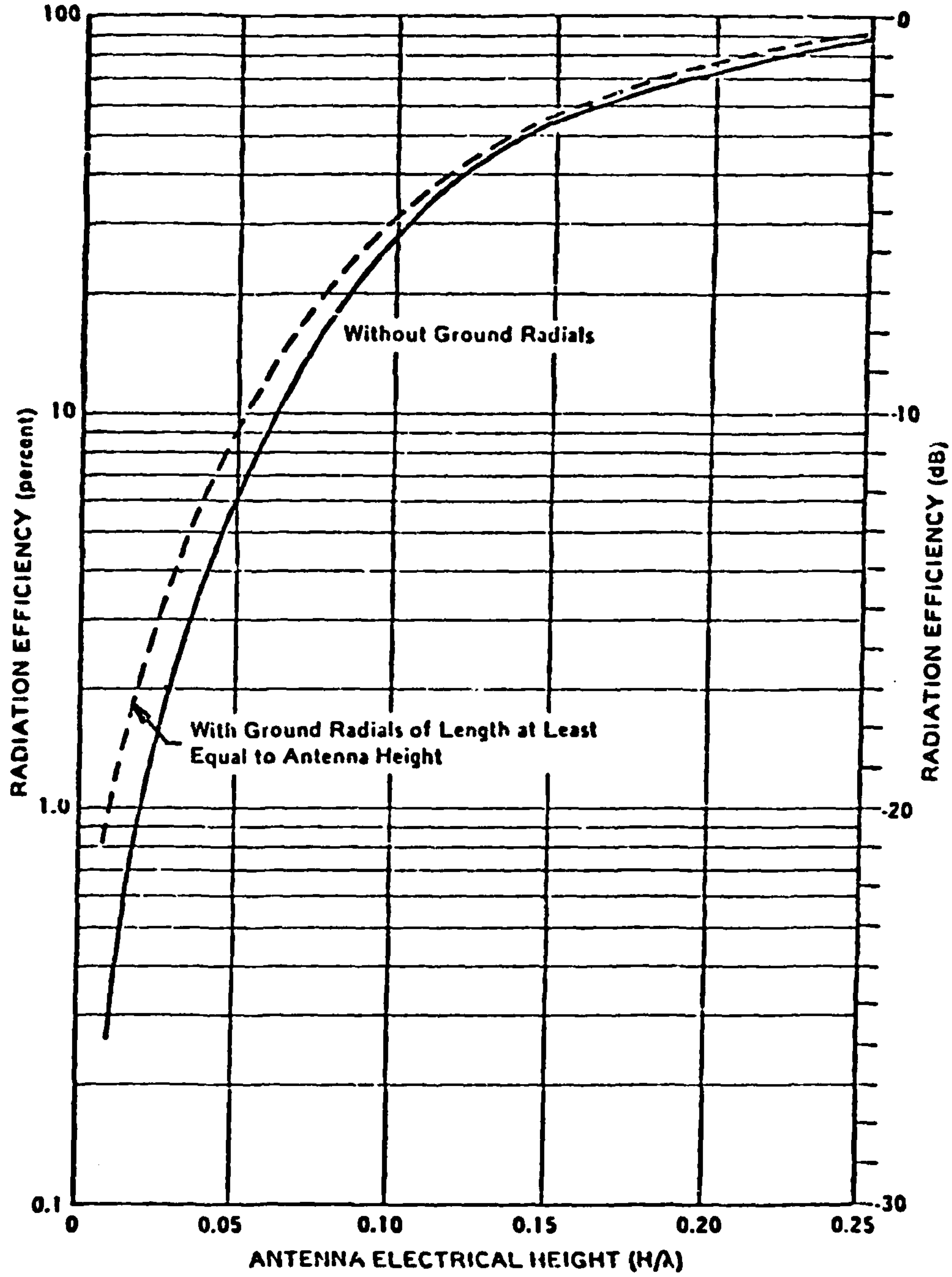

Fig. 4.1 Antenna Radiation Efficiency as a Function of Electrical Length for Base-Fed Vertical Whip

b. Range of SSB HF Voice Transmissions

From these considerations we have calculated the range of the SSB-HF radios described in Section 4.1 at three frequencies: 3 MHz, 10 MHz and 30 MHz, and for two types of propagation conditions: transmission over rural (flat) terrain and transmission in built-up (urban) areas. These predicted ranges are summarized in Table 4.1. From this table it can be seen that under favorable conditions (rural areas), the range of the SSB transmissions varies from 34 km at 3 MHz and 15 watts PEP (peak-envelope power) to 105 km at 30 MHz and 400 watts PEP . While ranges are close to the nominal ranges quoted by the radio manufacturers, the predicted ranges for these same radios in built-up areas are reduced to values between 0.8 km at 30 MHz and 15 watts PEP, to 17 km at 3 MHz and 400 watts PEP. The reduction in range is due to a combination of higher urban noise levels and increased attenuation due to the presence of buildings.

In general we can see from Table 4.1 that the range of the SSB transmissions in urban areas is lower than in rural areas by factors of 4.6 at 3 MHz, 8.0 at 10 MHz, and 59 at 30 MHz. The reduction in range is most severe at the higher frequencies. This is not surprising since the height of the buildings becomes comparable with the wavelength at 30 MHz. The reduction in range is somewhat pessimistic at 30 MHz though, as the theory used to calculate the ground wave attenuation in built-up areas (see Section 2.4) is marginably applicable. On the other hand, these ranges are somewhat lower (factor of 2) than those predicted by the theory of VHF propagation in built-up areas [see Ehrman and Parl, 1977] and measured experimentally at 27 MHz [Ehrman, Malaga and Ziolkowski, 1979].

TABLE 4.1

PREDICTED TRANSMISSION RANGE OF VARIOUS SSB-HF RADIOS

Transmitted Power, P_t (Watts PEP)	Radio Nomenclature	Transmission Range (km)					
		RURAL			URBAN		
		3 MHz	10 MHz	30 MHz	3 MHz	10 MHz	30 MHz
15	PRC-74	34*	36	46	7.5	4.6	0.8
20	PRC-104	37*	39	50	8.0	4.7	.85
40	PRC-70	44*	46	59	9.6	5.9	1.0
100	PRC-104/FRC-93	55*	58	74	12.	7.4	1.3
400	PRC-104/GRC-106 GRC-122	78*	82	105	17.	10.5	1.8

*Skyware interference at night.

c. Range of Teletype HF Transmissions

A similar calculation of the range of teletype data HF transmissions has been carried out for the Army HF radios which have this capability. The results are summarized in Table 4.2. It can be seen that the range of teletype data transmissions with less than 1% character error probabilities under favorable conditions (rural terrain) varies from 28.5 km at 3 MHz and 20 watts average transmitted power to 66 km at 30 MHz and 200 watts average transmitted power. In urban terrain these ranges are reduced to distances between .33 km at 30 MHz and 20 watts average transmitted power and 5.4 km at 3 MHz and 200 watts average transmitted power. In general, the range of teletype data transmission in urban areas is lower than in rural areas by factors of 9.4 at 3 MHz, 19.6 at 10 MHz, and 110 at 30 MHz. The range reduction factor for teletype data at a given frequency is twice as great as that for SSB transmission because the effects of Rayleigh fading are much more severe on data transmissions than on voice communications.

4.3 Implications of the Radio Analysis

In the previous section we analyzed the performance (range reduction) of six military HF radios in urban areas. The analysis was more general though and applies to any radio whose output power falls in the ranges listed in Tables 4.1 and 4.2.

The analysis shows that when the terrain is reasonably flat and obstruction free (such as rural terrain), slightly longer transmission ranges are achieved at the high edge of the HF band (30 MHz). The reasons are good antenna efficiency and lower noise levels. However when the terrain is built-up (such as in urban and suburban areas), the lower frequencies in the HF band (near 3 MHz) provide better coverage because the low antenna efficiencies and high noise levels at these frequencies

TABLE 4.2

PREDICTED TRANSMISSION RANGE FOR
TELETYPE DATA USING HF RADIOS

Average Transmitted Power P_t (Watts)	Radio Nomenclature	Transmission Range (km)					
		RURAL			URBAN		
		3 MHz	10 MHz	30 MHz	3 MHz	10 MHz	30 MHz
20	PRC-70	28.5	32	37	3.0	1.6	.33
200	GRC-106 GRC-122	51*	57	66	5.4	2.9	0.6

*Skyware interference at night.

are more than offset by the lower excess attenuation (introduced by the presence of buildings and other structures such as lamp posts). The excess attenuation is considerably higher at 30 MHz than at 3 MHz. In fact, the excess attenuation increases at a rate of 20 dB per decade (ten-fold increase in frequency) or 6 dB per octave (doubling of the frequency). This is over and above the ground wave attenuation which roughly increases at a rate of 40 dB per decade or 12 dB per octave.

The theoretical results given in Tables 4.1 and 4.2 show that radio transmission at 3 MHz provides 10 times greater range coverage than transmission at 30 MHz in built-up areas. This is very significant and it indicates that the lower portion of the HF band will provide much greater coverage in built-up areas than the military VHF band (30 MHz to 80 MHz). The improvement in coverage may be as high as 10 times greater if the radios are at ground level. Doubling in the coverage at VHF may be achieved by raising one antenna to a height of 30 feet or both antennas to a height of 15 feet. Antenna elevation at lower HF will not result in a significant improvement unless both antennas are elevated above roof top level.

SECTION 5
CONCLUSIONS AND RECOMMENDATIONS

5.1 Conclusions

Based on the results of this study, the following conclusions have been reached.

a. For radio wave propagation at HF using ground-based vertical whips, the ground wave will be dominant over the skywave up to distances of at least 70 km during daytime but only up to 35 km at night at frequencies below 5 MHz; above 5 MHz there is no skywave at night. These distances will vary somewhat depending on the propagation conditions.

b. The range of a radio at HF when operated street-to-street in an urban area will be significantly lower than when operated in a flat rural area. Typical ranges of various Army HF radios for voice and teletype data transmission in urban and rural areas are given in Tables 4-1 and 4-2.

c. All other things being equal, the range of a radio in an urban area is a strong function of frequency. The lower the frequency the greater the range.

d. The range of a radio in a rural area is on the other hand almost independent of frequency.

e. There is almost no data regarding the statistical behavior of HF signals in urban areas.

f. There is little quantitative data concerning signal attenuation in urban or suburban areas at HF.

g. There is little quantitative data regarding street-to-building, building-to-building communications or intrabuilding communications.

h. Antenna efficiency is a problem at the lower end of the HF band. As an example, the efficiency of a 9 ft whip at 3 MHz is -17 dB. A smaller antenna would be even less efficient.

i. From theoretical considerations, HF promises to provide significantly greater range (or area coverage) than VHF (factor of 5 times).

j. Due to antenna size considerations, HF may not be practical for street-to-building, building-to-building or intrabuilding communications.

k. Front-line units to higher echelon communications using 100 Watt HF radios will not be possible during the daytime if they are separated by more than 50 km especially when one end of the link is in a built-up area. At night communications is possible beyond 50 km at frequencies between 3 and 5 MHz.

5.2 Recommendations

In order to verify our conclusions regarding the improvement in range for MOBA we recommend that propagation measurements at HF be made in both urban and suburban areas. The measurements should be similar to those we made at VHF and UHF and the data reduction and analysis should be similar so that they can be used in a unified propagation model.